Widespread Nearshore and Shallow Marine Deposition within the Lower Jurassic Precipice Sandstone and Evergreen Formation in the Surat Basin, Australia

Andrew D. La Croix[1,2*], Jiahao Wang[1,3], Jianhua He[1,4], Carey Hannaford[5], Valeria Bianchi[6], Joan Esterle[6], and Jim R. Undershultz[7]

[1]Energy Initiative, University of Queensland, Brisbane 4072, Australia
[2]School of Science, University of Waikato, Hamilton 3240, New Zealand
[3]Key Laboratory of Petroleum Resources, China University of Geosciences, Wuhan 430074, China
[4]Key Laboratory of Oil and Gas Reservoir Geology and Exploitation, Chengdu University of Technology, Chengdu 610059, China
[5]MGPalaeo Pty Ltd, Perth 6090, Australia
[6]School of Earth and Environmental Sciences, University of Queensland, Brisbane 4072, Australia
[7]Centre for Coal Seam Gas, University of Queensland, Brisbane 4072, Australia

Corresponding author: Andrew D. La Croix, andrew.lacroix@waikato.ac.nz

Keywords: Precipice Sandstone; Evergreen Formation; Surat Basin; Jurassic; facies analysis; ichnology; sedimentology; palynology.

ABSTRACT

In the Surat Basin of eastern Australia, the Lower Jurassic Precipice Sandstone and Evergreen Formation are a highly prospective reservoir-seal pair for notional future carbon capture and storage. However, the succession remains poorly constrained from a paleo-depositional standpoint and this has impacted the capacity to construct predictive reservoir models. Here we integrate sedimentological, ichnological, and palynological data from ten cores located across a large region of the northern and central basin to produce conceptual depositional models.

Our analysis shows that the Lower Jurassic Series consists of fifteen recurring sedimentary facies that are arranged into six facies associations – braidplain, lower delta plain, subaqueous delta, delta-influenced shoreface, tidally influenced shoreline, and restricted marine shoals. The facies associations occur in the context of a large scale fluvio-deltaic system that developed within the basin. These results are supported by ichnological indications of marine and brackish water, and a coastal suite of palynomorphs including rare dinocysts, acritarchs, and copepod fragments. The very low abundance of marine palynomorphs are confined to the upper portion of the Evergreen Formation, and in combination with sedimentological and ichnological results suggest that marine influence increased through time.

The elucidation of marine influenced deposition contravenes all but the most recent facies interpretations of the Precipice Sandstone and Evergreen Formation, and suggests that the paleogeography of the Mesozoic of eastern Australia needs to be reconsidered. Importantly, the nearshore and shallow marine depositional affinity has important implications for the size, orientation, and distribution of geobodies when building geologically realistic static reservoir models for dynamic flow simulation.

1. Introduction

Facies analysis and paleoenvironmental interpretation are integral for predicting reservoir performance due to their implications for fluid flow properties (i.e., porosity and permeability; (Burton and Wood, 2013; Baniak et al., 2014; La Croix et al., 2017) and the continuity and connectedness of reservoirs and seals (Allen, 1978; Ainsworth, 2005). Facies data are fundamental inputs to high-resolution static reservoir models (Harding et al., 2005; Mikes and Geel, 2006; Ringrose and Bentley, 2015), and thus capturing detailed facies information can reduce uncertainty in the prediction of plume migration and pressure response in CO_2 injection scenarios.

Carbon capture and storage (CCS) in subsurface aquifers and depleted hydrocarbon reservoirs is a growing area of research and investment (Garnett et al., 2014; Neele et al., 2017; Worth et al., 2017). This is due to its large potential for mitigating emissions from coal- and gas-fired power generation and for the abatement of climate change (Metz et al., 2005; Agency, 2008). As a result, regional subsurface assessment of the sedimentary basins in Eastern Australia have identified the Surat Basin as being highly prospective because of its depth, temperature gradient, the presence of high-quality reservoir-seal pairs and its proximity to large point-source emissions (Bradshaw et al., 2011; Hodgkinson and Grigorescu, 2013; Garnett et al., 2014). Within the Surat Basin, the Lower Jurassic Precipice Sandstone and Evergreen Formation represent the primary reservoir and seal intervals with potential to meet commercial-scale storage requirements (Bradshaw et al., 2011).

The regional-scale geology of the Precipice Sandstone and Evergreen Formation is not well understood. This is because they are generally not hydrocarbon bearing strata, particularly in the deep central regions of the Surat Basin where CCS potential is greatest. Detailed depositional interpretations are few, hindering modelling efforts to help forecast reservoir performance and sealing potential. Most past studies have interpreted the Precipice Sandstone to represent braided river deposits with minimal effects of relative sea level (e.g., Sell et al., 1972; Exon, 1976; Exon and Burger, 1981; Martin, 1981; Green et al., 1997). More recently, an argument for marine influence has been put forth based on data from the outcrop belt and one core located in the northern portion of the basin (Bianchi et al., 2018b; Martin et al., 2018). The basal Evergreen Formation, on the other hand, has been interpreted as continental meandering river and freshwater lake deposits (Mollan et al., 1972; Dickins and Malone, 1973; Exon, 1976; Cosgrove and Mogg, 1985). Uppermost Evergreen Formation deposits have been interpreted as fluvio-lacustrine (Exon and Burger, 1981; Fielding, 1989, 1990; Cranfield et al., 1994), though marine incursions have been suggested to explain the presence of oolitic ironstone in the

Westgrove Ironstone Member (Mollan et al., 1969; Mollan et al., 1972; Exon, 1976; Beeston, 1979). Few studies to date have integrated multiple datasets across a large area to gain a regional perspective of the distribution of paleoenvironments and their representative sedimentary strata. Such regional integration of facies analysis for the Precipice Sandstone and Evergreen Formation needs to be revisited to establish an updated view of the depositional environments as this has not been undertaken for several decades.

The aim of this study was to analyse facies by integrating sedimentology, ichnology, and palynology from the Lower Jurassic- Precipice Sandstone and Evergreen Formation with a regional perspective in mind. We sought to construct depositional models that fit the large-scale distribution of facies and which document the progressive changes in environments through time. We focused on providing evidence of marine-influenced deposition, a topic that is still debated in the literature and holds important implications for the paleogeography of eastern Australia during the breakup of Gondwana. The results of this study are important for aiding sequence-stratigraphic interpretations (e.g., Wang et al., 2019), for predicting facies where data are sparse or absent (e.g., He et al., 2019), and ultimately to improve reservoir modelling for the purpose of CO_2 storage in the subsurface (Hodgkinson and Grigorescu, 2013).

2. Geological Setting

2.1 Structure and Basin Formation

The Surat Basin lies between latitudes 25° and 33° S, and from longitudes 147° to 152° E, enveloping an area of ~327, 000 km^2 in Queensland and New South Wales, Australia (Fig. 1). The Surat Basin is time equivalent to the Eromanga and Clarence-Moreton basins, separated from them by the Nebine and Kumbarilla ridges (structural highs) to the west and east, respectively (Power and Devine, 1970; Exon and Senior, 1976; Green et al., 1997). As a shallow platform depression sitting unconformably above the narrower Bowen and Gunnedah basins, the Surat Basin partly rests upon Palaeozoic basement rocks, and partly on sedimentary rocks of Permo-Triassic age. The basin axis trends north-south along the Mimosa Syncline, roughly corresponding to the Taroom Trough which is the thickest part of the underlying Bowen Basin (Exon, 1976; Fielding et al., 1990).

There are three differing basin formation models of the Surat Basin: 1) thermal subsidence (Korsch et al., 1989); 2) dynamic platform tilting (Gallagher et al., 1994; Korsch and Totterdell, 2009; Waschbusch et al., 2009); and, 3) intraplate rifting (Fielding, 1996). These differing interpretations stem from a poorly resolved tectonic history and debate over the intracratonic (Fielding, 1996; Yago and Fielding, 1996) *versus* pericratonic nature of the basin (Exon, 1976;

Exon and Senior, 1976; Veevers et al., 1982; Gallagher, 1990). Despite the relatively undeformed nature of its sedimentary fill, several important structural features occur within the Surat Basin (Fig. 1). The most prominent basement structures are the Auburn Arch in the southwest, the Yarraman Block in the northeast, and the Texas High in the southeast. These fault blocks were major sediment sources, but became less exposed as time progressed and the basin was filled (Green et al., 1997). The sedimentary succession is no longer at its maximum burial depths because up to 2500 m of sediment have been eroded from the northern and eastern parts of the basin in the last ~100Ma (Gallagher et al., 1994; Raza et al., 2009).

2.2 Sedimentation Cycles and Stratigraphy

The 2500 m thick fill of the Surat Basin was delivered in six major pulses (Exon and Burger, 1981). Each cycle broadly equates to a 2nd order transgressive-regressive cycle (10–20 Ma), with three cycles for the Jurassic section, one spanning the Jura-Cretaceous boundary, and two during the Cretaceous. The cycles are informally known as: (1) the Precipice-Evergreen, (2) the Hutton-Walloon, (3) the Springbok-Westbourne, (4) the Gubberamunda-Orallo, (5) the Mooga-Bungil, and (6) the Wallumbilla.

Stratigraphic correlation across the Surat Basin has garnered substantial effort over several decades (Gray, 1968; Power and Devine, 1970; Mollan et al., 1972; Exon, 1976; Green et al., 1997; Hoffmann et al., 2009; Totterdell et al., 2009; Wang et al., 2019). Yet, a set of lithostratigraphic terminology that is agreed upon and applied across the basin consistently has not been established (e.g., Mollan et al., 1972; Exon, 1976; McKellar, 1998). More recently, workers have focused on packaging rocks according to their age and genetic relationships using a sequence-stratigraphic framework (Wells et al., 1994; Hoffmann et al., 2009; Totterdell et al., 2009; Ziolkowski et al., 2014; Wang et al., 2019). The most recent stratigraphic scheme of Wang et al. (2019) for the Precipice Sandstone and Evergreen Formation comprises three 3rd-order sequences (Fig.2; Haq et al., 1987).

2.3 Palynology and Biostratigraphy

A substantial body of literature exists relating to the palynology of Jurassic–Cretaceous strata within the Surat Basin. In the Precipice Sandstone and Evergreen Formation, as well as time equivalent units in eastern Australia, palynology has mainly been used to understand the regional stratigraphy and timing of deposition (Evans, 1962, 1966; Reiser and Williams, 1969; Price, 1997; McKellar, 1998; de Jersey and McKellar, 2013). Other studies have documented the palynoflora from a taxonomic and paleoclimate point of view (de Jersey and Dearne, 1964; de Jersey and Paten, 1964b, a; de Jersey, 1965; Paten, 1967; Reiser and Williams, 1969; McKellar, 1974, 1998), noting a shift from warmer climates in the Early Jurassic corresponding to the *Callialasporites dampieri* Microflora to cooler climatic conditions represented by the *Microcachryidites* Microflora. This was under palaeolatitudinal control due to the position of the Pangea supercontinent, which was located towards the south pole at the time (McKellar, 1998). More recently, palynology has been applied to detailed paleoenvironmental interpretations with differing views on the (e.g., Ziolkowski et al., 2014) *versus* marine implications of the palynological suites (e.g., Martin et al., 2018). One problem that has hindered all previous studies, however, has been the relatively limited datasets in terms of number of wells used for analysis; most studies only considered a single well or few wells within a portion of the basin. Nonetheless, past studies set the stage for a regional-scale investigation of the palynology and especially one that combines with insights from sedimentology and ichnology.

3. Methods

Ten subsurface cores were logged to gain a regional perspective on the depositional environments and facies evolution of the Precipice–Evergreen succession: Chinchilla 4, Condabri MB9-H, Kenya East GW7, Moonie 31, Moonie 34, Reedy Creek MB3-H, Roma 8, Taroom 17, West Wandoan 1, and Woleebee Creek GW4 (Table 1). Cores were predominantly located in the northern portion of the Surat Basin, and to a lesser extent on the western and eastern flanks (Fig. 1). Cored intervals ranged from 7 m (Moonie 31) to 295 m thick (Woleebee Creek GW4). The succession was described in terms of lithology, physical sedimentary structures, and biogenic structures. Ichnological observations included bioturbation intensity using the bioturbation index (Taylor and Goldring, 1993), diversity of bioturbation, distribution of bioturbation between beds, and identification of trace fossils to the ichnogenus level.

Sixty-one samples were collected from mudstone or heterolithic (i.e., interbedded sandstone and mudstone) facies for palynological analysis. Samples were quantitatively analysed for the first 300 palynomorphs counted with only the presence of subsequent grains being recorded, but not included in the counts. Notably, counts did not account for reworking and re-deposition, sediment-gravity processes, windblown sedimentation, or other processes that might affect the distribution of palynomorphs.

To place our sedimentological, ichnological, and palynological observations into context and to facilitate comparison between wells, we describe the strata using the sequence stratigraphy of Wang et al. (2019) (Figs. 2 and 3).

4. Results and Interpretation

4.1 Sedimentary Facies

Fifteen discrete facies were identified from the Precipice Sandstone and Evergreen Formation (Table 2). These facies group together into six facies associations interpreted to represent braidplain, lower delta plain, subaqueous delta, delta-influenced shoreface, tidally influenced shoreline, and restricted marine shoal depositional environments. The Precipice Sandstone is overwhelmingly dominated by the braid plain association, whereas the Evergreen Formation comprises a complex mixture of lower delta plain, subaqueous delta, delta-influenced shoreface, tidally influenced shoreline, and restricted marine shoal deposits.

4.2 Facies Associations

4.2.1 Facies Association 1: Braid Plain

Facies Association 1 (FA1) predominantly consists of interbedded conglomerate and sandstone (Facies 1 (F1); Fig. 4A) representing lag deposits or channel bases, mud-clast breccia (Facies 2 (F2); Fig. 4B) interpreted as channel bank collapse or channel bases, and coarse-grained planar-tabular cross-bedded sandstone (Facies 3 (F3); Fig. 4C) deposited as the main channel fill (Table 2). Typical complete facies successions comprise F1 passing gradationally upwards into F3, with interspersed layers of 2 (Fig. 4). Individual packages range from 3–7 m, but they are commonly stacked into multi-storied packages up to 80 m thick, with the thickest occur near the axis of the basin along the Mimosa Syncline. The overall coarse grain size and thick cross-bedded layers of F3 suggests deposition under high flow velocities (Fig. 4C). Mud-clast breccias (F2) most commonly located near the base of individual fining-upward units indicates undercutting of the floodplain (Fig. 4B), whereas structureless layers (F1) indicate rapidly deposited sediment (Fig. 4A). The quartz-dominated nature of FA1 suggests that the sediment source area was rich in quartz. The sedimentological evidence and a general lack ichnological features indicates that FA1 was deposited in a braid plain system with abundant sediment supply (Miall, 1977). FA1 reflects the early stages of Surat Basin development as braided rivers flowed across the base-Surat unconformity surface following irregular topographic lows.

4.2.2 Facies Association 2: Lower Delta Plain

Facies Association 2 (FA2) is composed of planar-tabular to cross-bedded sandstone (Facies 4 (F4); Fig. 5A), structureless to planar-parallel laminated sandstone (Facies 5 (F5); Fig. 5B), carbonaceous sandstone and siltstone (Facies 6 (F6); Fig. 5C, D), coal (Facies 7 (F7); Fig.

5D), and bioturbated muddy sandstone and sandy mudstone (Facies 8 (F8); Fig. 5F). These are interpreted to represent distributary channel, levee and crevasse splay, floodplain, peat mire, and interdistributary bay deposits, respectively (Table 2). The association is characterized by an overall fining upward succession of F4 passing upward into F5, grading into F6, and capped with F7 (Fig. 5G). Facies 8 is interspersed at various stratigraphic positions, but is most commonly above F6. Facies successions vary between 3–13 m thick, with the thickest occurring towards the basin-centre. Sedimentological characteristics of the sandstone indicate quasi-steady unidirectional flow in channels (F4; Fig. 5A) with episodic breaching of the channel banks (F5; Fig. 5B). The thin nature of most channel deposits is interpreted to represent terminal distributary channels (Olariu and Bhattacharya, 2006). Thin coal deposits (F7; Fig. 5D) interbedded with carbonaceous siltstone and mudstone (F6; Fig. 5C) suggests a low-energy environment subject to river flooding. Peat forming environments would have required a sufficiently high water-table. Trace fossils produced by terrestrial insects or annelids – *Planolites*, *Taenidium,* and *Naktodemasis* – support the notion of a continental setting (Savrda et al., 2000). On the other hand, unstructured to crudely structured muddy sandstone and sandy mudstone (F8; Fig. 5F) suggests slow deposition rates between active zones of sediment delivery. Synaeresis cracks, rootlets, and a depauperate assemblage of marine burrows indicate normal to reduced marine salinity, which is consistent with the interpretation of interdistributary bays (MacEachern et al., 2007). The association between subaerial, freshwater subaqueous, and marine-influenced subaqueous deposits is taken to indicate that FA2 represents deposition within a lower delta plain setting.

4.2.3 Facies Association 3: Subaqueous Delta

Facies Association 3 (FA3) comprises wave to combined flow ripple laminated mouthbar sandstone (Facies 9 (F9); Fig. 6A), sand-dominated heterolithics representing the delta front (Facies 10 (F10); Fig. 6B, C), and muddy heterolithics deposited on the prodelta (Facies 11 (F11); Fig. 6D), arranged into coarsening-upward successions (Table 2). The association varies in thickness from 3–12 m, though individual facies are seldom thicker than 5 m. Typical facies successions consists of F11 passing gradationally upward into F10, and capped with F9, indicating overall progradational facies stacking (Fig. 6E). A dominance of combined flow rippled sandstone attests the close relationship with a channel system modified by waves and tides. Interbedded sharp-based mudstones with normal or inverse grading are interpreted to represent fluid mud deposits (Fig. 6D). Rare navichnia reflect sediment swimming behaviors as organisms were buried by fluid mud carried in hyperpycnal flows (Bhattacharya and MacEachern, 2009).

Synaeresis cracks combined with a depauperate marine ichnological assemblage indicate mixing of fresh and marine water (Fig. 6B; MacEachern et al., 2005). Finally, micro-faults suggest sediment loading and high deposition rates. The predominance of current generated physical structures, with subordinate wave and tide generated structures suggests a depositional setting dominated by fluvial processes, with secondary waves and tides (Ainsworth et al., 2011). The sedimentological and ichnological characteristics, in concert with the stratigraphic stacking patterns suggest that these deposits accumulated within the subaqueous portion of a delta.

4.2.4 Facies Association 4: Delta-Influenced Shoreface

Facies Association 4 (FA4), consists of a gradational transition from upper offshore bioturbated sandy mudstone with HCS (Facies 13 (F13); Fig. 7B) to bioturbated muddy sandstone (Facies 12 (F12); Fig. 7A) with wave-ripples and HCS of the lower shoreface, arranged into an upward-coarsening succession (Table 2; Fig. 7C). The association varies from 4–12 m thick. Wave and storm-generated physical structures and the increasing proportion of sandstone beds upwards reflects a change from deposition below fairweather wave base to above fairweather wave base where sediment was persistently agitated by wave energy. Interbedding between laminated sandstone and bioturbated mudstone is interpreted to represent alternation between fairweather depositional conditions and storm deposition (Fig. 7B). Sharp-based, graded mud beds represent hyperpycnal flows carrying fluid mud from nearby deltas (Bhattacharya and MacEachern, 2009). Highly bioturbated beds contain the most diverse suite of marine trace fossils in the Precipice Sandstone and Evergreen Formation (Fig. 7A, B) and suggests that the association represents a marine end-member. In consideration of the sedimentological and ichnological characteristics of FA4, the succession is interpreted to represent deposition on a delta-influenced shoreface.

4.2.5 Facies Association 5: Tidally Influenced Shoreline

Facies Association 5 (FA5) consists of mixed sandy and muddy heterolithics with tide-generated structures and uncommon to abundant bioturbation with marine trace fossils (Facies 14 (F14); Fig. 8 A, B; Table 2). The association is characterized by fining-upward heterolithic packages of strata (Fig. 8C). The association varies in thickness from 1–5 m. Current and tide-generated physical sedimentary structures dominate the succession (Fig. 8A, B), indicating alternating current directions. Rootlets suggest periodic subaerial exposure. Although bioturbation with marine trace fossils has completely homogenized portions of this facies, some beds and bedsets remain unburrowed. This is interpreted to indicate alternating physico-chemical environmental stresses in the depositional setting such as periodic subaerial exposure, as well as high and rapidly changing energy conditions (MacEachern et al., 2007). However, the bioturbation signature varies considerably in terms of intensity and distribution, and this might reflect differences in the location of deposition in relation to sources of freshwater influx (i.e., proximal or distal to a river mouth; (cf. Dashtgard, 2011)). Although FA5 is not common in the cored intervals, it demonstrates that tides were an important sediment transport and deposition mechanism, and suggests that parts of the basin were tidally influenced. The presences of tidal indicators also supports the notion of a marine influenced basin although we recognize that rarely tidal structures can be produced by meteorological tides (Ainsworth et al., 2012). FA5 is interpreted to represent deposition on tidal flats adjacent to active distributary channels, receiving some protection from wave fetch and freshwater input into the basin.

4.2.56 Facies Association 6: Restricted Marine Shoals

Facies 6 (FA6) is composed of oolitic ironstone (Facies 15A (F15A); Fig. 9A) and cemented ironstone (Facies 15B (F15B); Fig. 9B; Table 2). Rare horizontal planar parallel lamination or wave ripple lamination occurs in F15A, indicating periodic wave agitation of the sea floor. The absence of bioturbation suggests a physico-chemical environmental stress that precluded infaunal colonization. Facies 15B contains stylolites and is unstructured, suggesting overprinting of the original depositional texture (Fig. 9B). FA6 is nearly always interbedded with FA3, implying a close depositional affinity. Taken together, the characteristics of FA6 is interpreted to represent deposition in a restricted marine environment with freshwater influx, wave agitation, but protected (i.e. “restricted”) from abundant mixing of the water column such that the Fe context could be maintained long enough for mineralization of ooids; the restriction of mixing in the water column is most likely related to geomorphological barriers on the seafloor (cf. Hallam and Bradshaw, 1979), but the effects of embayments cannot be discounted. Hot fluids associated with structural features such as faults and fracturs account for the diagenetic overprint observed in the F15B sub-facies.

4.3 Sequence Stratigraphy

In the sequence stratigraphic scheme first introduced by Wang et al. (2019) the Precipice Sandstone and Evergreen Formation consist of 3 sequences from base to top (Fig. 2). The first and third sequences (i.e., SQ1 and SQ3) are defined by a basal unconformity (J10, SB2, J20, J30), contain a transgressive surface (TS1, TS3), a maximum flooding surface

(MFS1, MFS3), and are marked by an unconformity at their top. These segment the sequences into a lowstand systems tract, transgressive systems tract, and highstand systems tract, respectively. However, the second sequence (i.e., SQ2) is relatively thin and possibly incompletely preserved across the basin, and therefore, individual systems tracts were not defined. Thus, SQ2 is described as a single unit. The stratigraphy is composed of the surfaces: J10 (base-Surat unconformity), TS1, MFS1, SB2, J20, TS3, MFS3, and J30 (top Evergreen) from base to top.

4.4 Palynology

Palynological analysis identified a diverse spore-pollen assemblage as well as freshwater algae. In addition, spinose acritarchs, dinocysts, and copepod fragments were also identified in some of the samples. Although copepods can be found in both marine and non-marine settings those identified in these samples were accompanied by spinose acritarchs, thought to indicate brackish to marine influence (Figure 10; Table 3). Six sporomorph ecogroups (SEGs) were interpreted from the microplankton forms based on Abbink (1998) and Abbink et al. (2004). The SEGs consisted of: 1) marine forms, 2) coastal spores, 3) continental spores, 4) coastal pollen, 5) continental pollen, 6) freshwater algae, and 7) fungi. The marine SEG comprised dinoflagellates, acritarchs, and copepod fragments. The coastal spore SEG consisted of the genera *Retitriletes*. The coastal pollen SEG is composed of *Araucariacites, Callialasporites,* and *Corollina* / *Classpollis* . The remainder of spore, pollen, algae, and fungi were interpreted to represent non-marine to freshwater ecogroups. We describe the palynology by stratigraphic interval to give a sense of how the palynological signature changed through the vertical succession.

4.3.1 Lowstand Systems Tract 1

Palynological grains from the Precipice Sandstone (i.e., LST 1) were dominated by coastal pollen and continental pollen, with subordinate proportions of continental spores and coastal spores, and minor freshwater algae (Fig. 11; Table 4). Coastal spores ranged between 0% (Taroom 17 and West Wandoan 1) and 14.7% (Condabri MB9-H). Continental spores varied from 6.3% (Taroom 17) and 55.3% (Condabri MB9-H). The proportion of coastal pollen was in the range from 26.3% (Condabri MB9-H) to 85.0% (West Wandoan 1). Continental pollen content was between 2.7% (Condabri MB9-H) and 86.1% (Chinchilla 4). Finally, freshwater algae varied between 0.3% (Taroom 17) and 5.1% (Chinchilla 4). No fungi, dinocysts, acritarchs, or copepod fragments were recovered.

4.3.2 Transgressive Systems Tract 1

Grains counted from the lower Evergreen Formation (i.e., TST 1) were dominated by coastal pollen and continental pollen, with lesser amounts of continental spores and coastal spores, and minor freshwater algae (Fig. 11; Table 4). Coastal spores varied from 3.3% (Taroom 17) to 14.7% (Kenya East GW7). Continental spores ranged between 15.3% (Taroom 17) and 46.0% (Kenya East GW7). Coastal pollen proportions were from 14.6% (Kenya East GW7) to 65.3% (Kenya East GW7). Continental pollen content ranged between 8.3% (Condabri MB9-H) and 64.6% (Chinchilla 4). Lastly, freshwater algae varied between 0% (Woleebee Creek GW4) and 5.6% (Kenya East GW7). No fungi, dinocysts, acritarchs, or copepod grains were counted.

4.3.1 Highstand Systems Tract 1

Palynology grain counts for HST 1 were dominated by coastal pollen and continental pollen, with subordinate proportions of continental spores and coastal spores, and minor freshwater algae (Fig. 11; Table 4). Coastal spores ranged between 2.3% (Chinchilla 4) and 9.6% (Condabri MB9-H). Continental spores varied from 14.3% (Chinchilla 4) to 34.7% (Condabri MB9-H). The proportion of coastal pollen was in the range from 47.3% (Condabri MB9-H) to 63.5% (Chinchilla 4). Continental pollen content was between 6.7% (Condabri MB9-H) and 84.0% (Chinchilla 4). Freshwater algae varied between 0% (Taroom 17) and 2.0% (Reedy Creek MB3-H). Freshwater algae were only present in Chinchilla 4 at a proportion of 0.3%. No dinocysts, acritarchs, or copepod fragments were recovered.

4.3.1 Sequence 2

In Sequence 2 palynological analysis showed that mudstone samples were dominated by coastal pollen, continental pollen, and continental spores (Fig. 11; Table 4). Lesser proportions of coastal spores were observed and only a minor freshwater algae component was noted. No fungi, dinocysts, acritarchs, or copepod fragments were counted. The proportion of coastal spores varied between 4.6% (Woleebee Creek GW4) and 31.3% (Woleebee Creek GW4). Continental spores ranged from 25.05% (Taroom 17) and 52.3% (Condabri MB9-H). Coastal pollen grains comprise 24.7% (Condabri MB9-H) to 51.7% (Woleebee Creek GW4) of samples. Continental pollen consists of 2.3% (Roma 8 and Woleebee Creek GW4) to 41.8% (Reedy Creek MB3-H). Finally, freshwater algae varied between 0.3% (Reedy Creek MB9-H) and 6.0% (Roma 8).

4.3.1 Transgressive Systems Tract 3

Transgressive Systems Tract 3 comprised palynology grains dominated by coastal pollen and continental pollen, with lesser continental spores and coastal spores, and minor freshwater algae and marine indicators (i.e., dinocysts, acritarchs, copepoda; Fig. 11; Table 4). Samples consisted of between 1.3% (Chinchilla 4) and 30.0% (West Wandoan 1) coastal spores. Continental spores comprised between 7.0% (West Wandoan 1 and Woleebee Creek GW4) and 32.2% (West Wandoan 1) of samples. Coastal pollen ranged between 23.2% (Chinchilla 4) and 64.3% (Roma 8). Continental pollen varied from 8.0% (West Wandoan 1) and 81.5% (Chinchilla 4). The proportion of freshwater algae grains ranged between 0.9% (Roma 8) and 12.3% (Kenya East GW7). Marine indicators were as high as 6.1% of samples (West Wandoan 1). No fungi were observed.

4.3.1 Highstand Systems Tract 3

The palynology of Highstand Systems Tract 3 is dominated by coastal pollen, continental pollen, and continental spores, with lesser amounts of coastal spores (Fig. 11; Table 4). Minor freshwater algae content was observed, with trace indications of marine influence in the form of dinocysts, acritarchs, and copepoda. The proportion of coastal spores ranged from 6.1% (Condabri MB9-H) to 14.2% (Kenya East GW7). Continental spores varied between 15.7% (Roma 8) and 46.8% (Condabri MB9-H). Coastal pollen content is from 21.3% (Kenya East GW7) to 60.9% (Chinchilla 4). Continental pollen proportions vary from 5.8% (Condabri MB9-H) to 75.7% (Chinchilla 4). Freshwater algae comprise between 0.7% (Roma 8) and 5.3% (Roma 8). Finally, marine indicators were as high as 1.0% in Kenya East GW7. No fungi grains were counted.

5. Discussion

5.1 The Palynological Signal of Coastal Systems

Our dataset is consistent with the sporomorph ecogroup model proposed by Abbink et al. (2004), especially in the context of the other sedimentological and ichnological observations. In that framework, pollen such as *Corollina* / *Classopollis* represent flora (Cheirolepidiaceae) that inhabit salt marshes and mangroves at the transition from land to sea (Batten and MacLellan, 1984; Stukins et al., 2013; Galloway et al., 2015). Similarly our analysis would suggest that the pollen *Callialasporites* (Harris, 1979; Vakhrameev, 1991)*, Araucariacidites* (Grant-Mackie et al., 2000; Barron et al., 2006)*,* and the spores *Denisporites (Couper, 1958;*

Retallack, 1975, 1997), and *Retitriletes* (Balme, 1995) have a coastal to marginal marine affinity. It should be noted that previous workers interpreted a fully terrestrial depositional setting for the palynomorphs from the Precipice Sandstone and Evergreen Formation, and therefore our interpretation is not agreed upon by everyone (Ziolkowski et al., 2014).

Although the large proportion of coastal pollen and spores throughout the Precipice–Evergreen succession supports a nearshore depositional interpretation, the suite does not directly indicate marine influence *sensu stricto*. However, agglutinated foraminifera reported by Martin et al. (2018) supports the interpretation. There are a few possible mechanisms to explain the lack of dinocysts, acritarchs, and copepoda within Sequence 1 and Sequence 2. The first is flushing of the palynomorphs due to abundant freshwater run-off from distributary channels (Hardy and Wrenn, 2009). A second explanation is low preservation potential due to distributary channels cannibalizing marine influenced facies as they migrate across a low-accommodation delta plain. This problem remains unresolved, however, and is a potential area of future research. Finally, marine influence on deposition of Sequence 3 is clearly illustrated by the dominance of coastal pollen and spores and the small proportion of marine palynomorphs.

5.2 Facies Evolution and Depositional Model

Differences in the distribution of facies occur both across the basin and up stratigraphic section through the Precipice–Evergreen succession. The facies evolution displays differences related to along-strike variation as well as proximal to distal relationships. The basin axis occurs along the Mimosa Syncline (Fig. 1) and contains the thickest and most complete succession, recorded in wells such as West Wandoan 1 and Woleebee Creek (Table 1). Towards the basin margins, the succession is thinner, and in some cases the basal part is missing. Wells such as Roma 8, Moonie 31, and Moonie 34 show this relationship (Table 1). However, the same general stratigraphic evolution is observed in all ten wells with each well recording different proximal to distal positions within the basin. Broadly speaking, from proximal to distal we rank the wells: Roma 8 (Fig. 12), Moonie 31 (Fig. 13), Moonie 34 (Fig. 14), Chinchilla 4 (Fig. 15), Condabri MB9-H (Fig. 16), Kenya East GW7 (Fig. 17), Taroom 17 (Fig. 18), Reedy Creek MB3-H (Fig. 19), West Wandoan 1 (Fig. 20), and Woleebee Creek GW4 (Fig. 21). We describe the evolution of sedimentary facies in the context of the sequence stratigraphy and display block models showing the major depositional environments and their stratal stacking relationships (Figs. 22–24). Notably, we make no attempt to show the specific geographic distribution of facies; the diagrams are conceptual and intended to show the broad-scale arrangement of depositional environments through time.

5.2.1 Lowstand Systems Tract 1 (J10–TS1)

The base of the Precipice Sandstone is manifest as a sharp, erosive contact overlain by coarse-grained structureless to planar-tabular cross-bedded sandstone (F3) containing rip up clasts (F2) and pebble lags (F1). The entire lowstand systems tract consists of a series of amalgamated (aggradational) small-scale (i.e., 2–6 m thick) fining-upward packages. The succession is thicker and cleaner in terms of mudstone content in West Wandoan 1 (Fig. 20) and Woleebee Creek (Fig. 21), along the axis of the basin. Towards the basin margins the proportion of mudstone interbeds increases slightly, such as in Chinchilla 4 (Fig. 15) and Taroom 17 (Fig. 18). The basal part of the succession is missing in Roma 8 (Fig. 12) which is located near the edge of the basin, as well as in Moonie 31 (Fig. 13) and Moonie 34 (Fig. 14). Up section, facies transition to finer grained sandstone (F4–5) with increasing proportions of mudstone, coal, and heterolithics (F6–11). We interpret this to reflect progressive infilling of basin topography through time, where the basin centre was situated within the middle of a braidplain (FA1) and the basin margins underwent periodic deposition within a lower delta plain (FA2) and subaqueous delta (FA3) (Fig. 22A). Palynological content, which consists primarily of subequal proportions of continental pollen and spores and coastal pollen and spores suggests that the braidplain was situated in the upper delta plain.

5.2.2 Transgressive Systems Tract 1 (TS1–MFS1)

The transgressive systems tract is characterized by an overall fining-upward succession (Fig. 22B). Along the axis of the basin, at West Wandoan 1 (Fig. 20) and Woleebee Creek GW4 (Fig. 21) the interval displays a series of small-scale fining-upward packages consisting of cross-bedded sandstones (F4) that transition into heterolithic strata (F9–11). Towards the basin margins, near Chinchilla 4 (Fig. 15) and Taroom 17 (Fig. 18), the succession comprises cross-bedded (F4) and planar parallel laminated (F5) sandstones passing gradationally upward into carbonaceous mudstones (F6) and coal (F7). Bioturbated sandy mudstone and muddy sandstone (F8) occurs sporadically distributed through both successions. All wells across the basin become progressively muddier towards their top. The stratigraphic architecture and facies transitions are taken to represent retrogradational facies stacking. Along the basin axis depositional environments transition from distal lower delta plain (FA2) into the subaqueous delta (FA3). Further up depositional dip, away from the basin centre, lower delta plain (FA2) strata dominate, but with a gradual transition to proximal delta front packages (FA3) recorded. Variations between facies patterns in the most closely spaced wells reflect along-strike variation in environments. A sub-equal mixture of continental spore-pollen and coastal spore-pollen suggests deposition consistently occurred in proximity to a marine basin, and the bioturbate textures in FA2 and FA3 support this notion.

5.2.3 Highstand Systems Tract 1 (MFS1–SB2)

Highstand Systems Tract 1 displays a coarsening-upward succession that consists of smaller-scale coarsening- and fining-upward packages (Fig. 22C). Generally, the highstand systems tract is thin (approximately 10–20 m), and is characterized by heterolithic strata (F10–11) overlain by cross-bedded (F4) and combined-flow ripple laminated (F9) sandstones. Towards the basin margins – up depositional dip – facies packages consist of carbonaceous mudstones (F6) and coals (F7) overlying cross-bedded (F4) and planar parallel laminated (F5) sandstone. In wells such as Chinchilla 4, the highstand is composed of moderate to highly bioturbated heterolithics showing alternations in current direction (F14). The facies evolution is interpreted to reflect progradational tacking patterns. In distal depositional positions progradation is manifest as lower delta plain (FA2) strata building outwards atop the subaqueous delta (FA3). In more proximal locations (Roma 8, Moonie 31 and 34), progradational motifs are poorly expressed and difficult to differentiate from autogenic shifts in environments. However, along-strike variation in deposition is clearly evident through the shift from lower delta plain (FA2) to tidally influenced shoreline (FA5) strata, which are recorded between wells displaying the same proximal-distal relationship (i.e., Chinchilla 4 versus Taroom 17). A mixture of continental spore-pollen and coastal spore-pollen suggests there was subtle marine influence on deposition, further evidence of which is manifest in the recurrence of marine trace fossils in FA2–FA6.

5.2.4 Sequence 2 (SB2–J20)

Sequence 2 rests atop a sharp, and sometimes erosive interface at the top of highstand deposits in Sequence 1. The sequence is thin (25–60 m) suggesting limited accommodation space (Wang et al., 2019). At the basin centre, near Woleebee Creek GW4 (Fig. 21), stacked cross-bedded sandstones (F4) give way to muddy (F11) and heterolithic (F9 and F10) strata with coarsening-upward characteristics. Packages are initially mud prone, becoming sand-dominated gradually up section (Fig. 21). Further up depositional dip, the sections in Chinchilla 4 (Fig. 15) and Taroom 17 (Fig. 17) have thicker sandstone successions at their base (Fig. 22A) and become muddier upward but to a lesser extent (Fig. 22B, C). Finally, in the most proximal positions, such as Roma 8 (Fig. 12), the succession primarily consists of cross-bedded sandstones (F4) alternating with bioturbated muddy sandstone (F8) and combined-flow ripple laminated sandstone (F9) with a subtle fining-upward character. Together the stratigraphic stacking and facies evolution suggest the full succession from lowstand through transgression to highstand are recorded in Sequence 2. Marine influenced on deposition is indicated by the presence of substantial proportions of coastal spores and pollen, in concert with bioturbation by marine organisms.

5.2.5 Lowstand Systems Tract 3 (J20–TS3)

The lowstand systems tract in Sequence 3, otherwise known as the Boxvale Sandstone Member (Fig. 2), is marked by an abrupt lithological change from the underlying mudstone across the J20 unconformity . Along the axis of the Mimosa Syncline in West Wandoan 1 (Fig. 20) and Woleebee Creek (Fig. 21), the lowstand is characterized by amalgamated cross-bedded (F4) or combined-flow ripple laminated sandstone (F5). The lowstand systems tract thins towards the basin margins where it is composed of cross-bedded sandstone (F4), such as in Taroom 17 (Fig. 18). Up stratigraphic section the strata shift towards heterolithic deposits (F10) in most wells. Distributary channel and mouthbar sandstone deposits display aggradational stacking patterns representing the lower delta plain (FA2) and proximal subaqueous delta facies (FA3), respectively (Fig. 24A). The large spacing between wells is too great to resolve the detail of along-strike variation in facies. However, the c presence of coastal spores and coastal pollen indicate a persistently marine-influenced depositional setting through large portions of the basin. However, very little bioturbation is observed in this interval to aid in the interpretation.

5.2.6 Transgressive Systems Tract 3 (TS3–MFS3)

Transgressive Systems Tract 3 displays an overall fining-upward succession (Fig. 24B) and is also known as the Westgrove Ironstone Member (Fig. 2). In the basin centre, near West Wandoan 1 (Fig. 20) and Woleebee Creek GW4 (Fig. 21), the succession displays small-scale fining-upward packages consisting of combined-flow ripple laminated sandstone (F9) passing upward into heterolithic sandstone and mudstone (F10–11). Interbedded layers of oolitic ironstone (F15) define individual fining-upward packages. In Roma 8 (Fig. 12) at the basin margin, the transgressive systems tract consists of alternations between cross-bedded sandstone (F4), combined-flow ripple laminated sandstone (F9), and heterolithic sandstone and mudstone (F10–11) with interspersed oolitic ironstone (F15). Up stratigraphic section, all cored intervals become progressively muddier, with fewer sandstone layers. In the context of the stratigraphy, and considering the vertical and lateral distribution of facies, the succession displays a retrogradational facies stacking pattern interpreted to be associated with relative sea level rise. Along the basin axis subaqueous delta (FA3) facies are interbedded with restricted marine shoals (FA6). Further up depositional dip and away from the basin centre, proximal subaqueous delta (FA3) to distal lower delta plain (FA2) facies dominate. Along-strike variation is demonstrated in the shift from lower delta plain (FA2) strata in Reedy Creek MB3-H (Fig. 19) to delta-influenced shoreface packages (FA5) in Condabri MB9-H (Fig. 16) and Kenya East GW7 (Fig. 17) at approximately the same stratigraphic level. A low proportion of marine palynomorphs, including dinocysts, acritarchs, and copepod fragments, as well as ichnological assemblages composed of marine trace fossils are a strong indication of significant marine influenced deposition.

To explain the mechanisms for iron enrichment and the formation of widespread oolitic ironstone, we propose that it was due to slight wave and / or tide agitation in a geographically restricted marine setting. It is most likely that the physical restriction was a topographic low or trough on the sea floor that prevented mixing of water (Hallam and Bradshaw, 1979; Turner et al., 2009). It is possible that humic acid assisted in liberating iron from clay minerals that were later precipitated to form ironstone (Tombacz et al., 2004). A potential contributor may have been microbes, acting to reduce the iron from clays (Liu et al., 2017). Minor paralic lakes and bays might also have been conducive depositional settings to accumulate ironstone, being in connection to the basin and sharing similar chemistry (Veevers and Wells, 1959; Gibson et al., 1994).

5.2.7 Highstand Systems Tract 3 (MFS3–J30)

Finally, Highstand Systems Tract 3 is characterized by a coarsening-upward succession (Fig. 24C) comprising a series of meter-scale coarsening-upward packages that become thicker up section. The highstand at the basin-centre, near West Wandoan 1 (Fig. 20) and Woleebee Creek (Fig. 21), is manifest as stacked combined-flow ripple laminated (F9) to heterolithic sandstone and mudstone (F10–11) packages. At more proximal positions near the basin margins, the succession is very similar but contains a few cross-bedded sandstone layers (F4) or tidal heterolithic sandstone and mudstone (F14). Chinchilla 4 demonstrates these facies relationships (Fig. 15). The progradational stratal stacking patterns in concert with the types of facies observed, leads to the interpretation that the basin was predominantly occupied by subaqueous deltas (FA3) at the basin centre, and in more proximal positions was characterized by lower delta plain (FA2) and tidal shoreline (FA5) environments. Along-strike variation in deposition is not conspicuous at this stratigraphic level, probably due to the wide spacing between cores. Low proportions of dinocysts, acritarchs, and copepod fragments shows quite clearly that marine influence was steadily increasing up-section. The most diverse assemblages of marine traces also occur in this stratigraphic interval.

5.3 Implications for the Paleogeography of Eastern Australia

Relatively few paleogeographic maps of eastern Australia have been published, and existing interpretations of the Lower Jurassic Series – corresponding to the Precipice Sandstone and lower Evergreen Formation – show an eastern Australia dominated by “fluvial”, “lacustrine”, and “fluvial-lacustrine” depositional conditions (e.g., Bradshaw and Yeung, 1990; Struckmeyer and Totterdell, 1990; Bradshaw and Yeung, 1992). Notably, the outcrop belt and northern Surat Basin region have been re-interpreted as fluvio-deltaic systems with paleo-flow directions to the east of the Surat Basin (Bianchi et al., 2018b). Our results bolster those of Bianchi et al. (2018b), and extend the interpretation of nearshore to shallow marine deposition across all of the northern and central Surat Basin. This suggests that the paleogeography of all Mesozoic basins of eastern Australia needs to be re-considered, especially in light of the increasing sedimentological (Bianchi et al., 2018a; Bianchi et al., 2018b; Martin et al., 2018) and stratigraphic evidence (Wang et al., 2019) of relative sea-level control on deposition.

5.4 Impact on Reservoir Characterization and Modelling

The work presented in this paper suggests that reservoir models of the Precipice–Evergreen interval should be constructed of flow units that are controlled by geobody geometries consistent with coastal to shallow marine depositional systems (Bianchi et al., 2018a). Geometric constraints on geobody size and distribution can be distilled from studies of distributary channels (Bridge and Tye, 2000; Gibling, 2006), interdistributary bays (Elliott, 1974), mouthbars (Bhattacharya, 2006), and delta lobes (Howell et al., 2008; Enge et al., 2010). The differentiation of nearshore and shallow marine facies and environments (e.g., Miall, 1985; Jorgensen and Fielding, 1996; Lang et al., 2000) means that more accurate and geologically-realistic facies models can be constructed and used to parameterize flow units. This is especially applicable to the Transgressive Systems Tract 1 through to Sequence 2 interval where previous interpretations have potentially overpredicted the lateral extent and connectivity of sandstone bodies

In addition to the reservoir modelling implications, facies interpretation also affects the ways in which reservoir characteristics are mapped and predicted. For example, siderite cements within sandstones might have different occurrence patterns given fluvial (Gibson et al., 1994; Al-Agha et al., 1995) *versus* nearshore and shallow marine depositional interpretations (Machemer and Hutcheon, 1988; Mozley, 1989; Pye et al., 1990; Huggett et al., 2000). Differences in bioturbate textures that are genetically related to the sedimentary environment would also be expected to impact the distribution of porosity and permeability (Pemberton and Gingras, 2005; Gingras et al., 2012; La Croix et al., 2013; La Croix et al., 2017).

6. Conclusions

The integration of sedimentological, ichnological, and palynological observations from core has yielded an improved view of the facies characteristics and paleodepositional environments of the Precipice Sandstone and Evergreen Formation. The major conclusions that can be drawn from this facies analysis are:

1) The succession consists of fifteen recurring facies that were observed in ten cores across the north and central portions of the Surat Basin.
2) Facies are arranged into 6 distinct associations representing braidplain, lower delta plain, subaqueous delta, delta-influenced shoreface, tidally influenced shoreline, and restricted marine shoal environments. These associations are interpreted to occur within the context of a large-scale fluvio-deltaic system that occupied the basin.
3) Using a sporomorph ecogroup model to interpret the palynology showed that there is a significant component of coastal pollen and coastal spores which independently support the facies interpretations from sedimentology and ichnology.
4) Increasing marine influence on deposition through time is supported by increased, yet minor proportion of dinocysts, acritarchs, and copepod fragments up-section. Sedimentological and ichnological characteristics suggest increasing marine influence as well.

Our results indicate that the paleogeography of eastern Australia during the Jurassic should be reconsidered to incorporate a greater degree of marine influence – similar deposits might exist in the neighboring Eromanga and Clarence-Moreton Basins. Finally, the updated view of depositional environments has important implications for reservoir characterization and modelling for CO_2 storage; geobody distribution, orientation, and dimensions should utilize nearshore to shallow marine concepts to produce the most geologically-realistic static reservoir models.

7. Acknowledgements

We thank the Australian Government, through the CCS RD&D Programme, ACA Low Emissions Technology (ACALET), and the University of Queensland for financial support of this project. The DNRM Exploration Data Centre staff in Zillmere, Queensland, were helpful in providing access to core data. We also thank APLNG, CTSCo, Origin Energy, and QGC for data access. AppleCore software from Mike Ranger was utilized in drafting lithologs. Discussions with Mike Martin, Mark Reilly, Andrew Garnett, Sebastian Gonzalez, Jochen Kassan, and John McKellar helped focus the scope and develop ideas. Finally, we thank Associate Editor Luis Buatois, Fiona Burns, and an anonymous reviewer for constructive feedback to improve the quality of the manuscript

8. References

Abbink, O.A., 1998. Palynological Investigations in the Jurassic of the North Sea Region: Palynologisch Onderzoek in de Jura Van Het Noordzeegebied. Univ.

Abbink, O.A., Cittert, V.K.-V., Visscher, H., 2004. A sporomorph ecogroup model for the Northwest European Jurassic - Lower Cretaceous: concepts and framework. Netherlands Journal of Geosciences 83, 17-38.

Agency, I.E., 2008. Energy technology perspectives, Paris, France.

Ainsworth, R.B., 2005. Sequence stratigraphic-based analysis of depositional architecture-a case study from a marginal marine depositional setting. Petroleum Geoscience 11, 257-276.

Ainsworth, R.B., Hasiotis, S.T., Amos, K.J., Krapf, C.B.E., Payenberg, T.H.D., Sandstrom, M.L., Vakarelov, B.K., Lang, S.C., 2012. Tidal signatures in an intracratonic playa lake. Geology 40, 607-610.

Ainsworth, R.B., Vakarelov, B.K., Nanson, R.A., 2011. Dynamic spatial and temporal prediction of changes in depositional processes on clastic shorelines: towards improved subsurface uncertainty reduction and management. American Association of Petroleum Geologists Bulletin.

Al-Agha, M.R., Burley, S.D., Curtis, C.D., Esson, J., 1995. Complex cementation textures and authigenic mineral assemblages in Recent concretions from the Lincolnshire Wash (east coast, UK) drive by Fe(0) to Fe(II) oxidation. Journal of the Geological Society of London 152, 157-171.

Allen, J.R.L., 1978. Studies in fluviatile sedimentation; an exploratory quantitative model for the architecture of avulsion-controlled alluvial sites. Sedimentary Geology 21, 129-147.

Balme, B.E., 1995. Fossil in situ spores and pollen grains: An annotated catalogue. Review of Palaeobotany and Palynology 87, 81-323.

Baniak, G.M., La Croix, A.D., Polo, C.A., Playter, T.L., Pemberton, S.G., Gingras, M.K., 2014. Associating x-ray microtomography with permeability contrasts in bioturbated media. Ichnos 21, 234-250.

Barron, E., Gomez, J.J., Goy, A., Pieren, A.P., 2006. The Triassic–Jurassic boundary in Asturias (northern Spain): Palynological characterisation and facies. Review of Palaeobotany and Palynology 138, 187-208.

Batten, D.J., MacLellan, A.M., 1984. The paleoenvironmental significance of the conifer family Cheirolepidiaceae in the Cretaceous of Portugal, in: Reif, W., Westphal, F. (Eds.), Symposium on Mesozoic Terrestrial Ecosystems. Tubigen University Press, Tubingen, Germay, pp. 7-12.

Beeston, J.W., 1979. Field conference: Taroom-Wandoan-Millmerran. Geological Society of Australia, Queensland Division, p. 47.

Bhattacharya, J.P., 2006. Deltas, in: Posamentier, H.W., Walker, R.G. (Eds.), Facies Models Revisited. SEPM (Sociey for Sedimentary Geology), Tulsa, pp. 237-292.

Bhattacharya, J.P., MacEachern, J.A., 2009. Hyperpycnal rivers and prodeltaic shelves in the Cretaceous seaway of North America. Journal of Sedimentary Research 79, 184-209.

Bianchi, V., Pistellato, D., Zhou, F., Boccardo, S., Esterle, J., 2018a. Outcrop analogue models of the Precipice Sandstone, ANLEC Final Reports. ANLEC, Brisbane, Queensland, p. 69.

Bianchi, V., Zhou, F., Pistellato, D., Martin, M., Boccardo, S., Esterle, J., 2018b. Mapping a coastal transition in braided systems: an example from the Precipice Sandstone, Surat Basin. Australian Journal of Earth Sciences 65, 483-502.

Bradshaw, B.E., Spencer, L.K., Lahtinen, A.-L., Khider, K., Ryan, D.J., Colwell, J.B., Chirinos, A., Bradshaw, J., Draper, J.J., Hodgkinson, J., McKillop, M., 2011. An assessment of Queensland's CO2 geological storage prospectivity – the Queensland CO2 Geological Storage Atlas. Energy Procedia 4, 4583-4590.

Bradshaw, M., Yeung, M., 1990. The Jurassic Palaeogeography of Australia. Bureau of Mineral Resources, Geology and Geophysics, p. 60.

Bradshaw, M., Yeung, M., 1992. Palaeogeographic Atlas of Australia. Bureau of Mineral Resources, Canberra, ACT.

Bridge, J.S., Tye, R.S., 2000. Interpreting the dimensions of ancient fluvial channel bars, channels, and channel belts from wireline-logs and cores. AAPG Bulletin 84, 1205-1228.

Burton, D., Wood, L.J., 2013. Geologically-based permeability anisotropy estimates for tidally-influenced reservoirs using quantitative shale data. Petroleum Geoscience 19, 3-20.

Cosgrove, J.L., Mogg, W.G., 1985. Recent exploration and hydrocarbon potential of the Roma Shelf, Queensland. Australian Petroleum Exploration Association (APEA) Journal 25, 216-234.

Couper, R.A., 1958. British Mesozoic microspores and pollen grains. A systematic and stratigraphic study. Palaeontographica Abteilung B 103, 75-179.

Cranfield, L.C., Carmichael, B.C., Wells, A.T., 1994. Ferruginous oolite and associated lithofacies from the Clarence-Moreton and related basins in southeast Queensland, in: Wells, A.T., O'Brien, R.E. (Eds.), Geology and petroleum poetential of the Clarence-Moreton Basin, New South Wales and Queensland. Australian Geological Survey Organisation, pp. 144-163.

Dashtgard, S.E., 2011. Neoichnology of the lower delta plain: Fraser River Delta, British Columbia, Canada: Implications for the ichnology of deltas. Palaeogeography, Palaeoclimatology, Palaeoecology 307, 98-108.

de Jersey, N.J., 1965. Plant microfossils in some crude oil samples. Geological Survey of Queensland, p. 9.

de Jersey, N.J., Dearne, D.W., 1964. Palynological report on samples from Cabawin No.1 well. Appendix 1-6. Bureau of Mineral Resources, Australia, Queensland, pp. 53-78.

de Jersey, N.J., McKellar, J.L., 2013. The palynology of the Triassic-Jurassic transition in southeastern Queensland, Australia, and correlation with New Zealand. Palynology 37.

de Jersey, N.J., Paten, R.J., 1964a. Jurassic spores and pollen grains from the Surat Basin. Geological Survey of Queensland, p. 18.

de Jersey, N.J., Paten, R.J., 1964b. Palynology of samples from Union-Kern-A.O.G. Moonie Nos. 1 and 3 wells. Appendix 2. Bureau of Mineral Resources, Australia, Queensland, pp. 29-055.

Dickins, J.M., Malone, E.J., 1973. Geology of the Bowen Basin, Queensland, Bulletin. Bureau of Mineral Resources, Geology and Geophysics, Canberra, Australia, p. 154.

Elliott, T., 1974. Interdistributary bay sequences and their genesis. Sedimentology 21, 611-622.

Enge, H.D., Howell, J.A., Buckley, S.J., 2010. Quantifying clinothem geometry in a forced-regressive river-dominated delta, Panther Tongue Member, Utah, USA. Sedimentology 57, 1750-1770.

Evans, P.R., 1962. Microfossils association with the “Bundamba Group” of the Surat Bain, Queensalnd. Department of National Development, Bureau of Mineral Resources Geology and Geophysics, Canberta, ACT, p. 115.

Evans, P.R., 1966. Mesozoic stratigraphic palynology in Australia. Australian Oil and Gas Journal 12, 58-63.

Exon, N.F., 1976. Geology of the Surat Basin in Queensland. Bureau of Mineral Resources, Geology and Geophysics, Canberra, Australia, p. 160.

Exon, N.F., Burger, D., 1981. Sedimentary cycles in the Surat Basin and global changes in sea level. BMR Journal of Australian Geology and Geophysics 6, 153-159.

Exon, N.F., Senior, B.R., 1976. The Cretaceous of the Eromanga and Surat basins. BMR Journal of Australian Geology and Geophysics 1, 33-50.

Fielding, C.R., 1989. Hummocky cross-stratification from the Boxvale Sandstone Member in the northern Surat Basin, Queensland. Australian Journal of Earth Sciences 36, 469-471.

Fielding, C.R., 1990. Reply to discussion: Hummocky cross-stratification from the Boxvale Sandstone Member in the northern Surat Basin, Queensland. Australian Journal of Earth Sciences 37, 379-380.

Fielding, C.R., 1996. Mesozoic sedimentary basins and resources in eastern Australia – a review of current understanding, Mesozoic Geology of the Eastern Australia Plate Conference. Geological Society of Australia, Brisbane, Queensland, pp. 180-185.

Fielding, C.R., Gray, A.R.G., Harris, G.I., Saloman, J.A., 1990. The Bowen Basin and overlying Surat Basin, in: Finlayson, D.M. (Ed.), The Eromanga–Brisbane Geoscience Transect: A Guide to Basin Development Across Phanerozoic Australia in Southern Queensland. Australian Government Publishing Service, Canberra, ACT.

Gallagher, K., 1990. Permian-Cretaceous subsidence history along the Eromanga Brisbane geoscience transect, in: Finlayson, D.M. (Ed.), The Eromanga Brisbane Geoscience Transect: a Guide to Basin Development Across Phanerozoic Australia in Southern Queensland. Bureau of Mineral Resources, Canberra, ACT, pp. 133-151.

Gallagher, K., Dumitru, T.A., Gleadow, A.J.W., 1994. Constraints on the vertical motion of eastern Australia during the Mesozoic. Basin Research 6, 77-94.

Galloway, J.M., Tullius, D.N., Evenchick, C.A., Swindles, G.T., Hadlari, T., Ambry, A., 2015. Early Cretaceous vegetation and climate change at high latitude: Palynological evidence from Isachsen Formation, Arctic Canada. Cretaceous Research 56, 399-420.

Garnett, A.J., Greig, C.R., Oettinger, M., 2014. ZeroGen IGCC with CCS: a case history. The University of Queensland, Brisbane, Australia, p. 483.

Gibling, M.R., 2006. Width and thickness of fluvial channel bodies and valley fills in the geological record: a literature compilation and classification. Journal of Sedimentary Research 76, 731-770.

Gibson, P.J., Shaw, H.F., Spiro, B., 1994. The nature and origin of sideritic ironstone bands in the Tertiary Lowmead and Duaringa Basins, Queensland. Australian Journal of Earth Sciences 41, 255-263.

Gingras, M.K., Baniak, G.M., Gordon, J., Hovikowski, J., Konhauser, K.O., La Croix, A.D., Lemiski, R.T., Mendoza, C.A., Pemberton, S.G., Polo, C., Zonneveld, J.P., 2012. Porosity and permeability in bioturbated sediments, in: Knaust, D., Bromley, R.G. (Eds.), Trace Fossils as Indicators of Sedimentary Environments. Elsevier, pp. 837-868.

Grant-Mackie, J.A., Aita, Y., Balme, B.E., Campbell, H., Crallinor, A.B., MacFarlane, D.A.B., Thulborn, R.A., 2000. Jurassic paleobiogeography of Australiasia. Memoir of the Australasian Association of Palaeontologists 23, 311-353.

Gray, A.R.G., 1968. Stratigraphic drilling the Surat and Bowen basins, 1965-1966. Queensland Geological Survey, p. 34.

Green, P.M., Hoffmann, K.L., Brain, T.J., Gray, A.R.G., 1997. The Surat and Bowen Basins, south-east Queensland, Queensland Minerals and Energy Review Series. Queensland Department of Mines and Energy, Brisbane, Queensland, p. 244.

Hallam, A., Bradshaw, M.J., 1979. Bituminous shales and oolitic ironstones as indicators of transgressions and regressions. Journal of the Geological Society of London 136, 157-164.

Haq, B.U., Hardenbol, J., Vail, P.R., 1987. Chronology of fluctuating sea levels since the Triassic. Science 235, 1156-1167.

Harding, A., Strebelle, S., Levy, M., Thorne, J., Xie, D., Leigh, S., Preece, R., Scamman, R., 2005. Reservoir Facies Modelling: New Advances in MPS, in: Leuangthong, O., Deutsch, C.V. (Eds.), Geostatistics Banff 2004. Springer Netherlands, Dordrecht, pp. 559-568.

Hardy, M.J., Wrenn, J.H., 2009. Palynomorph distribution in modern tropical deltaic and shelf sediments - Mahakam Delta, Borneo, Indonesia. Palynology 33, 19-42.

Harris, T.M., 1979. The Yorkshire Jurassic flora, V. Coniferales. British Museum of Natural History, London.

He, J., La Croix, A.D., Wang, J., Ding, W., Underschultz, J.R., 2019. Using neural networks and the Markov Chain approach for facies analysis and prediction from well logs in the Precipice Sandstone and Evergreen Formation, Surat Basin, Australia. Marine and Petroleum Geology 101, 410-427.

Hodgkinson, J., Grigorescu, M., 2013. Background research for selection of potential geostorage targets – case studies from the Surat Basin, Queensland. Australian Journal of Earth Sciences 60, 71-89.

Hoffmann, K.L., Totterdell, J.M., Dixon, O., Simpson, G.A., Brakel, A.T., Wells, A.T., Mckellar, J.L., 2009. Sequence stratigraphy of Jurassic strata in the lower Surat Basin succession, Queensland. Australian Journal of Earth Sciences 56, 461-476.

Howell, J.A., Skorstad, A., MacDonald, A., Fordham, A., Flint, S., Fjellvoll, B., Manzocchi, 2008. Sedimentological parameterization of shallow-marine reservoirs. Petroleum Geoscience 14, 17-34.

Huggett, J., Dennis, P., Gale, A., 2000. Geochemistry of early siderite cements from the eocene succession of Whitecliff Bay, Hamshire Basin, U.K. Journal of Sedimentary Research 70, 1107-1117.

Jorgensen, P.J., Fielding, C.R., 1996. Facies architecture of alluvial floodbasin deposits: three dimensional data from the Upper Triassic Callide Coal Measures of east-central Queensland, Australia. Sedimentology 43, 479-495.

Korsch, R.J., O'Brien, P.E., Sexton, M.J., Wake-Dyster, K.D., Wells, A.T., 1989. Development of Mesozoic transtensional basins in easternmost Australia. Australian Journal of Earth Sciences 36, 13-28.

Korsch, R.J., Totterdell, J.M., 2009. Subsidence history and basin phases of the Bowen, Gunnedah and Surat Basins, eastern Australia. Australian Journal of Earth Sciences 56, 335-353.

La Croix, A.D., Gingras, M.K., Pemberton, S.G., Mendoza, C.A., MacEachern, J.A., Lemiski, R.T., 2013. Biogenically enhanced reservoir properties in the Medicine Hat gas field, Alberta, Canada. Marine and Petroleum Geology 43, 464-477.

La Croix, A.D., MacEachern, J.A., Ayranci, K., Hsieh, A., Dashtgard, S.E., 2017. An ichnological-assemblage approach to reservoir heterogeneity assessment in bioturbated strata: Insights from the Lower Cretaceous Viking Formation, Alberta, Canada. Marine and Petroleum Geology 86, 636-654.

Lang, S.C., Kassan, J., Benson, J.M., Grasso, C.A., Avenell, L.C., 2000. Applications of modern and ancient geological analogues in characterization of fluvial and fluvial-lacustrine deltaic reservoirs in the Copper Basin. APPEA Journal 40, 393-416.

Liu, G., Qiu, S., Liu, B., Pu, Y., Gao, Z., Wang, J., Jin, R., Zhou, J., 2017. Microbial reduction of Fe(III)-bearing clay minerals in the presence of humic acids. Scientific Reports 7, 1-9.

MacEachern, J.A., Bann, K.L., Bhattacharya, J.P., Howell, C.D.J., 2005. Ichnology of deltas: Organism responses to the dynamic interplay of rivers, waves, storms, and tides, in: Giosan, L., Bhattacharya, J.P. (Eds.), River Deltas - Concepts, Models, and Examples. SEPM Society for Sedimentary Geology, Tulsa, USA, pp. 49-85.

MacEachern, J.A., Pemberton, S.G., Bann, K.L., Gingras, M.K., 2007. Departures from the Archetypal Ichnofacies: Effective Recognition of Physico-Chemical Stresses in the Rock Record, in: MacEachern, J.A., Bann, K.L., Gingras, M.K., Pemberton, S.G. (Eds.), Applied Ichnology. SEPM, Tulsa, USA, pp. 65-93.

Machemer, S.D., Hutcheon, I., 1988. Geochemistry of early carbonate cements in the Cardium Formation, central Alberta. Journal of Sedimentary Petrology 58, 136-147.

Martin, K.R., 1981. Deposition of the Precipice Sandstone and the evolution of the Surat Basin in the Early Jurassic. The APPEA Journal 21, 16-23.

Martin, M.A., Wakefield, M., Bianchi, V., Esterle, J., Zhou, F., 2018. Evidence for marine influence in the Lower Jurassic Precipice Sandstone, Surat Basin, eastern Australia. Australian Journal of Earth Sciences 65, 75-91.

McKellar, J.K., 1974. Jurassic miospores from the upper Evergreen Formation, Hutton Sandstone, and basal Injune Creek Group, north-eastern Surat Basin. Geological Survey of Queensland, Queensland, p. 89.

McKellar, J.K., 1998. Late Early to Late Jurassic palynology, biostratigraphy and palaeogeography of the Roma Shelf area, northwestern Surat Basin, Queensland, Australia, Department of Earth Sciences. University of Queensland, Brisbane, Queensland, p. 620.

Metz, B., Davidson, O., de Coninck, H., Loos, M., Meyer, L., 2005. IPCC special report on carbon dioxide capture and storage, New York, NY.

Miall, A.D., 1977. A review of the braided-river depositional environment. Earth-Science Reviews 13, 1-62.

Miall, A.D., 1985. Archtectural-element analysis: a new method of facies analysis applied to fluvial deposits. Earth-Science Reviews 22, 261-308.

Mikes, D., Geel, C.R., 2006. Standard facies models to incorporate all heterogeneity levels in a reservoir model. Marine and Petroleum Geology 23, 943-959.

Mollan, R.G., Dickins, J.M., Kirkegaard, A.G., Exon, N.F., 1969. Geology of the Springsure 1:250,000 sheet area, Queensland. Bureau of Mineral Resources, Geologic Survey of Queensland, p. 138.

Mollan, R.G., Forbes, V.R., Jensen, A.R., Exon, N.F., Gregory, C.M., 1972. Geology of the Eddystone, Taroom and western part of the Munduberra Sheet areas, Queensland. Bureau of Mineral Resources, Geology and Geophysics, Australia.

Mozley, P.S., 1989. Relation between depositional environment and the elemental composition of early diagenetic siderite. Geology 17, 704-706.

Neele, F., Vanderwijer, V., Mayyan, H., Sharma, S.R.K., Kamal, D., 2017. Options for CO2 sequestration in Kuwait. Energy Procedia 114, 2827-2835.

Olariu, C., Bhattacharya, J.P., 2006. Terminal distributary channels and delta front architecture of river-dominated delta systems. Journal of Sedimentary Research 76, 212-233.

Paten, R.J., 1967. Microfloral distribution in the Lower Jurassic Evergreen Formation of the Boxvale area, Surat Basin, Queensland. Queensland Government Mining Journal 68, 345-349.

Pemberton, S.G., Gingras, M.K., 2005. Classification and characterizations of biogenically enhanced permeability. American Association of Petroleum Geologists Bulletin 89, 1493-1517.

Power, P.E., Devine, S.B., 1970. Surat Basin, Australia – subsurface stratigraphy, history, and petroleum. American Association of Petroleum Geologists Bulletin 54, 2410-2437.

Price, P.L., 1997. Permian to Jurassic palynostratigraphic nomenclature of the Bowen and Surat bains, in: Green, P.M. (Ed.), The Surat and Bowen Basins, southeast Queensland. Queensland Department of Mines and Enegy, Brisbane, Queensland, pp. 137-178.

Pye, K., Dickson, J.A.D., Schiavon, N., Coleman, M.L., Cox, M., 1990. Formation of siderite–Mg-calcite–iron sulphide concretions in intertidal marsh and sandflat sediments, north Norfolk, England. Sedimentology 37, 325-343.

Raza, A., Hill, K.C., Korsch, R.J., 2009. Mid-Cretaceous uplift and denudation of the Bowen and Surat Basins, eastern Australia: relationship to Tasman Sea rifting from apatite and fission-track and vitrinite-reflectance data. Australian Journal of Earth Sciences 56, 501-531.

Reiser, R.F., Williams, A.J., 1969. Palynology of the Lower Jurassic sediments of the northern Surat Basin, Queensland. Geological Survey of Queensland Brisbane, Queensland, p. 24.

Retallack, G.J., 1975. The life and times of a Triassic lycopod. Alcheringa 1, 3-29.

Retallack, G.J., 1997. Earliest Triassic origin of Isoetes and quillwort adaptive. Journal of Paleontology 71, 35-45.

Ringrose, P.S., Bentley, M., 2015. Reservoir Model Design - a Practictioner's Guide. Springer, Dordrecht Heidelberg New York London.

Savrda, C.E., Blanton-Hooks, A.D., Collier, J.W., Drake, R.A., Graves, R.L., Hall, A.G., Nelson, A.I., Slone, J.C., Williams, D.D., Wood, H.A., 2000. *Taenidium* and associated ichnofossils in fluvial deposits, Cretaceous Tuscaloosa Formation, Eastern Alabama, Southeastern U.S.A. Ichnos 7, 227-242.

Sell, B.H., Brown, L.N., Groves, R.D., 1972. Basal Jurassic sands of the Roma area. Queensland Government Mining Journal 73, 309-321.

Struckmeyer, H.I., Totterdell, J.M., 1990. Australia: Evolution of a continent. Australian Government Publishing Service, Canberra, ACT.

Stukins, S., Jolley, D.W., McIlroy, D., Hartley, A.J., 2013. Middle Jurassic vegetation dynamics from allochthonous palynological assemblages: An example from a marginal marine depositional setting; Lajas Formation, Neuquen Basin, Argentina. Palaeogeography, Palaeoclimatology, Palaeoecology 392, 117-127.

Taylor, A.M., Goldring, R., 1993. Descriptions and analysis of bioturbation and ichnofabric. Journal of the Geological Society (London) 150, 141-148.

Tombacz, E., Libor, Z., Illes, E., Majzik, A., Klumpp, E., 2004. The role of reactive surface sites and complexation by humic acids in the interaction of clay mineral and iron oxide particles. Organic Geochemistry 35, 257-267.

Totterdell, J.M., Moloney, J., Korsch, R.J., Krassay, A.A., 2009. Sequence stratigraphy of the Bowen-Gunnedah and Surat basins in New South Wales. Australian Journal of Earth Sciences 56, 433-459.

Turner, S., Bean, L.B., Dettmann, M., McKellar, J.L., McLoughlin, S., Thulborn, T., 2009. Australian Jurassic sedimentary and fossil successions: current work and future prospects for marine and non-marine correlation. GFF 131, 49-70.

Vakhrameev, V.A., 1991. Jurassic and Cretaceous floras and climates of the Earth. Cambridge University Press, Cambridge.

Veevers, J.J., Jones, J.R., Powell, C.M., 1982. Tectonic framework of Australia's sedimentary basins. Australian Petroleum Exploration Association Journal 22, 283-300.

Veevers, J.J., Wells, A.T., 1959. Pisolitic ironstone deposits, Port Hedland area, Western Australia. Department of National Development, Bureau of Mineral Resources, Geology and Geophysics, p. 10.

Wang, J., La Croix, A.D., Gonzalez, S., He, J., Underschultz, J.R., 2019. Sequence stratigraphic analysis of the Lower Jurassic Precipice and Evergreen Formations in the Surat Basin, Australia: implications for the architecture of reservoirs and seals for CO2 storage. Marine and Petroleum Geology 102, 829-843.

Waschbusch, P., Korsch, R.J., C., B., 2009. Geodynamic modelling of aspects of the Bowen, Gunnedah, Surat and Eromanga Basins from the perspective of convergent margin processes. Australian Journal of Earth Sciences 56, 309-334.

Wells, A.T., Brakel, A.T., Totterdell, J.M., Korsch, R.J., Nicoll, R.S., 1994. Sequence stratigraphic interpretation of seismic data north of 26°S, Bowen and Surat basins, Queensland. Marine, Petroleum, and Sedimentary Resources Division, Canberra, ACT, p. 25.

Worth, K., White, D., Chalaturnyk, R., Sorensen, J., Hawkes, C., Rostron, B., Risk, D., Young, A., Sacuta, N., 2017. Aquistore: Year one - injection, data, results. Energy Procedia 114, 5624-5635.

Yago, J.V.R., Fielding, C.R., 1996. Sedimentology of the Middle Jurassic Walloon Coal Measures in the Great Artesian Basin, eastern Australia, Mesozoic Geology of the Eastern Australia Plate Conference. Geological Society of Australia, Brisbane, Queensland.

Ziolkowski, V., Hodgkinson, J., McKillop, M., Grigorescu, M., McKellar, J.L., 2014. Sequence stratigraphic analysis of the Lower Jurassic succession in the Surat Basin, Queensland - preliminary findings, Queensland Minerals and Energy Review Series. Department of Natural Resources and Mines, Brisbane, Queensland, p. 30.

8. Figure and Table Captions

Table 1 – Core locations and intervals logged as part of this study.

Table 2 – Detailed facies descriptions and interpretations of the nineteen discrete facies observed in the Precipice Sandstone and Evergreen Formation.

Table 3 – List of the palynomorphs encountered during palynological analysis of the Precipice Sandstone and Evergreen Formation.

Table 4 – Summary table of the palynomorph counts for each sample analyzed from the Precipice Sandstone and Evergreen Formation.

Figure 1 – The geographic location and major structural elements of the Surat Basin in eastern Australia. Black dots indicate the location of cored wells that were analyzed in this study. The dashed black line indicates the location of the lines of section displayed in Figure 3.

Figure 2 – Stratigraphic nomenclature of the Lower Jurassic in the Surat Basin. The lithostratigraphy is after McKellar (11998), the sequence stratigraphy is based on Wang et al. (2019), and the global sea level curve is from Haq et al. (1987). The sequence stratigraphy consists of three 3rd order sequences (SQ1–SQ3), and is sub-divided into systems tracts by the sequence boundaries J10, SB2, J20, and J30, the transgressive surfaces TS1 and TS3, and the maximum flooding surfaces MFS1 and MFS3. Notably, SQ2 was not subdivided into systems tracts due to its very thin preservation across the basin; Sequence 2 represents a relatively minor stratal package and no systems tracts were defined within it.

Figure 3 – North-south and west-east oriented cross sections showing the sequence stratigraphic sub-division of the cored wells. See Figure 1 for location of lines of section.

Figure 4 – Core photographs of the facies that comprise Facies Association 1 (FA1) – braidplain. (A) F1, interbedded conglomerate and sandstone from Chinchilla 4, 1063.91 m. (B) F2, mud-clast breccia in Kenya East GW7, 1152.6 m. (C) F3, coarse-grained cross-bedded sandstone from Chinchilla 4, 1219.7 m. (D) Litholog from Chinchilla 4 showing the aggrading, fining-upward sandstone packages that characterizes FA1.

Figure 5 – Core photographs of Facies Association 2 (FA2) – lower delta plain. (A) F4, fine-grained cross-bedded to current ripple laminated sandstone from Woleebee Creek GW4, 1518.5 m. (B) F5, planar parallel laminated sandstone from Woleebee Creek GW4, 1297.25 m. (C) F5, structureless sandstone from Woleebee Creek GW4, 1081.3 m. (D) F6, apparently structureless mudstone from Roma 8, 1076.5 m. (E) F7, coal from Chinchilla 4, 1107.40 m. (F) F8, bioturbated muddy sandstone with juxtaposition of roots (Ro) and *Teichichnus* (Te) from Chinchilla 4, 1003.75 m. (G) Litholog from Condabri MB9-H showing fining-upward channel packages stacked with coarsening-upward interdistributary bay deposits that comprise FA2.

Figure 6 – Core photographs of the constituent facies in Facies Association 3 (FA3) – subaqueous delta. (A) F9, wave-ripple laminated sandstone from Taroom 17, 336.74 m. Note the juxtaposition of roots (Ro) and *Lockeia* (Lo) within the wave ripples (wr). (B) F10, sandstone-dominated heterolithics with *Planolites* (Pl) and synaeresis cracks (syn) from Chinchilla 4, 1026.45 m. (C) F10, mixed sandy and muddy heterolithics with *Planolites* and *Lockeia* from Chinchilla 4, 987.70 m. (D) F11, mudstone-dominated heterolithics with combined flow ripples (cf) and *Planolites* (Pl) from Roma 8, 1006.25 m. (E) Litholog from Woleebee Creek GW4 displaying the coarsening-upward prodelta to delta front and mouthbar succession that is typical of FA3.

Figure 7 – Core photographs of Facies Association 4 (FA4) – shoreface – and its primary facies. (A) F12, bioturbated muddy sandstone with wave-ripple to HCS interbeds from Kenya East GW7, 1013.40 m. The facies displays laminated beds interpreted as tempestites (tm), *Palaeophycus* (Pa), *Planolites* (Pl), *Teichichnus* (Te), *Phycosiphon* (Ph), and *Scolicia* (Sc). (B) F13, bioturbated sandy mudstone with wave ripples, *Diplocraterion* (Di), *Palaeophycus* (Pa), and *Phycosiphon* (Ph) from Kenya East GW7, 1013.70 m. (C) Litholog from Kenya East GW7 showing the coarsening upwards transition from upper offshore to lower shoreface deposits in FA4.

Figure 8 – Core photographs of Facies Association 5 (FA5) – tidal shoreline. (A) F14, tidally influenced heterolithics (muddy end-member) with *Planolites* (Pl) and *Palaeophycus* (Pa) from Chinchilla 4, 983.80 m. (B) F14, tidally influenced heterolithics (sandy end-member) displaying lenticular bedding (len), synaeresis cracks (syn), as well as *Planolites* (Pl) and *Palaeophycus* (Pa) from Taroom 17, 302.70 m. (C) Litholog from Chinchilla 4 displaying the overall fining-upwards nature of deposits in FA5.

Figure 9 – Core photographs of Facies Association 6 (FA6) – restricted marine shoals. (A) F15A, oolitic ironstone from Chinchilla 4, 1036.87 m. (B) F15B, cemented ironstone from Chinchilla 4, 1030.50 m. (C) Litholog from Kenya East GW7 showing alternating ironstone layers of FA6 alternating with prodelta strata of FA3.

Figure 10 – Photomicrographs of palynomorph taxa identified from the Precipice Sandstone and Evergreen interval. (A) The coastal pollen *Araucariacites australis* from Chinchilla 4, 983.00. m. (B) The coastal pollen *Corollina spp*. from Roma 8, 1041.00 m. (C) The coastal

pollen *Callialasporites dampierii* from Chinchilla 4, 983.00 m. (D) The coastal pollen *Callialasporites turbatus* from Kenya East GW7, 1023.60 m. (E) The continental spore *Stereisporites antiquasporites* from Moonie 31, 1724.25 m. (F) The continental spore *Kekryphalospora distincta* from Woleebee Creek GW4, 1356.785 m. (G) The algae *Leiosphaeres spp.* from West Wandoan 1, 1011.86 m. (H) The continental spore *Cadargasporites baculatus* from Condabri MB9-H, 1461.22 m. (I) The continental spore *Sculptisporites moretonensis* from Taroom 17, 397.35 m. (J) The coastal spore *Retitriletes australoclavatidites* from Woleebee Creek GW4, 1485.44 m. (K) The continental spore *Apiculatisporites pristadentatus* from Kenya East GW7, 1181.50 m. (L) The algae *Botryococcus spp.* from Moonie 31, 1724.25 m. (M) The acritarch *Multiplicisphaeridium spp.* from Woleebee Creek GW4, 1336.70 m. (N) Undifferentiated dinocyst from West Wandoan 1, 1011.86 m. (O) Copepod fragment from Chinchilla 4, 1017.00 m.

Figure 11 – The proportion of palynomorphs in each of the wells analyzed organized into their sporomorph ecogroups (SEGs) based on Abbink (1998) and Abbink et al. (2004). D / A / C denotes the proportion of the marine SEG which comprise dinocysts, acritarchs, and copepod fragments.

Figure 12 – Detailed lithological description of the Precipice Sandstone and Evergreen Formation in Roma 8 from 1059.70 m to 954.00 m. The descriptions include physical sedimentary structures and accessories, trace fossils and bioturbation intensity, facies, and the sequence stratigraphic sub-division of the core.

Figure 13 – Detailed lithological description of the Precipice Sandstone and Evergreen Formation in Moonie 31 from 1731.20 m to 1724.60 m. The descriptions include physical sedimentary structures and accessories, trace fossils and bioturbation intensity, facies, and the sequence stratigraphic sub-division of the core.

Figure 14 – Detailed lithological description of Moonie 34 from 1780.20 m to 1758.40 m. The descriptions include physical sedimentary structures and accessories, trace fossils and bioturbation intensity, facies, and the sequence stratigraphic sub-division of the core.

Figure 15 – Detailed lithological description of the Precipice Sandstone and Evergreen Formation in Chinchilla 4 from 1226.60 m to 983.20 m. The descriptions include physical

sedimentary structures and accessories, trace fossils and bioturbation intensity, facies, and the sequence stratigraphic sub-division of the core.

Figure 16 – Detailed lithological description of the Precipice Sandstone and Evergreen Formation in Condabri MB9-H from 1528.50 m to 1399.70 m. The descriptions include physical sedimentary structures and accessories, trace fossils and bioturbation intensity, facies, and the sequence stratigraphic sub-division of the core.

Figure 17 – Detailed lithological description of the Precipice Sandstone and Evergreen Formation in Kenya East GW7 from 1220.50 m to 973.00 m. The descriptions include physical sedimentary structures and accessories, trace fossils and bioturbation intensity, facies, and the sequence stratigraphic sub-division of the core.

Figure 18 – Detailed lithological description of the Precipice Sandstone and Evergreen Formation in Taroom 17 from 500.20 m to 270.80 m. The descriptions include physical sedimentary structures and accessories, trace fossils and bioturbation intensity, facies, and the sequence stratigraphic sub-division of the core.

Figure 19 – Detailed lithological description of the Precipice Sandstone and Evergreen Formation in Reedy Creek MB3-H from 1351.70 m to 1150.60 m. The descriptions include physical sedimentary structures and accessories, trace fossils and bioturbation intensity, facies, and the sequence stratigraphic sub-division of the core.

Figure 20 – Detailed lithological description of the Precipice Sandstone and Evergreen Formation in West Wandoan 1 from 1237.00m to 953.80 m. The descriptions include physical sedimentary structures and accessories, trace fossils and bioturbation intensity, facies, and the sequence stratigraphic sub-division of the core.

Figure 21 – Detailed lithological description of the Precipice Sandstone and Evergreen Formation in Woleebee Creek GW4 from 1573.60 m to 1285.20 m. The descriptions include physical sedimentary structures and accessories, trace fossils and bioturbation intensity, facies, and the sequence stratigraphic sub-division of the core.

Figure 22 – Depositional block model for Sequence 1 showing the major depositional environments and their associated facies. The models are sub-divided into the lowstand (Lowstand Systems Tract 1), transgressive systems tract (Transgressive Systems Tract 1), and highstand (Highstand Systems Tract 1). No implications for scale or paleogeographic orientation are intended.

Figure 23 – Depositional block model for Sequence 2 showing the major depositional environments and their associated facies. The models are sub-divided into a lowstand, transgressive systems tract, and highstand systems tract; these packages were not defined by stratigraphic surfaces due to the thin and potentially incomplete preservation of this sequence across the basin. No implications for scale or paleogeographic orientation are intended.

Figure 24 – Depositional block model for Sequence 3 showing the major depositional environments and their associated facies. The models are sub-divided into the lowstand (Lowstand Systems Tract 1), transgressive systems tract (Transgressive Systems Tract 1), and highstand (Highstand Systems Tract 1). No implications for scale or paleogeographic orientation are intended.

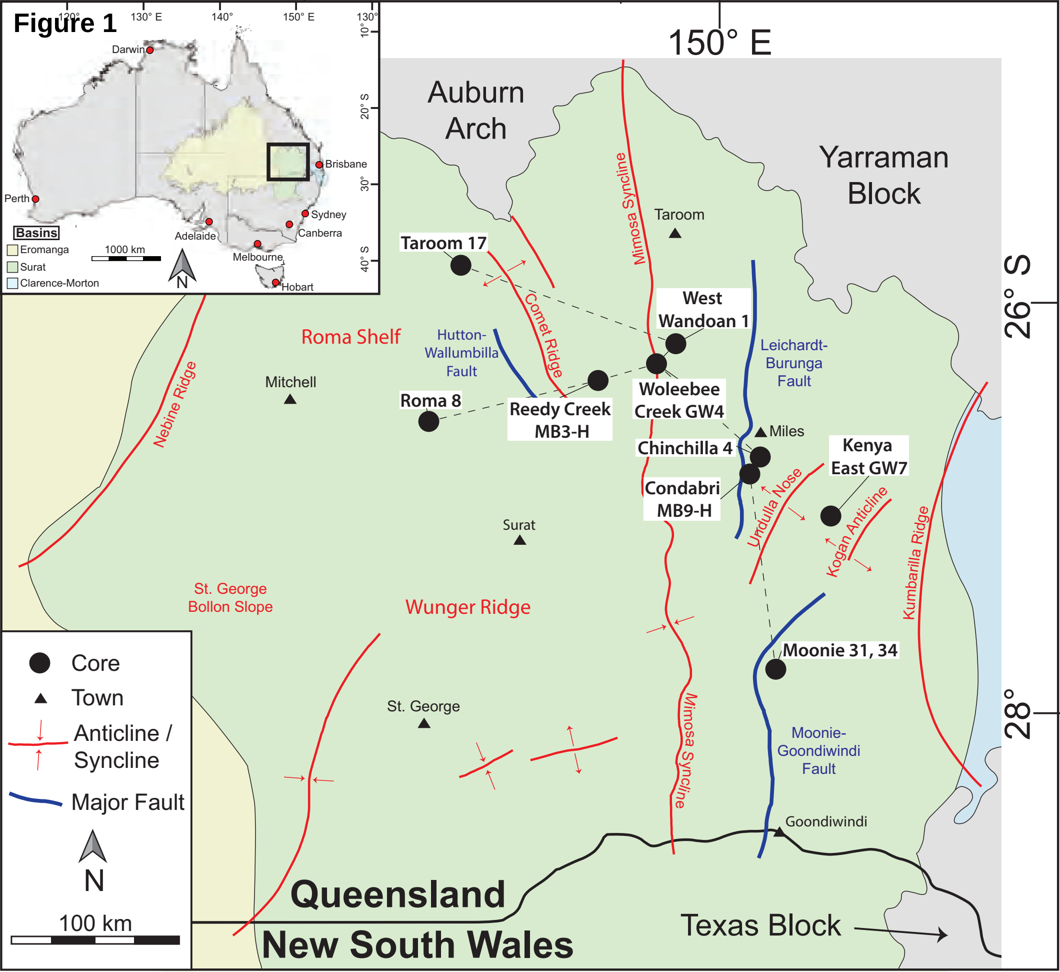

Figure 1
120°
130° E
140°
150° E
130°
10° S
20° S
30° S
40° S
Darwin
Brisbane
Perth
Sydney
Adelaide
Canberra
Melbourne
Hobart
Basins
Eromanga
Surat
Clarence-Morton
1000 km
N
150° E
Auburn Arch
Yarraman Block
Taroom
Taroom 17
Mimosa Syncline
Comet Ridge
West Wandoan 1
Roma Shelf
Hutton-Wallumbilla Fault
Leichardt-Burunga Fault
Mitchell
Roma 8
Reedy Creek MB3-H
Woleebee Creek GW4
Miles
Chinchilla 4
Kenya East GW7
Condabri MB9-H
Undulla Nose
Kogan Anticline
Kumbarilla Ridge
Nebine Ridge
Surat
St. George Bollon Slope
Wunger Ridge
Moonie 31, 34
St. George
Moonie-Goondiwindi Fault
Mimosa Syncline
Goondiwindi
26° S
28°
Core
Town
Anticline / Syncline
Major Fault
N
100 km
Queensland
New South Wales
Texas Block

Figure 2

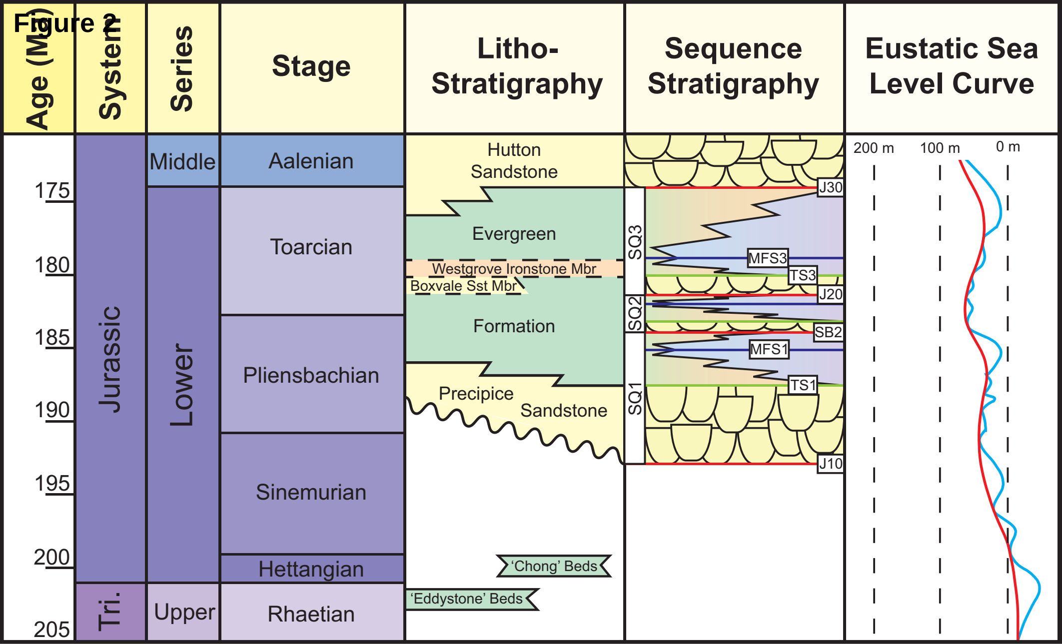
Age (Ma)
System
Series
Stage
Litho-Stratigraphy
Sequence Stratigraphy
Eustatic Sea Level Curve
175
180
185
190
195
200
205
Jurassic
Tri.
Middle
Lower
Upper
Aalenian
Toarcian
Pliensbachian
Sinemurian
Hettangian
Rhaetian
Hutton Sandstone
Evergreen
Westgrove Ironstone Mbr
Boxvale Sst Mbr
Formation
Precipice
Sandstone
'Chong' Beds
'Eddystone' Beds
SQ3
SQ2
SQ1
J30
MFS3
TS3
J20
SB2
MFS1
TS1
J10
200 m
100 m
0 m

Figure 3

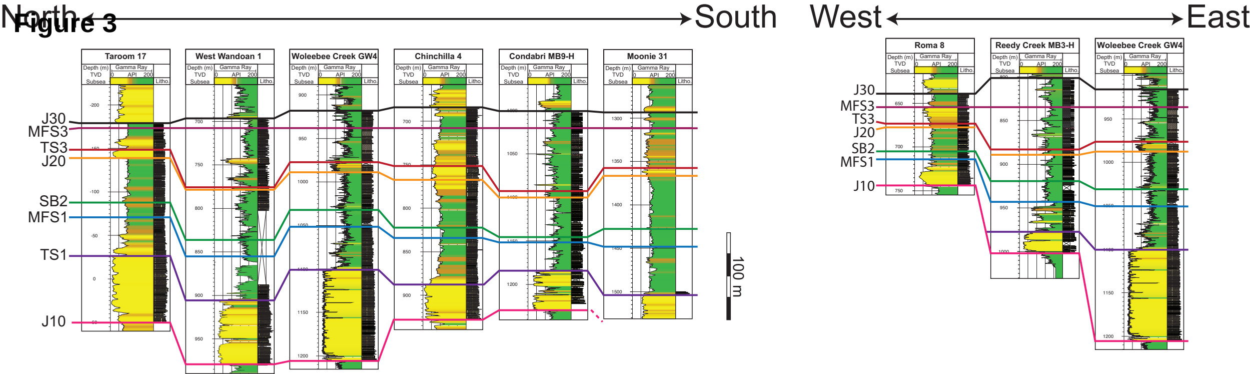
North
South
West
East
Taroom 17
West Wandoan 1
Woleebee Creek GW4
Chinchilla 4
Condabri MB9-H
Moonie 31
Roma 8
Reedy Creek MB3-H
Woleebee Creek GW4
Depth (m) TVD Subsea
Gamma Ray API 0 200
Litho.
J30
MFS3
TS3
J20
SB2
MFS1
TS1
J10
100 m

Figure 4

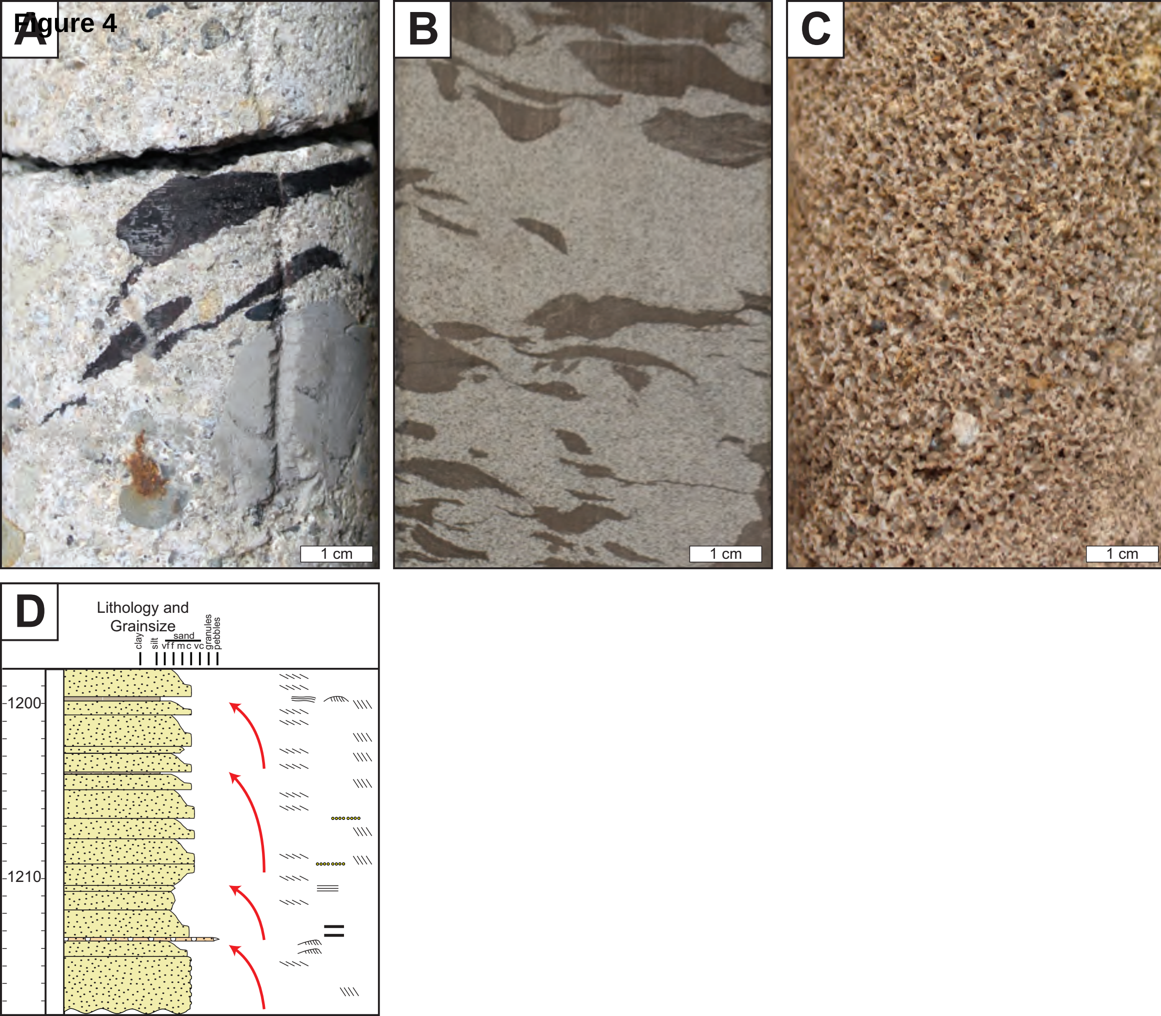
A
B
C
1 cm
1 cm
1 cm
D
Lithology and Grainsize
clay
silt
sand
vf f m c vc
granules
pebbles
1200
1210

Figure 5

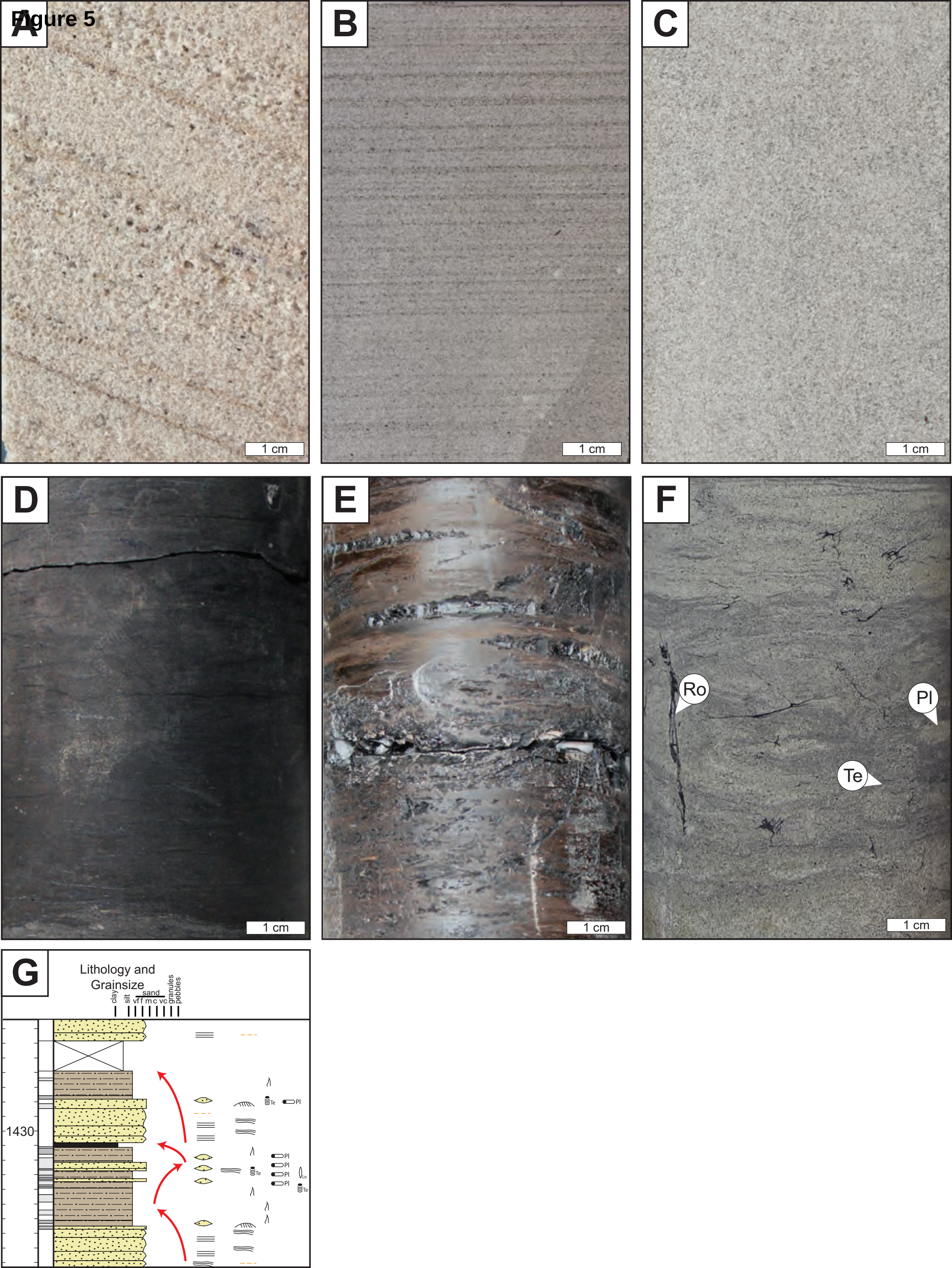
A
1 cm
B
1 cm
C
1 cm
D
1 cm
E
1 cm
F
Ro
Pl
Te
1 cm
G
Lithology and Grainsize
clay
silt
sand
vf f m c vc
granules
pebbles
1430
Te
Pl
Lo

Figure 6

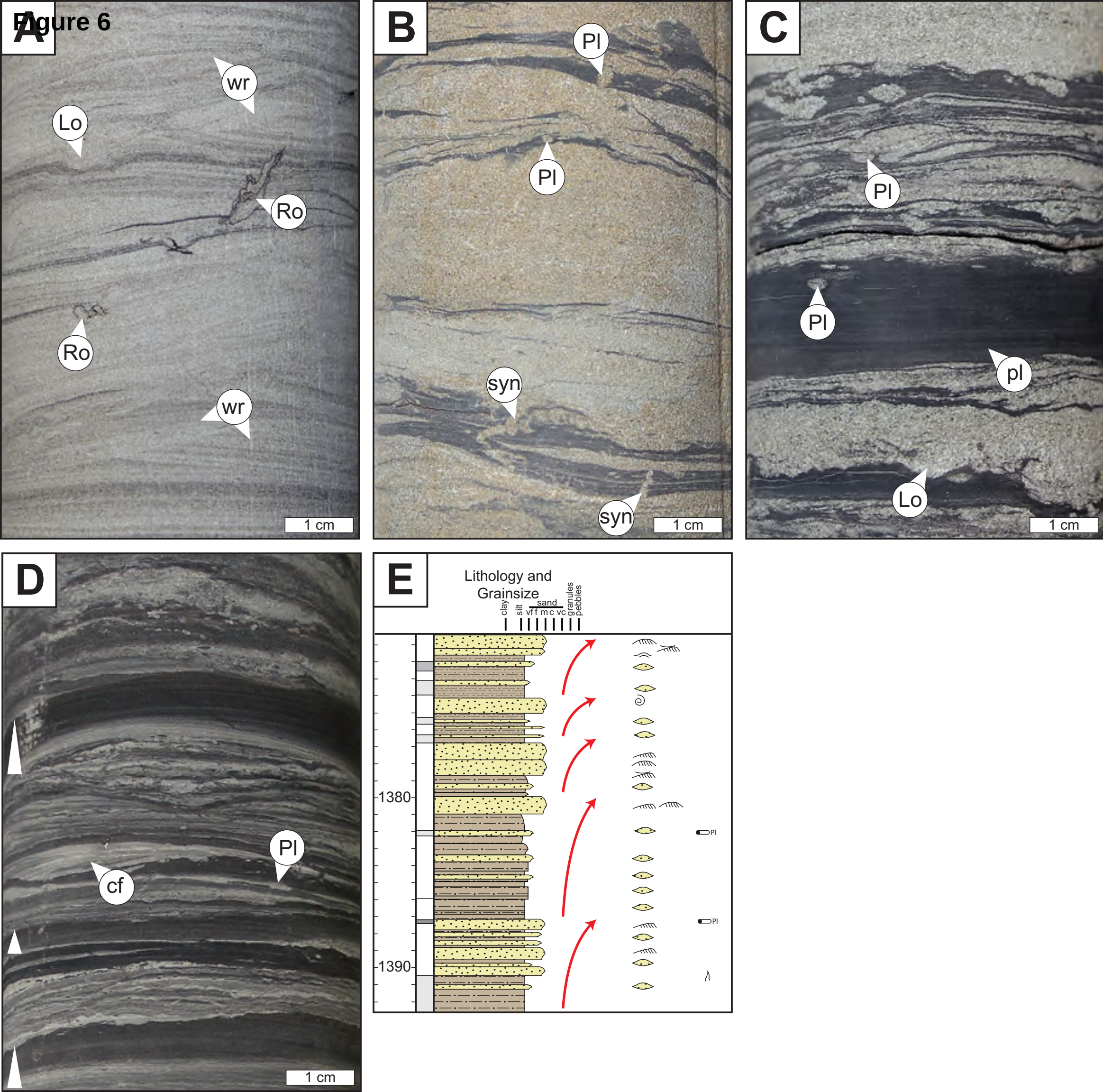
A
wr
Lo
Ro
Ro
wr
1 cm
B
Pl
Pl
syn
syn
1 cm
C
Pl
Pl
pl
Lo
1 cm
D
Pl
cf
1 cm
E
Lithology and Grainsize
clay
silt
sand
vf f m c vc
granules
pebbles
1380
1390
Pl
Pl

Figure 7

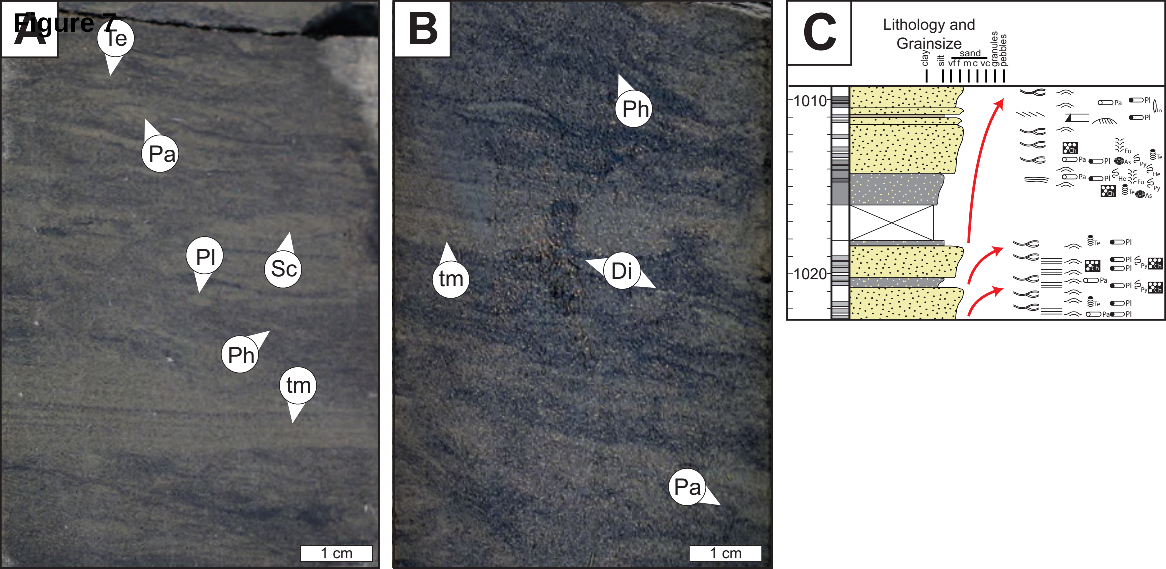
A
Te
Pa
Pl
Sc
Ph
tm
1 cm
B
Ph
tm
Di
Pa
1 cm
C
Lithology and
Grainsize
clay
silt
sand
vf f m c vc
granules
pebbles
1010
1020
Pa
Pl
Lo
Ch
Fu
Te
As
Py
He

Figure 8

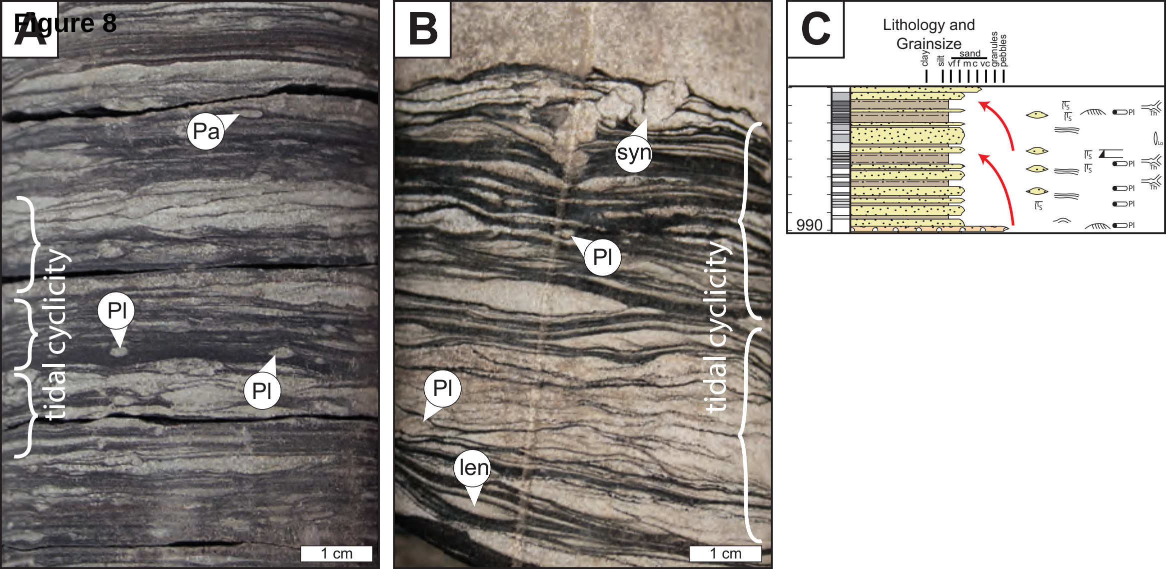
A
Pa
Pl
Pl
tidal cyclicity
1 cm
B
syn
Pl
Pl
len
tidal cyclicity
1 cm
C
Lithology and
Grainsize
clay
silt
sand
vf f m c vc
granules
pebbles
990
Pl
Pl
Pl
Pl
Pl
Th
Th
Th
Lo

Figure 9

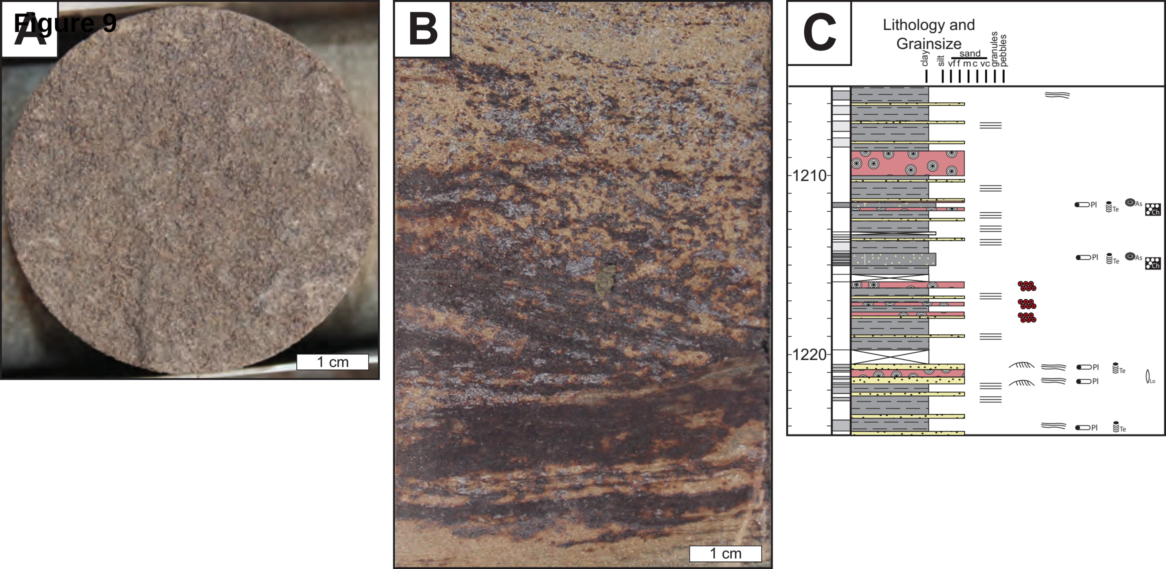
A
1 cm
B
1 cm
C
Lithology and Grainsize
clay
silt
sand
vf f m c vc
granules
pebbles
1210
1220
Pl
Te
As
Ch
Lo

Figure 10

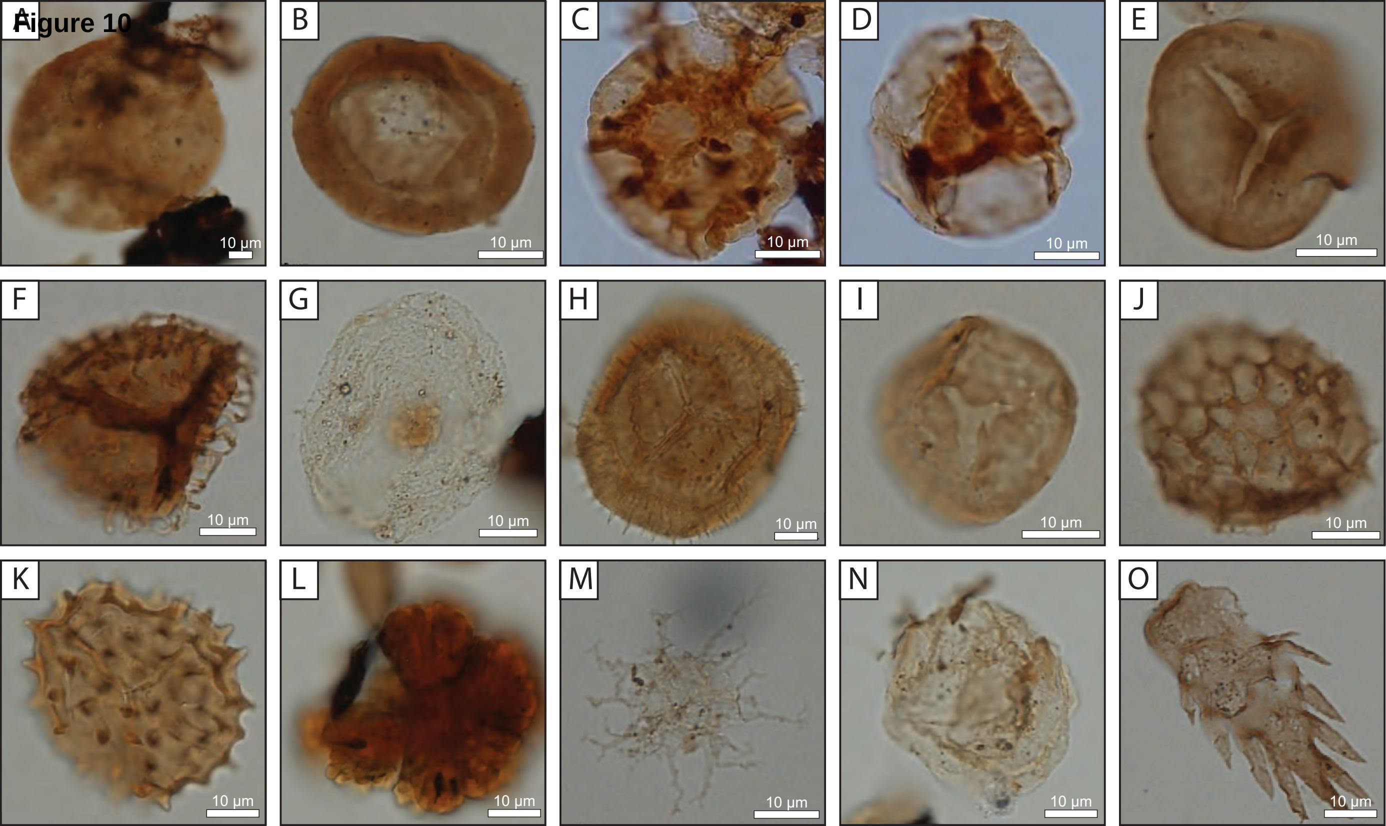

Figure 11

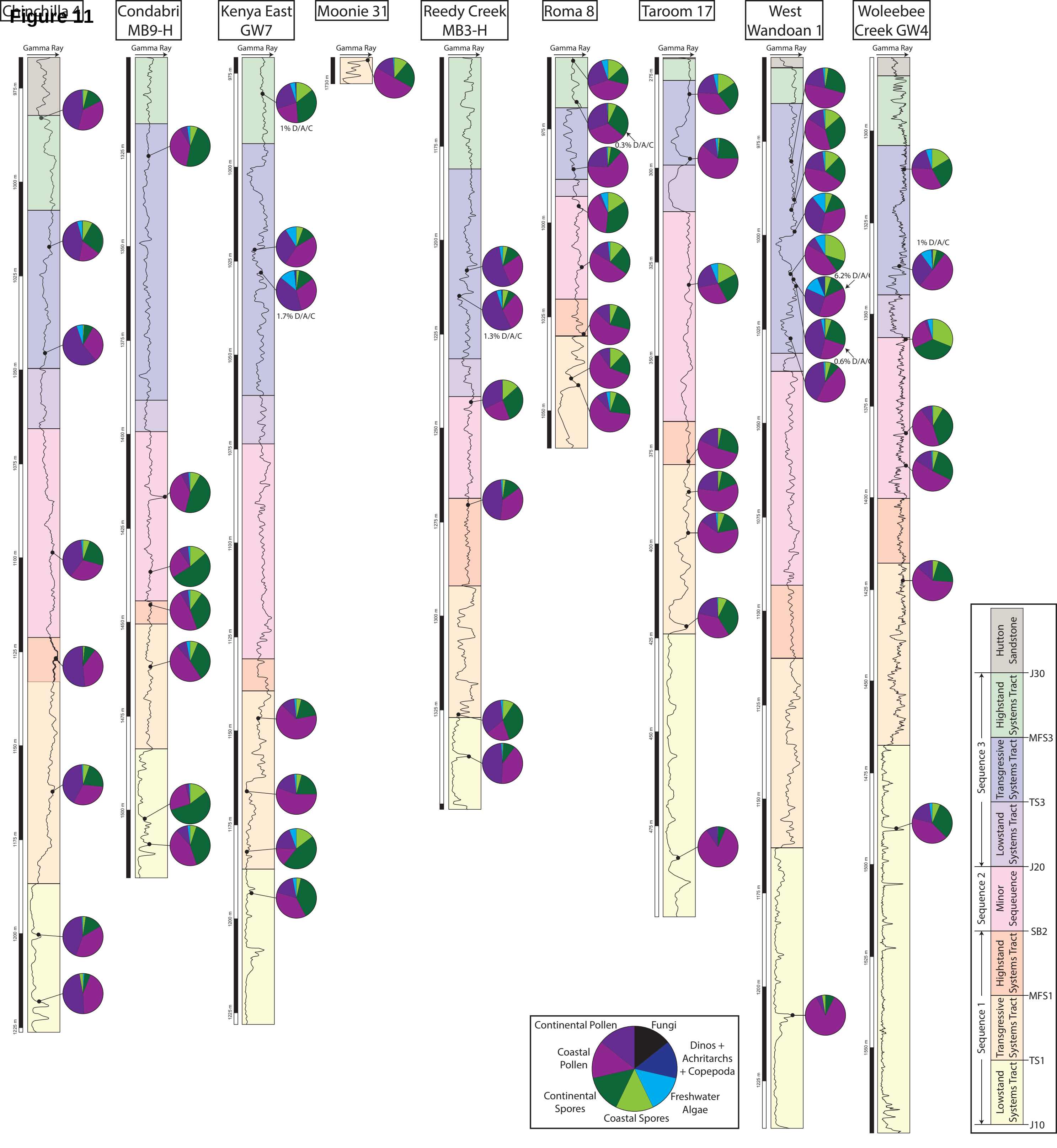

Chinchilla 4
Condabri MB9-H
Kenya East GW7
Moonie 31
Reedy Creek MB3-H
Roma 8
Taroom 17
West Wandoan 1
Woleebee Creek GW4
Gamma Ray
1% D/A/C
1.7% D/A/C
1.3% D/A/C
0.3% D/A/C
6.2% D/A/C
0.6% D/A/C
Continental Pollen
Fungi
Coastal Pollen
Dinos + Achritarchs + Copepoda
Continental Spores
Freshwater Algae
Coastal Spores
Hutton Sandstone
Highstand Systems Tract
Transgressive Systems Tract
Lowstand Systems Tract
Minor Sequeuence
Sequence 1
Sequence 2
Sequence 3
J30
MFS3
TS3
J20
SB2
MFS1
TS1
J10

Figure 12

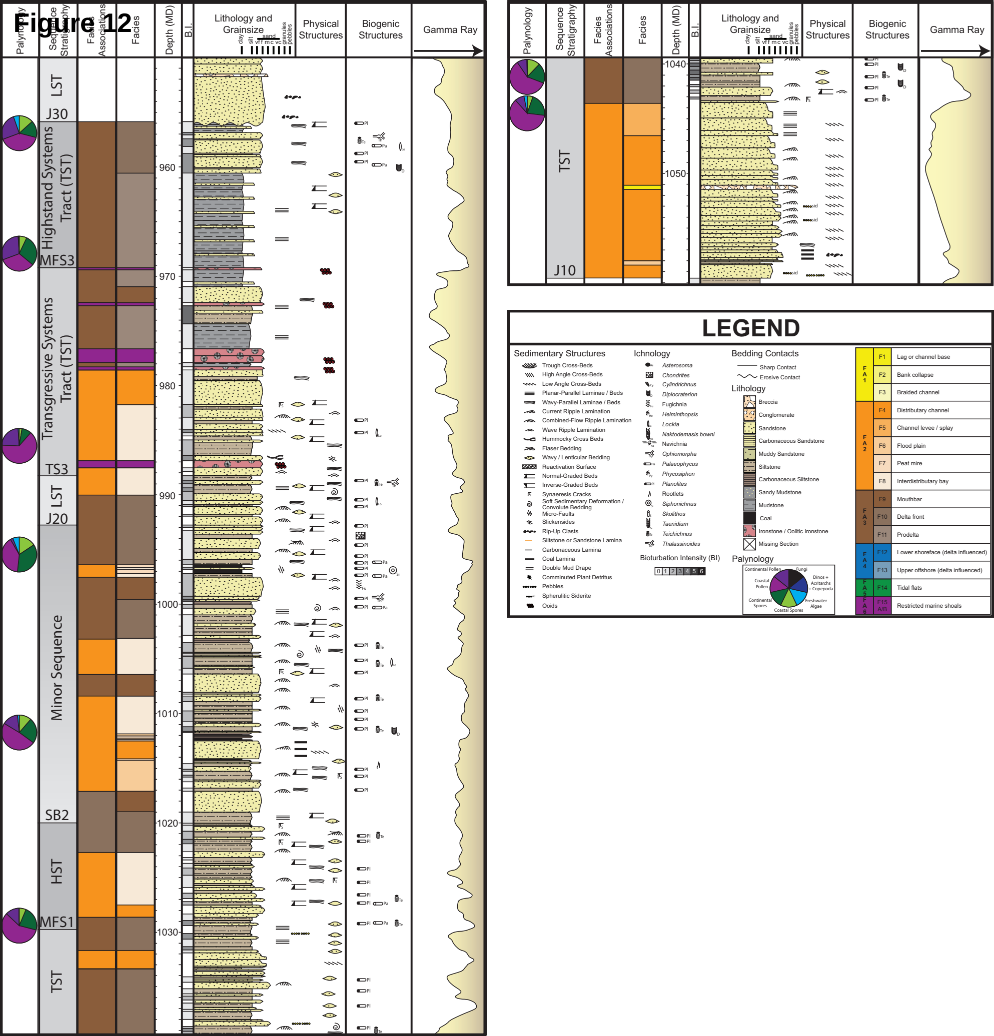

Palynology
Sequence Stratigraphy
Facies Associations
Facies
Depth (MD)
B.I.
Lithology and Grainsize
clay silt vf f m c vc sand granules pebbles
Physical Structures
Biogenic Structures
Gamma Ray
LST
J30
Highstand Systems Tract (TST)
MFS3
Transgressive Systems Tract (TST)
TS3
LST
J20
Minor Sequence
SB2
HST
MFS1
TST
J10
960
970
980
990
1000
1010
1020
1030
1040
1050
LEGEND
Sedimentary Structures
Trough Cross-Beds
High Angle Cross-Beds
Low Angle Cross-Beds
Planar-Parallel Laminae / Beds
Wavy-Parallel Laminae / Beds
Current Ripple Lamination
Combined-Flow Ripple Lamination
Wave Ripple Lamination
Hummocky Cross Beds
Flaser Bedding
Wavy / Lenticular Bedding
Reactivation Surface
Normal-Graded Beds
Inverse-Graded Beds
Synaeresis Cracks
Soft Sedimentary Deformation / Convolute Bedding
Micro-Faults
Slickensides
Rip-Up Clasts
Siltstone or Sandstone Lamina
Carbonaceous Lamina
Coal Lamina
Double Mud Drape
Comminuted Plant Detritus
Pebbles
Spherulitic Siderite
Ooids
Ichnology
Asterosoma
Chondrites
Cylindrichnus
Diplocraterion
Fugichnia
Helminthopsis
Lockia
Naktodemasis bowni
Navichnia
Ophiomorpha
Palaeophycus
Phycosiphon
Planolites
Rootlets
Siphonichnus
Skolithos
Taenidium
Teichichnus
Thalassinoides
Bioturbation Intensity (BI)
0 1 2 3 4 5 6
Bedding Contacts
Sharp Contact
Erosive Contact
Lithology
Breccia
Conglomerate
Sandstone
Carbonaceous Sandstone
Muddy Sandstone
Siltstone
Carbonaceous Siltstone
Sandy Mudstone
Mudstone
Coal
Ironstone / Oolitic Ironstone
Missing Section
Palynology
Continental Pollen
Fungi
Coastal Pollen
Dinos + Acritarchs + Copepoda
Continental Spores
Freshwater Algae
Coastal Spores
FA1
F1 Lag or channel base
F2 Bank collapse
F3 Braided channel
FA2
F4 Distributary channel
F5 Channel levee / splay
F6 Flood plain
F7 Peat mire
F8 Interdistributary bay
FA3
F9 Mouthbar
F10 Delta front
F11 Prodelta
FA4
F12 Lower shoreface (delta influenced)
F13 Upper offshore (delta influenced)
FA5
F14 Tidal flats
FA6
F15 A/B Restricted marine shoals

Figure 13

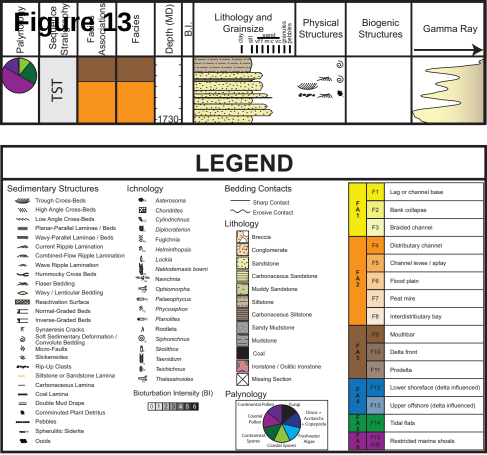
Palynology
Sequence Stratigraphy
Facies Associations
Facies
Depth (MD)
B.I.
Lithology and Grainsize
clay
silt
vf f m c vc
sand
granules
pebbles
Physical Structures
Biogenic Structures
Gamma Ray
TST
1730
LEGEND
Sedimentary Structures
Trough Cross-Beds
High Angle Cross-Beds
Low Angle Cross-Beds
Planar-Parallel Laminae / Beds
Wavy-Parallel Laminae / Beds
Current Ripple Lamination
Combined-Flow Ripple Lamination
Wave Ripple Lamination
Hummocky Cross Beds
Flaser Bedding
Wavy / Lenticular Bedding
Reactivation Surface
Normal-Graded Beds
Inverse-Graded Beds
Synaeresis Cracks
Soft Sedimentary Deformation / Convolute Bedding
Micro-Faults
Slickensides
Rip-Up Clasts
Siltstone or Sandstone Lamina
Carbonaceous Lamina
Coal Lamina
Double Mud Drape
Comminuted Plant Detritus
Pebbles
Spherulitic Siderite
Ooids
Ichnology
Asterosoma
Chondrites
Cylindrichnus
Diplocraterion
Fugichnia
Helminthopsis
Lockia
Naktodemasis bowni
Navichnia
Ophiomorpha
Palaeophycus
Phycosiphon
Planolites
Rootlets
Siphonichnus
Skolithos
Taenidium
Teichichnus
Thalassinoides
Bioturbation Intensity (BI)
0 1 2 3 4 5 6
Bedding Contacts
Sharp Contact
Erosive Contact
Lithology
Breccia
Conglomerate
Sandstone
Carbonaceous Sandstone
Muddy Sandstone
Siltstone
Carbonaceous Siltstone
Sandy Mudstone
Mudstone
Coal
Ironstone / Oolitic Ironstone
Missing Section
Palynology
Continental Pollen
Fungi
Coastal Pollen
Dinos + Acritarchs + Copepoda
Continental Spores
Freshwater Algae
Coastal Spores
FA 1
F1 Lag or channel base
F2 Bank collapse
F3 Braided channel
FA 2
F4 Distributary channel
F5 Channel levee / splay
F6 Flood plain
F7 Peat mire
F8 Interdistributary bay
FA 3
F9 Mouthbar
F10 Delta front
F11 Prodelta
FA 4
F12 Lower shoreface (delta influenced)
F13 Upper offshore (delta influenced)
FA 5
F14 Tidal flats
FA 6
F15 A/B Restricted marine shoals

Figure 14

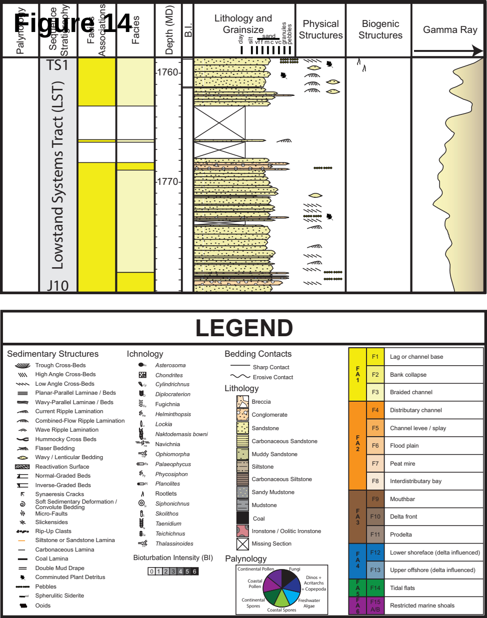
Palynology
Sequence Stratigraphy
Facies Associations
Facies
Depth (MD)
B.I.
Lithology and Grainsize
clay
silt
sand
vf f m c vc
granules
pebbles
Physical Structures
Biogenic Structures
Gamma Ray
TS1
Lowstand Systems Tract (LST)
J10
1760
1770
LEGEND
Sedimentary Structures
Trough Cross-Beds
High Angle Cross-Beds
Low Angle Cross-Beds
Planar-Parallel Laminae / Beds
Wavy-Parallel Laminae / Beds
Current Ripple Lamination
Combined-Flow Ripple Lamination
Wave Ripple Lamination
Hummocky Cross Beds
Flaser Bedding
Wavy / Lenticular Bedding
Reactivation Surface
Normal-Graded Beds
Inverse-Graded Beds
Synaeresis Cracks
Soft Sedimentary Deformation / Convolute Bedding
Micro-Faults
Slickensides
Rip-Up Clasts
Siltstone or Sandstone Lamina
Carbonaceous Lamina
Coal Lamina
Double Mud Drape
Comminuted Plant Detritus
Pebbles
Spherulitic Siderite
Ooids
Ichnology
Asterosoma
Chondrites
Cylindrichnus
Diplocraterion
Fugichnia
Helminthopsis
Lockia
Naktodemasis bowni
Navichnia
Ophiomorpha
Palaeophycus
Phycosiphon
Planolites
Rootlets
Siphonichnus
Skolithos
Taenidium
Teichichnus
Thalassinoides
Bioturbation Intensity (BI)
0 1 2 3 4 5 6
Bedding Contacts
Sharp Contact
Erosive Contact
Lithology
Breccia
Conglomerate
Sandstone
Carbonaceous Sandstone
Muddy Sandstone
Siltstone
Carbonaceous Siltstone
Sandy Mudstone
Mudstone
Coal
Ironstone / Oolitic Ironstone
Missing Section
Palynology
Continental Pollen
Fungi
Dinos + Acritarchs + Copepoda
Coastal Pollen
Continental Spores
Freshwater Algae
Coastal Spores
FA1
F1 Lag or channel base
F2 Bank collapse
F3 Braided channel
FA2
F4 Distributary channel
F5 Channel levee / splay
F6 Flood plain
F7 Peat mire
F8 Interdistributary bay
FA3
F9 Mouthbar
F10 Delta front
F11 Prodelta
FA4
F12 Lower shoreface (delta influenced)
F13 Upper offshore (delta influenced)
FA5
F14 Tidal flats
FA6
F15 A/B Restricted marine shoals

Figure 15

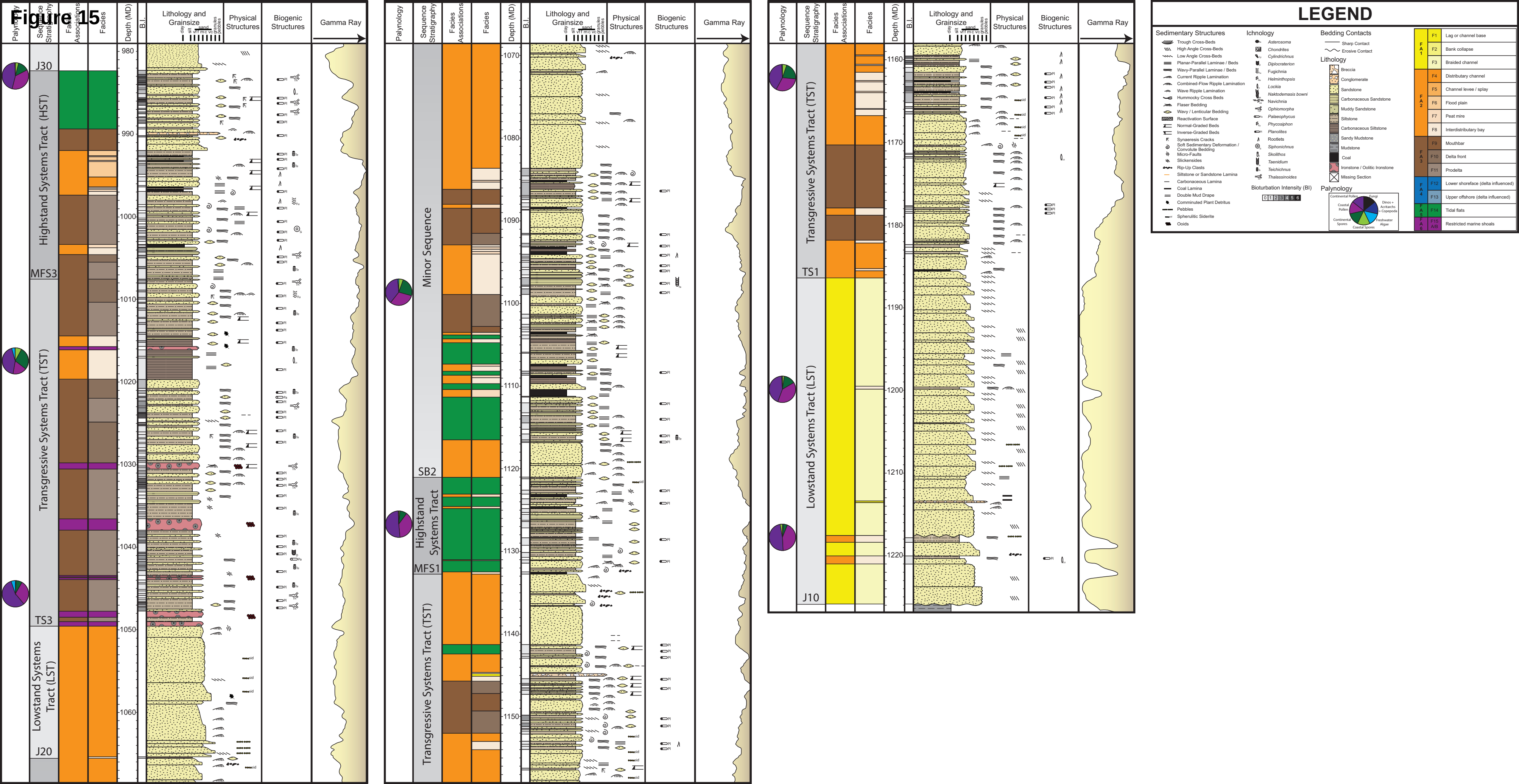

Palynology
Sequence Stratigraphy
Facies Associations
Facies
Depth (MD)
B.I.
Lithology and Grainsize
clay silt vf f m c vc sand granules pebbles
Physical Structures
Biogenic Structures
Gamma Ray
J30
Highstand Systems Tract (HST)
MFS3
Transgressive Systems Tract (TST)
TS3
Lowstand Systems Tract (LST)
J20
Minor Sequence
SB2
Highstand Systems Tract
MFS1
Transgressive Systems Tract (TST)
TS1
Lowstand Systems Tract (LST)
J10
LEGEND
Sedimentary Structures
Trough Cross-Beds
High Angle Cross-Beds
Low Angle Cross-Beds
Planar-Parallel Laminae / Beds
Wavy-Parallel Laminae / Beds
Current Ripple Lamination
Combined-Flow Ripple Lamination
Wave Ripple Lamination
Hummocky Cross-Beds
Flaser Bedding
Wavy / Lenticular Bedding
Reactivation Surface
Normal-Graded Beds
Inverse-Graded Beds
Synaeresis Cracks
Soft Sedimentary Deformation / Convolute Bedding
Micro-Faults
Slickensides
Rip-Up Clasts
Siltstone or Sandstone Lamina
Carbonaceous Lamina
Coal Lamina
Double Mud Drape
Comminuted Plant Detritus
Pebbles
Spherulitic Siderite
Ooids
Ichnology
Asterosoma
Chondrites
Cylindrichnus
Diplocraterion
Fugichnia
Helminthopsis
Lockia
Naktodemasis bowni
Navichnia
Ophiomorpha
Palaeophycus
Phycosiphon
Planolites
Rootlets
Siphonichnus
Skolithos
Taenidium
Teichichnus
Thalassinoides
Bioturbation Intensity (BI)
0 1 2 3 4 5 6
Bedding Contacts
Sharp Contact
Erosive Contact
Lithology
Breccia
Conglomerate
Sandstone
Carbonaceous Sandstone
Muddy Sandstone
Siltstone
Carbonaceous Siltstone
Sandy Mudstone
Mudstone
Coal
Ironstone / Oolitic Ironstone
Missing Section
Palynology
Continental Pollen
Fungi
Coastal Pollen
Dinos + Acritarchs + Copepoda
Continental Spores
Freshwater Algae
Coastal Spores
FA1
F1 Lag or channel base
F2 Bank collapse
F3 Braided channel
FA2
F4 Distributary channel
F5 Channel levee / splay
F6 Flood plain
F7 Peat mire
F8 Interdistributary bay
FA3
F9 Mouthbar
F10 Delta front
F11 Prodelta
FA4
F12 Lower shoreface (delta influenced)
F13 Upper offshore (delta influenced)
FA5
F14 Tidal flats
FA6
F15 A/B Restricted marine shoals

Figure 16

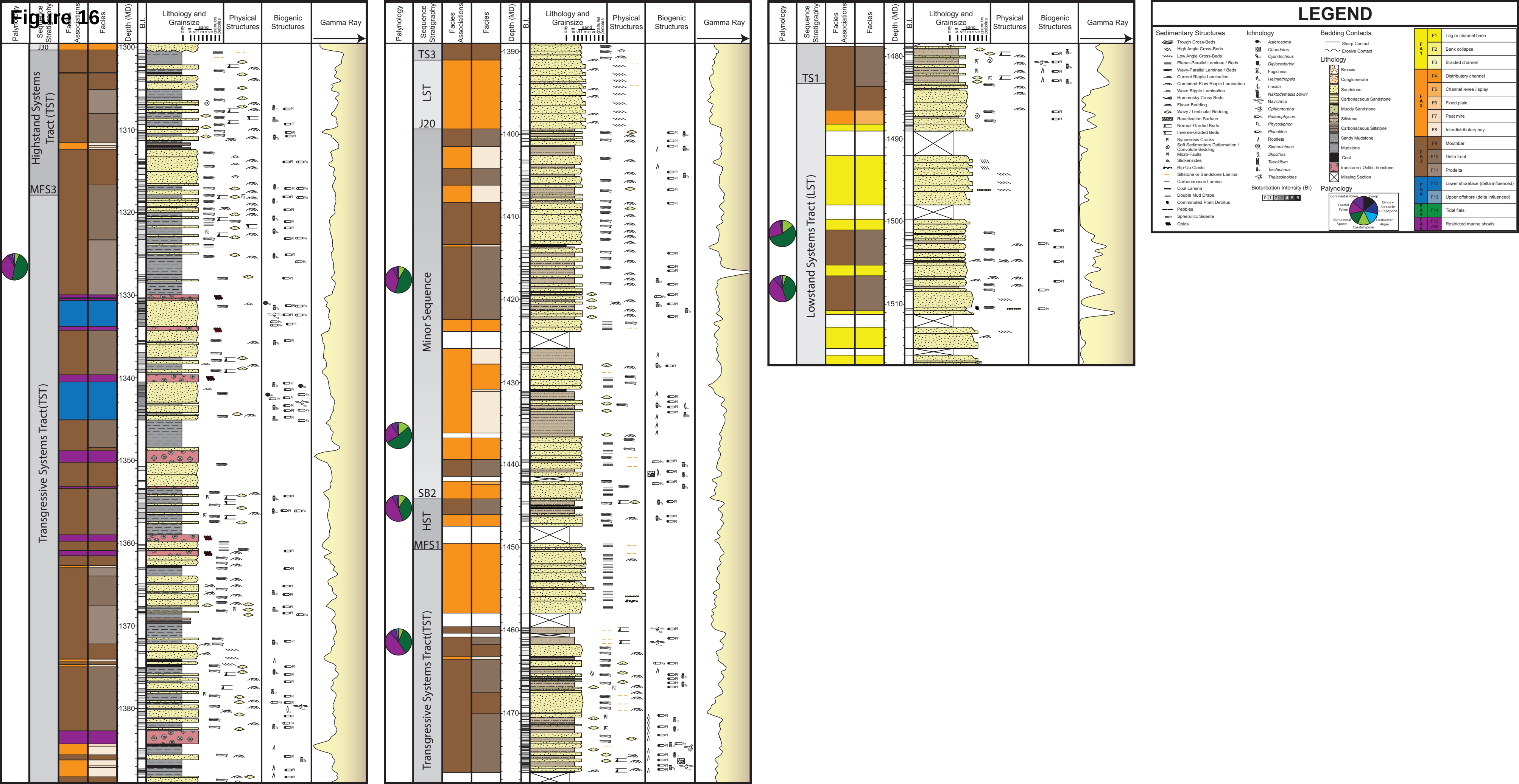

Palynology
Sequence Stratigraphy
Facies Associations
Facies
Depth (MD)
B.I.
Lithology and Grainsize
clay silt sand vf f m c vc granules pebbles
Physical Structures
Biogenic Structures
Gamma Ray
J30
Highstand Systems Tract (TST)
MFS3
Transgressive Systems Tract(TST)
1300
1310
1320
1330
1340
1350
1360
1370
1380
TS3
LST
J20
Minor Sequence
SB2
HST
MFS1
Transgressive Systems Tract(TST)
1390
1400
1410
1420
1430
1440
1450
1460
1470
TS1
Lowstand Systems Tract (LST)
1480
1490
1500
1510
LEGEND
Sedimentary Structures
Trough Cross-Beds
High Angle Cross-Beds
Low Angle Cross-Beds
Planar-Parallel Laminae / Beds
Wavy-Parallel Laminae / Beds
Current Ripple Lamination
Combined-Flow Ripple Lamination
Wave Ripple Lamination
Hummocky Cross Beds
Flaser Bedding
Wavy / Lenticular Bedding
Reactivation Surface
Normal-Graded Beds
Inverse-Graded Beds
Synaeresis Cracks
Soft Sedimentary Deformation / Convolute Bedding
Micro-Faults
Slickensides
Rip-Up Clasts
Siltstone or Sandstone Lamina
Carbonaceous Lamina
Coal Lamina
Double Mud Drape
Comminuted Plant Detritus
Pebbles
Spherulitic Siderite
Ooids
Ichnology
Asterosoma
Chondrites
Cylindrichnus
Diplocraterion
Fugichnia
Helminthopsis
Lockia
Naktodemasis bowni
Navichnia
Ophiomorpha
Palaeophycus
Phycosiphon
Planolites
Rootlets
Siphonichnus
Skolithos
Taenidium
Teichichnus
Thalassinoides
Bioturbation Intensity (BI)
0 1 2 3 4 5 6
Bedding Contacts
Sharp Contact
Erosive Contact
Lithology
Breccia
Conglomerate
Sandstone
Carbonaceous Sandstone
Muddy Sandstone
Siltstone
Carbonaceous Siltstone
Sandy Mudstone
Mudstone
Coal
Ironstone / Oolitic Ironstone
Missing Section
Palynology
Continental Pollen
Fungi
Coastal Pollen
Dinos + Acritarchs + Copepoda
Continental Spores
Freshwater Algae
Coastal Spores
FA1
F1 Lag or channel base
F2 Bank collapse
F3 Braided channel
FA2
F4 Distributary channel
F5 Channel levee / splay
F6 Flood plain
F7 Peat mire
F8 Interdistributary bay
FA3
F9 Mouthbar
F10 Delta front
F11 Prodelta
FA4
F12 Lower shoreface (delta influenced)
F13 Upper offshore (delta influenced)
FA5
F14 Tidal flats
FA6
F15 A/B Restricted marine shoals

Figure 17

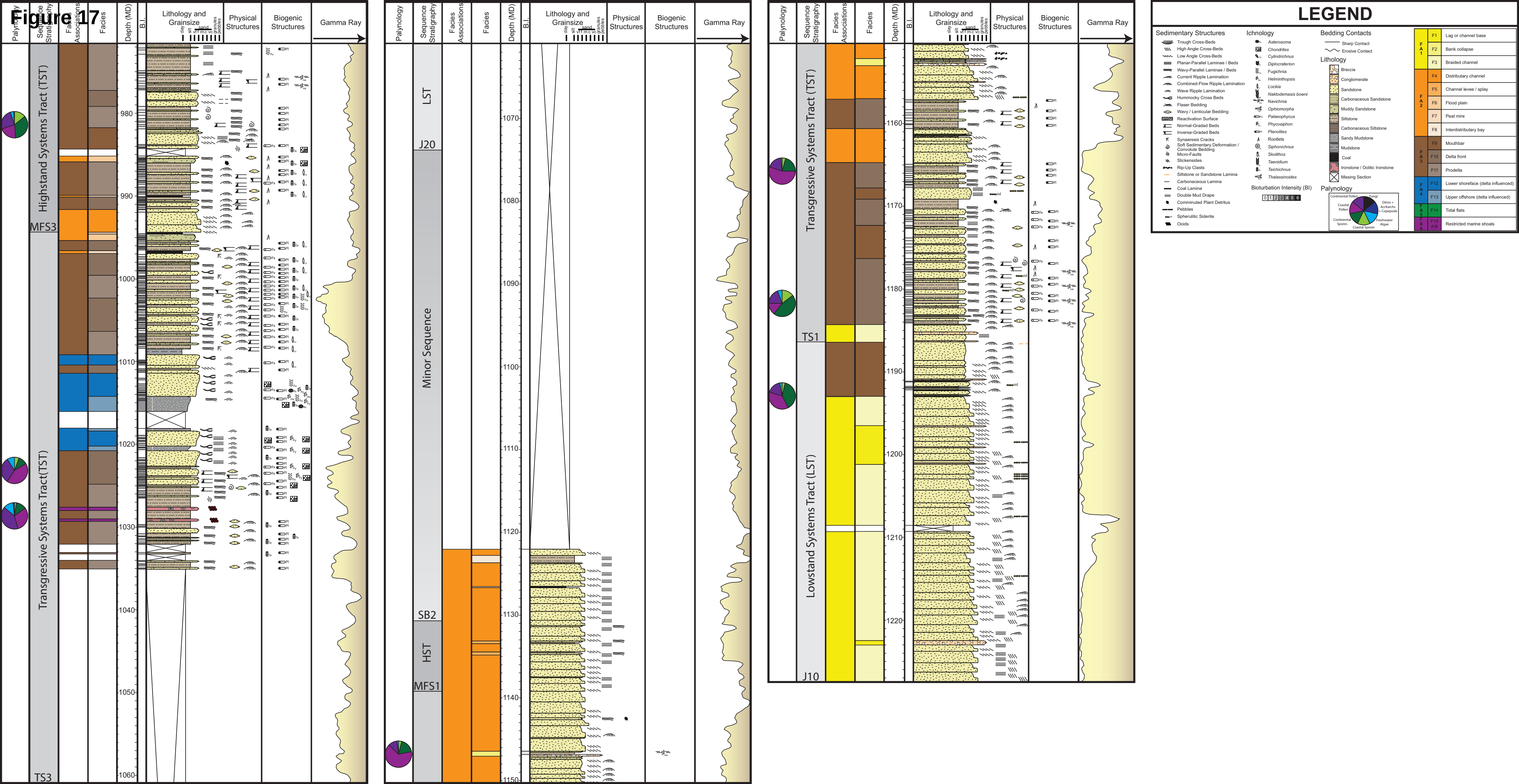
Palynology
Sequence Stratigraphy
Facies Associations
Facies
Depth (MD)
B.I.
Lithology and Grainsize
clay silt vf f m c vc granules pebbles
sand
Physical Structures
Biogenic Structures
Gamma Ray
Highstand Systems Tract (HST)
MFS3
Transgressive Systems Tract(TST)
TS3
LST
J20
Minor Sequence
SB2
HST
MFS1
Transgressive Systems Tract (TST)
TS1
Lowstand Systems Tract (LST)
J10
980
990
1000
1010
1020
1030
1040
1050
1060
1070
1080
1090
1100
1110
1120
1130
1140
1150
1160
1170
1180
1190
1200
1210
1220
LEGEND
Sedimentary Structures
Trough Cross-Beds
High Angle Cross-Beds
Low Angle Cross-Beds
Planar-Parallel Laminae / Beds
Wavy-Parallel Laminae / Beds
Current Ripple Lamination
Combined-Flow Ripple Lamination
Wave Ripple Lamination
Hummocky Cross Beds
Flaser Bedding
Wavy / Lenticular Bedding
Reactivation Surface
Normal-Graded Beds
Inverse-Graded Beds
Synaeresis Cracks
Soft Sedimentary Deformation / Convolute Bedding
Micro-Faults
Slickensides
Rip-Up Clasts
Siltstone or Sandstone Lamina
Carbonaceous Lamina
Coal Lamina
Double Mud Drape
Comminuted Plant Detritus
Pebbles
Spherulitic Siderite
Ooids
Ichnology
Asterosoma
Chondrites
Cylindrichnus
Diplocraterion
Fugichnia
Helminthopsis
Lockia
Naktodemasis bowni
Navichnia
Ophiomorpha
Palaeophycus
Phycosiphon
Planolites
Rootlets
Siphonichnus
Skolithos
Taenidium
Teichichnus
Thalassinoides
Bioturbation Intensity (BI)
0 1 2 3 4 5 6
Bedding Contacts
Sharp Contact
Erosive Contact
Lithology
Breccia
Conglomerate
Sandstone
Carbonaceous Sandstone
Muddy Sandstone
Siltstone
Carbonaceous Siltstone
Sandy Mudstone
Mudstone
Coal
Ironstone / Oolitic Ironstone
Missing Section
Palynology
Continental Pollen
Fungi
Coastal Pollen
Dinos + Acritarchs + Copepoda
Continental Spores
Freshwater Algae
Coastal Spores
FA1
F1 Lag or channel base
F2 Bank collapse
F3 Braided channel
FA2
F4 Distributary channel
F5 Channel levee / splay
F6 Flood plain
F7 Peat mire
F8 Interdistributary bay
FA3
F9 Mouthbar
F10 Delta front
F11 Prodelta
FA4
F12 Lower shoreface (delta influenced)
F13 Upper offshore (delta influenced)
FA5
F14 Tidal flats
FA6
F15 A/B Restricted marine shoals

Figure 18

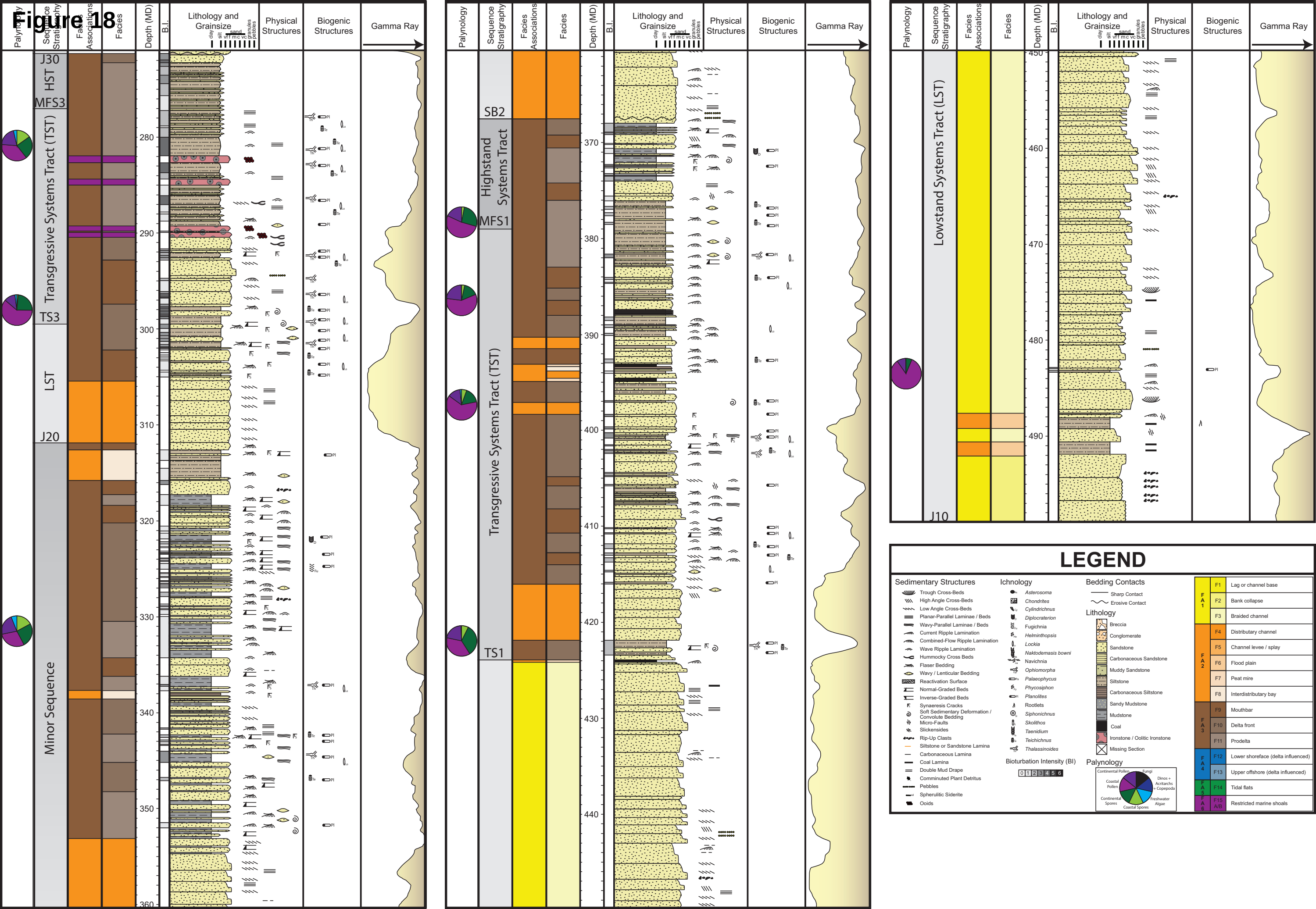

Palynology
Sequence Stratigraphy
Facies Associations
Facies
Depth (MD)
B.I.
Lithology and Grainsize
clay silt vf f m c vc sand granules pebbles
Physical Structures
Biogenic Structures
Gamma Ray
J30
HST
MFS3
Transgressive Systems Tract (TST)
TS3
LST
J20
Minor Sequence
280
290
300
310
320
330
340
350
360
SB2
Highstand Systems Tract
MFS1
Transgressive Systems Tract (TST)
TS1
370
380
390
400
410
420
430
440
Lowstand Systems Tract (LST)
J10
450
460
470
480
490
LEGEND
Sedimentary Structures
Trough Cross-Beds
High Angle Cross-Beds
Low Angle Cross-Beds
Planar-Parallel Laminae / Beds
Wavy-Parallel Laminae / Beds
Current Ripple Lamination
Combined-Flow Ripple Lamination
Wave Ripple Lamination
Hummocky Cross Beds
Flaser Bedding
Wavy / Lenticular Bedding
Reactivation Surface
Normal-Graded Beds
Inverse-Graded Beds
Synaeresis Cracks
Soft Sedimentary Deformation / Convolute Bedding
Micro-Faults
Slickensides
Rip-Up Clasts
Siltstone or Sandstone Lamina
Carbonaceous Lamina
Coal Lamina
Double Mud Drape
Comminuted Plant Detritus
Pebbles
Spherulitic Siderite
Ooids
Ichnology
Asterosoma
Chondrites
Cylindrichnus
Diplocraterion
Fugichnia
Helminthopsis
Lockia
Naktodemasis bowni
Navichnia
Ophiomorpha
Palaeophycus
Phycosiphon
Planolites
Rootlets
Siphonichnus
Skolithos
Taenidium
Teichichnus
Thalassinoides
Bioturbation Intensity (BI)
0 1 2 3 4 5 6
Bedding Contacts
Sharp Contact
Erosive Contact
Lithology
Breccia
Conglomerate
Sandstone
Carbonaceous Sandstone
Muddy Sandstone
Siltstone
Carbonaceous Siltstone
Sandy Mudstone
Mudstone
Coal
Ironstone / Oolitic Ironstone
Missing Section
Palynology
Continental Pollen
Fungi
Coastal Pollen
Dinos + Acritarchs + Copepoda
Continental Spores
Coastal Spores
Freshwater Algae
FA1
F1 Lag or channel base
F2 Bank collapse
F3 Braided channel
FA2
F4 Distributary channel
F5 Channel levee / splay
F6 Flood plain
F7 Peat mire
F8 Interdistributary bay
FA3
F9 Mouthbar
F10 Delta front
F11 Prodelta
FA4
F12 Lower shoreface (delta influenced)
F13 Upper offshore (delta influenced)
FA5
F14 Tidal flats
FA6
F15 A/B Restricted marine shoals

Figure 19

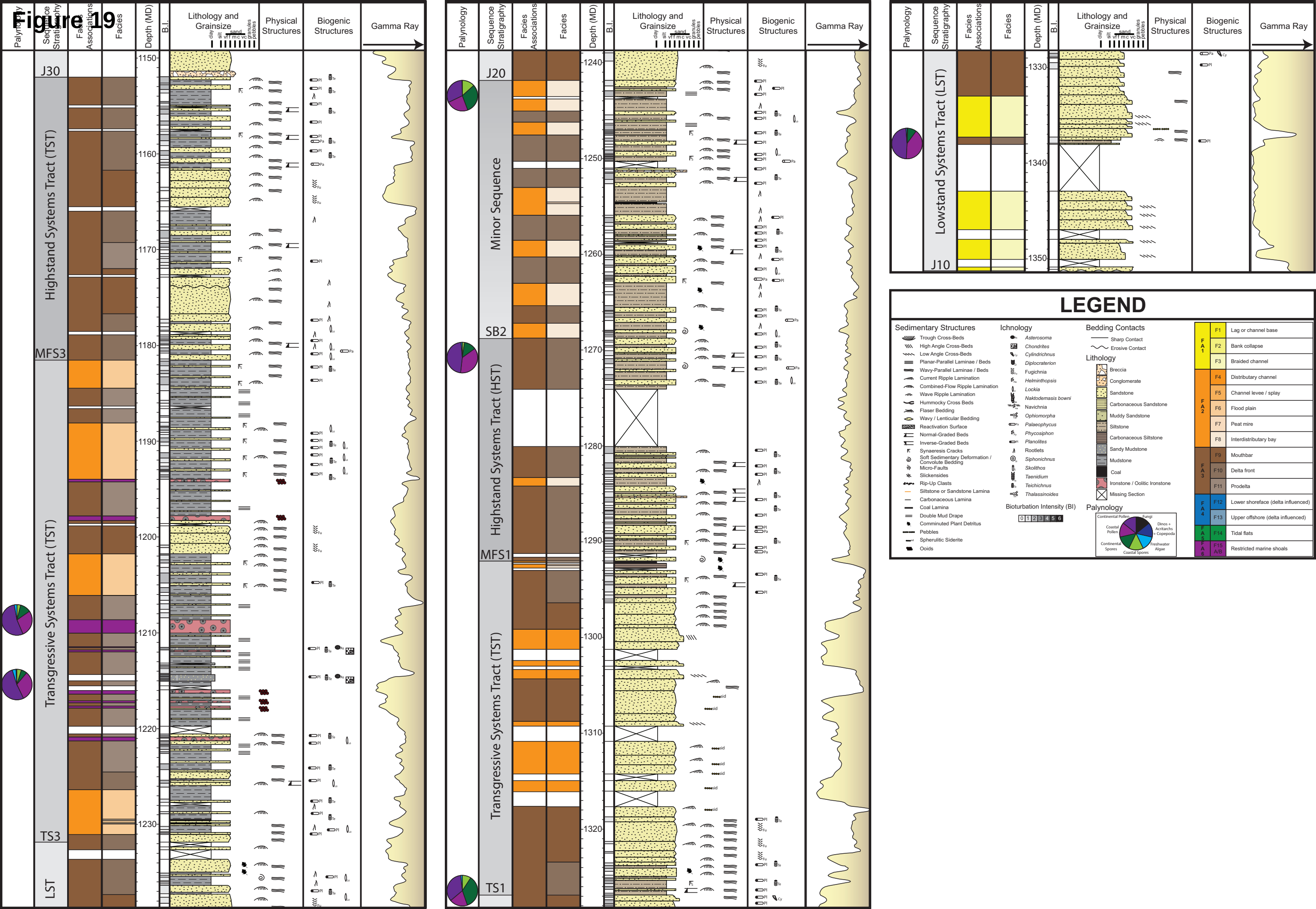

Palynology
Sequence Stratigraphy
Facies Associations
Facies
Depth (MD)
B.I.
Lithology and Grainsize
Physical Structures
Biogenic Structures
Gamma Ray
J30
Highstand Systems Tract (HST)
MFS3
Transgressive Systems Tract (TST)
TS3
LST
J20
Minor Sequence
SB2
MFS1
TS1
Lowstand Systems Tract (LST)
J10
LEGEND
Sedimentary Structures
Trough Cross-Beds
High Angle Cross-Beds
Low Angle Cross-Beds
Planar-Parallel Laminae / Beds
Wavy-Parallel Laminae / Beds
Current Ripple Lamination
Combined-Flow Ripple Lamination
Wave Ripple Lamination
Hummocky Cross Beds
Flaser Bedding
Wavy / Lenticular Bedding
Reactivation Surface
Normal-Graded Beds
Inverse-Graded Beds
Synaeresis Cracks
Soft Sedimentary Deformation / Convolute Bedding
Micro-Faults
Slickensides
Rip-Up Clasts
Siltstone or Sandstone Lamina
Carbonaceous Lamina
Coal Lamina
Double Mud Drape
Comminuted Plant Detritus
Pebbles
Spherulitic Siderite
Ooids
Ichnology
Asterosoma
Chondrites
Cylindrichnus
Diplocraterion
Fugichnia
Helminthopsis
Lockia
Naktodemasis bowni
Navichnia
Ophiomorpha
Palaeophycus
Phycosiphon
Planolites
Rootlets
Siphonichnus
Skolithos
Taenidium
Teichichnus
Thalassinoides
Bioturbation Intensity (BI)
Bedding Contacts
Sharp Contact
Erosive Contact
Lithology
Breccia
Conglomerate
Sandstone
Carbonaceous Sandstone
Muddy Sandstone
Siltstone
Carbonaceous Siltstone
Sandy Mudstone
Mudstone
Coal
Ironstone / Oolitic Ironstone
Missing Section
Palynology
Continental Pollen
Fungi
Coastal Pollen
Dinos + Acritarchs + Copepoda
Continental Spores
Coastal Spores
Freshwater Algae
FA1
F1 Lag or channel base
F2 Bank collapse
F3 Braided channel
FA2
F4 Distributary channel
F5 Channel levee / splay
F6 Flood plain
F7 Peat mire
F8 Interdistributary bay
FA3
F9 Mouthbar
F10 Delta front
F11 Prodelta
FA4
F12 Lower shoreface (delta influenced)
F13 Upper offshore (delta influenced)
FA5
F14 Tidal flats
FA6
F15 A/B Restricted marine shoals

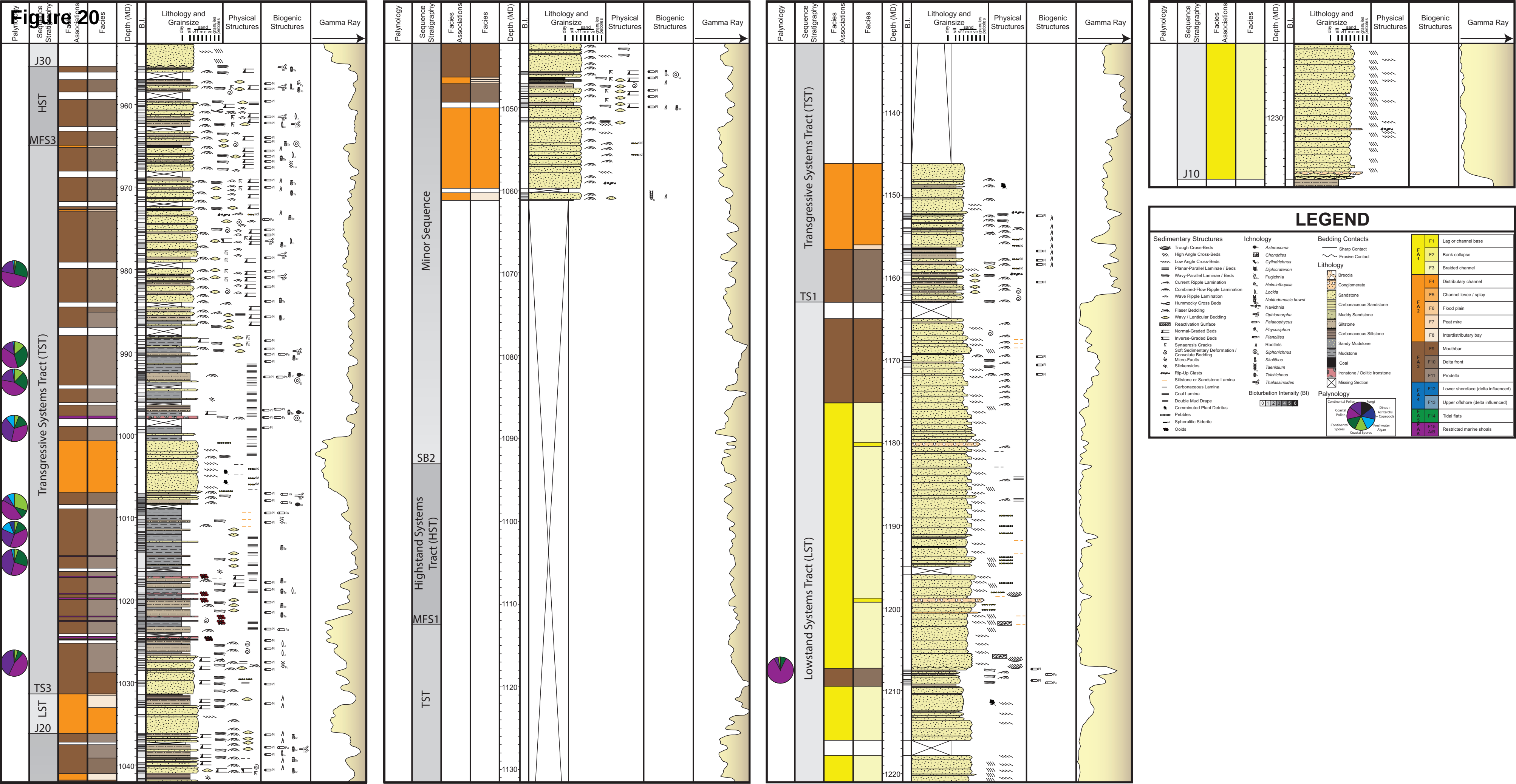

Palynology
Sequence Stratigraphy
Facies Associations
Facies
Depth (MD)
B.I.
Lithology and Grainsize
clay silt vf f m c vc sand granules pebbles
Physical Structures
Biogenic Structures
Gamma Ray
J30
HST
MFS3
Transgressive Systems Tract (TST)
TS3
LST
J20
Minor Sequence
SB2
Highstand Systems Tract (HST)
MFS1
TST
Transgressive Systems Tract (TST)
TS1
Lowstand Systems Tract (LST)
J10
960
970
980
990
1000
1010
1020
1030
1040
1050
1060
1070
1080
1090
1100
1110
1120
1130
1140
1150
1160
1170
1180
1190
1200
1210
1220
1230
LEGEND
Sedimentary Structures
Trough Cross-Beds
High Angle Cross-Beds
Low Angle Cross-Beds
Planar-Parallel Laminae / Beds
Wavy-Parallel Laminae / Beds
Current Ripple Lamination
Combined-Flow Ripple Lamination
Wave Ripple Lamination
Hummocky Cross Beds
Flaser Bedding
Wavy / Lenticular Bedding
Reactivation Surface
Normal-Graded Beds
Inverse-Graded Beds
Synaeresis Cracks
Soft Sedimentary Deformation / Convolute Bedding
Micro-Faults
Slickensides
Rip-Up Clasts
Siltstone or Sandstone Lamina
Carbonaceous Lamina
Coal Lamina
Double Mud Drape
Comminuted Plant Debris
Pebbles
Spherulitic Siderite
Ooids
Ichnology
Asterosoma
Chondrites
Cylindrichnus
Diplocraterion
Fugichnia
Helminthopsis
Lockia
Naktodemasis bowni
Navichnia
Ophiomorpha
Palaeophycus
Phycosiphon
Planolites
Rootlets
Siphonichnus
Skolithos
Taenidium
Teichichnus
Thalassinoides
Bioturbation Intensity (BI)
0 1 2 3 4 5 6
Bedding Contacts
Sharp Contact
Erosive Contact
Lithology
Breccia
Conglomerate
Sandstone
Carbonaceous Sandstone
Muddy Sandstone
Siltstone
Carbonaceous Siltstone
Sandy Mudstone
Mudstone
Coal
Ironstone / Oolitic Ironstone
Missing Section
Palynology
Continental Pollen
Fungi
Coastal Pollen
Dinos + Acritarchs + Copepoda
Continental Spores
Freshwater Algae
Coastal Spores
FA1
F1 Lag or channel base
F2 Bank collapse
F3 Braided channel
FA2
F4 Distributary channel
F5 Channel levee / splay
F6 Flood plain
F7 Peat mire
F8 Interdistributary bay
FA3
F9 Mouthbar
F10 Delta front
F11 Prodelta
FA4
F12 Lower shoreface (delta influenced)
F13 Upper offshore (delta influenced)
FA5
F14 Tidal flats
FA6
F15 A/B Restricted marine shoals

Figure 20

Figure 21

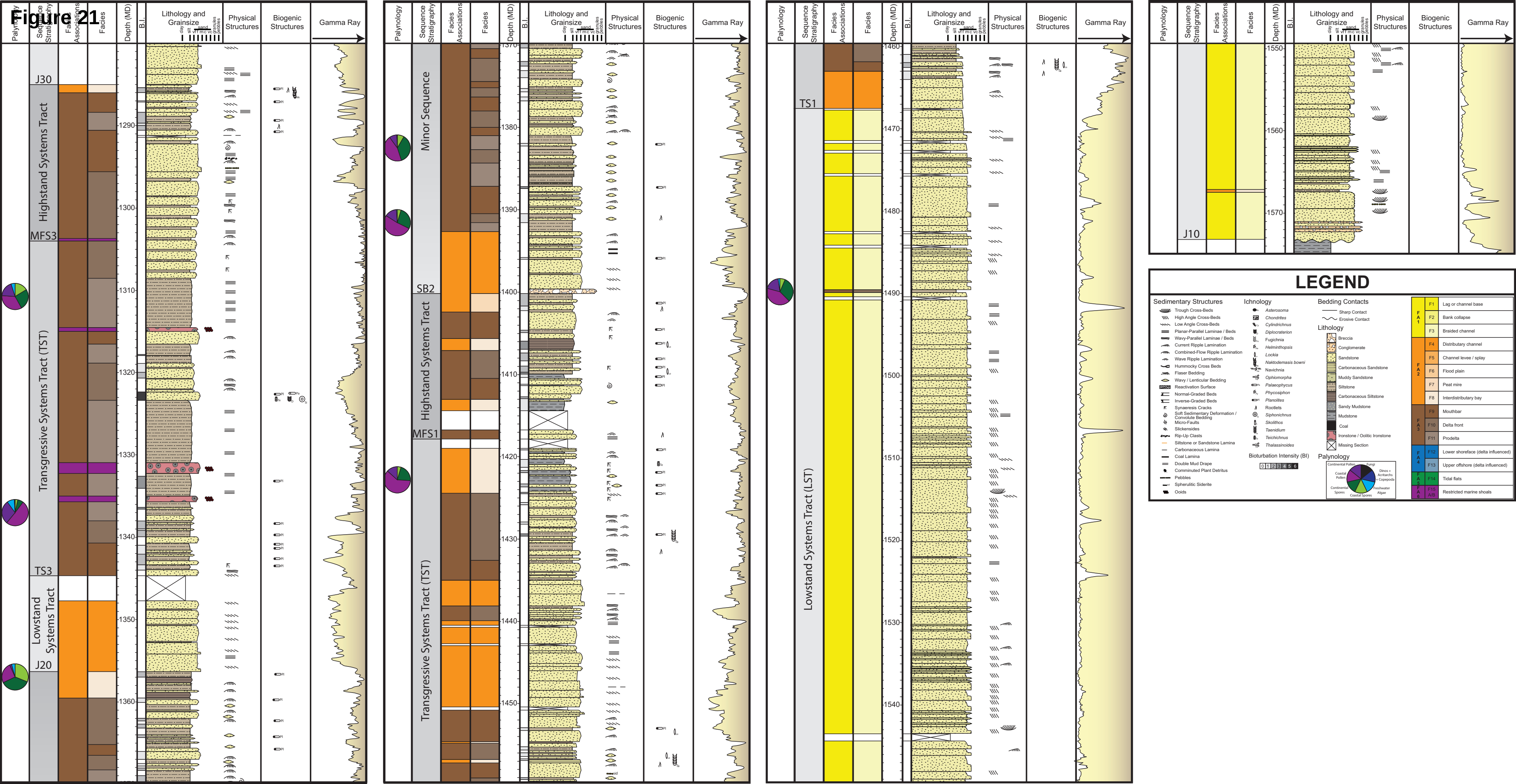

Palynology
Sequence Stratigraphy
Facies Associations
Facies
Depth (MD)
B.I.
Lithology and Grainsize
clay silt vf f m c vc sand granules pebbles
Physical Structures
Biogenic Structures
Gamma Ray
J30
Highstand Systems Tract
MFS3
Transgressive Systems Tract (TST)
TS3
Lowstand Systems Tract
J20
Minor Sequence
SB2
Highstand Systems Tract
MFS1
Transgressive Systems Tract (TST)
TS1
Lowstand Systems Tract (LST)
J10
1290
1300
1310
1320
1330
1340
1350
1360
1370
1380
1390
1400
1410
1420
1430
1440
1450
1460
1470
1480
1490
1500
1510
1520
1530
1540
1550
1560
1570
LEGEND
Sedimentary Structures
Trough Cross-Beds
High Angle Cross-Beds
Low Angle Cross-Beds
Planar-Parallel Laminae / Beds
Wavy-Parallel Laminae / Beds
Current Ripple Lamination
Combined-Flow Ripple Lamination
Wave Ripple Lamination
Hummocky Cross Beds
Flaser Bedding
Wavy / Lenticular Bedding
Reactivation Surface
Normal-Graded Beds
Inverse-Graded Beds
Synaeresis Cracks
Soft Sedimentary Deformation / Convolute Bedding
Micro-Faults
Slickensides
Rip-Up Clasts
Siltstone or Sandstone Lamina
Carbonaceous Lamina
Coal Lamina
Double Mud Drape
Comminuted Plant Detritus
Pebbles
Spherulitic Siderite
Ooids
Ichnology
Asterosoma
Chondrites
Cylindrichnus
Diplocraterion
Fugichnia
Helminthopsis
Lockia
Naktodemasis bowni
Navichnia
Ophiomorpha
Palaeophycus
Phycosiphon
Planolites
Rootlets
Siphonichnus
Skolithos
Taenidium
Teichichnus
Thalassinoides
Bioturbation Intensity (BI)
0 1 2 3 4 5 6
Bedding Contacts
Sharp Contact
Erosive Contact
Lithology
Breccia
Conglomerate
Sandstone
Carbonaceous Sandstone
Muddy Sandstone
Siltstone
Carbonaceous Siltstone
Sandy Mudstone
Mudstone
Coal
Ironstone / Oolitic Ironstone
Missing Section
Palynology
Continental Pollen
Fungi
Coastal Pollen
Dinos + Acritarchs + Copepoda
Continental Spores
Freshwater Algae
Coastal Spores
FA1
F1 Lag or channel base
F2 Bank collapse
F3 Braided channel
FA2
F4 Distributary channel
F5 Channel levee / splay
F6 Flood plain
F7 Peat mire
F8 Interdistributary bay
FA3
F9 Mouthbar
F10 Delta front
F11 Prodelta
FA4
F12 Lower shoreface (delta influenced)
F13 Upper offshore (delta influenced)
FA5
F14 Tidal flats
FA6
F15 A/B Restricted marine shoals

Figure 22

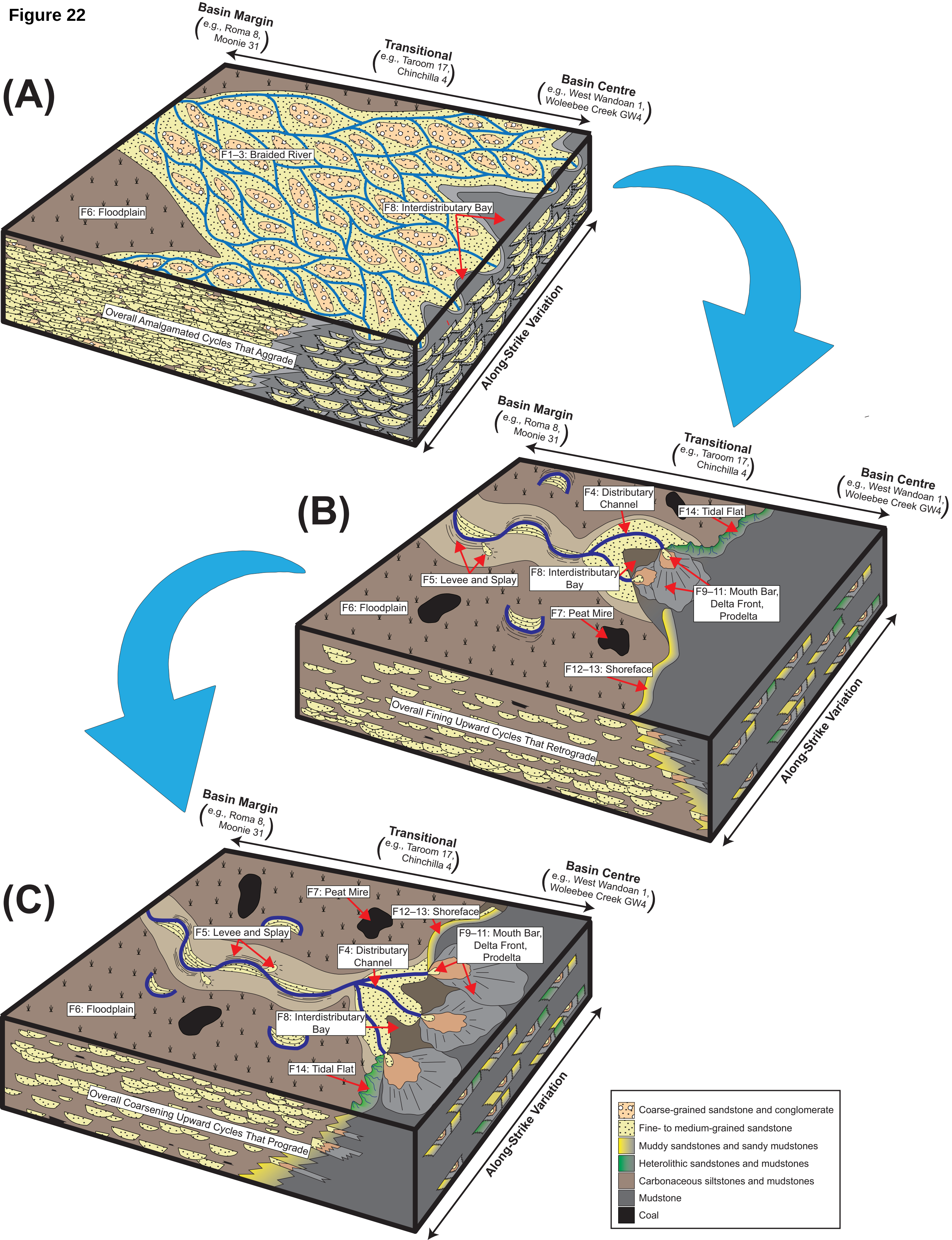

(A)
Basin Margin
(e.g., Roma 8, Moonie 31)
Transitional
(e.g., Taroom 17, Chinchilla 4)
Basin Centre
(e.g., West Wandoan 1, Woleebee Creek GW4)
F1–3: Braided River
F6: Floodplain
F8: Interdistributary Bay
Overall Amalgamated Cycles That Aggrade
Along-Strike Variation
(B)
Basin Margin
(e.g., Roma 8, Moonie 31)
Transitional
(e.g., Taroom 17, Chinchilla 4)
Basin Centre
(e.g., West Wandoan 1, Woleebee Creek GW4)
F4: Distributary Channel
F14: Tidal Flat
F5: Levee and Splay
F8: Interdistributary Bay
F9–11: Mouth Bar, Delta Front, Prodelta
F6: Floodplain
F7: Peat Mire
F12–13: Shoreface
Overall Fining Upward Cycles That Retrograde
Along-Strike Variation
(C)
Basin Margin
(e.g., Roma 8, Moonie 31)
Transitional
(e.g., Taroom 17, Chinchilla 4)
Basin Centre
(e.g., West Wandoan 1, Woleebee Creek GW4)
F7: Peat Mire
F12–13: Shoreface
F5: Levee and Splay
F9–11: Mouth Bar, Delta Front, Prodelta
F4: Distributary Channel
F6: Floodplain
F8: Interdistributary Bay
F14: Tidal Flat
Overall Coarsening Upward Cycles That Prograde
Along-Strike Variation
Coarse-grained sandstone and conglomerate
Fine- to medium-grained sandstone
Muddy sandstones and sandy mudstones
Heterolithic sandstones and mudstones
Carbonaceous siltstones and mudstones
Mudstone
Coal

Figure 23

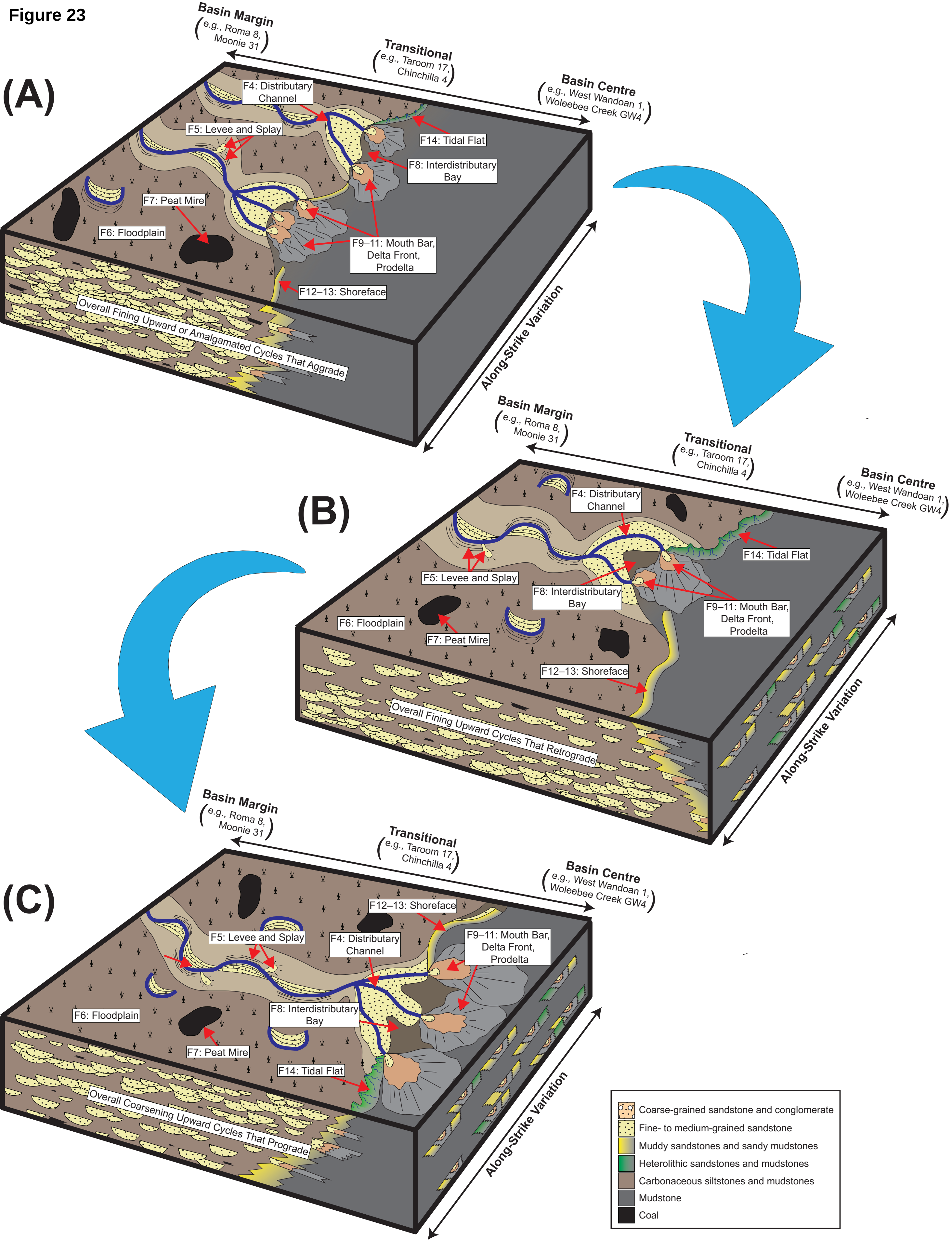
(A)
Basin Margin
(e.g., Roma 8, Moonie 31)
Transitional
(e.g., Taroom 17, Chinchilla 4)
Basin Centre
(e.g., West Wandoan 1, Woleebee Creek GW4)
F4: Distributary Channel
F5: Levee and Splay
F14: Tidal Flat
F8: Interdistributary Bay
F7: Peat Mire
F6: Floodplain
F9–11: Mouth Bar, Delta Front, Prodelta
F12–13: Shoreface
Overall Fining Upward or Amalgamated Cycles That Aggrade
Along-Strike Variation
(B)
Basin Margin
(e.g., Roma 8, Moonie 31)
Transitional
(e.g., Taroom 17, Chinchilla 4)
Basin Centre
(e.g., West Wandoan 1, Woleebee Creek GW4)
F4: Distributary Channel
F14: Tidal Flat
F5: Levee and Splay
F8: Interdistributary Bay
F9–11: Mouth Bar, Delta Front, Prodelta
F6: Floodplain
F7: Peat Mire
F12–13: Shoreface
Overall Fining Upward Cycles That Retrograde
Along-Strike Variation
(C)
Basin Margin
(e.g., Roma 8, Moonie 31)
Transitional
(e.g., Taroom 17, Chinchilla 4)
Basin Centre
(e.g., West Wandoan 1, Woleebee Creek GW4)
F12–13: Shoreface
F5: Levee and Splay
F4: Distributary Channel
F9–11: Mouth Bar, Delta Front, Prodelta
F6: Floodplain
F8: Interdistributary Bay
F7: Peat Mire
F14: Tidal Flat
Overall Coarsening Upward Cycles That Prograde
Along-Strike Variation
Coarse-grained sandstone and conglomerate
Fine- to medium-grained sandstone
Muddy sandstones and sandy mudstones
Heterolithic sandstones and mudstones
Carbonaceous siltstones and mudstones
Mudstone
Coal

Figure 24

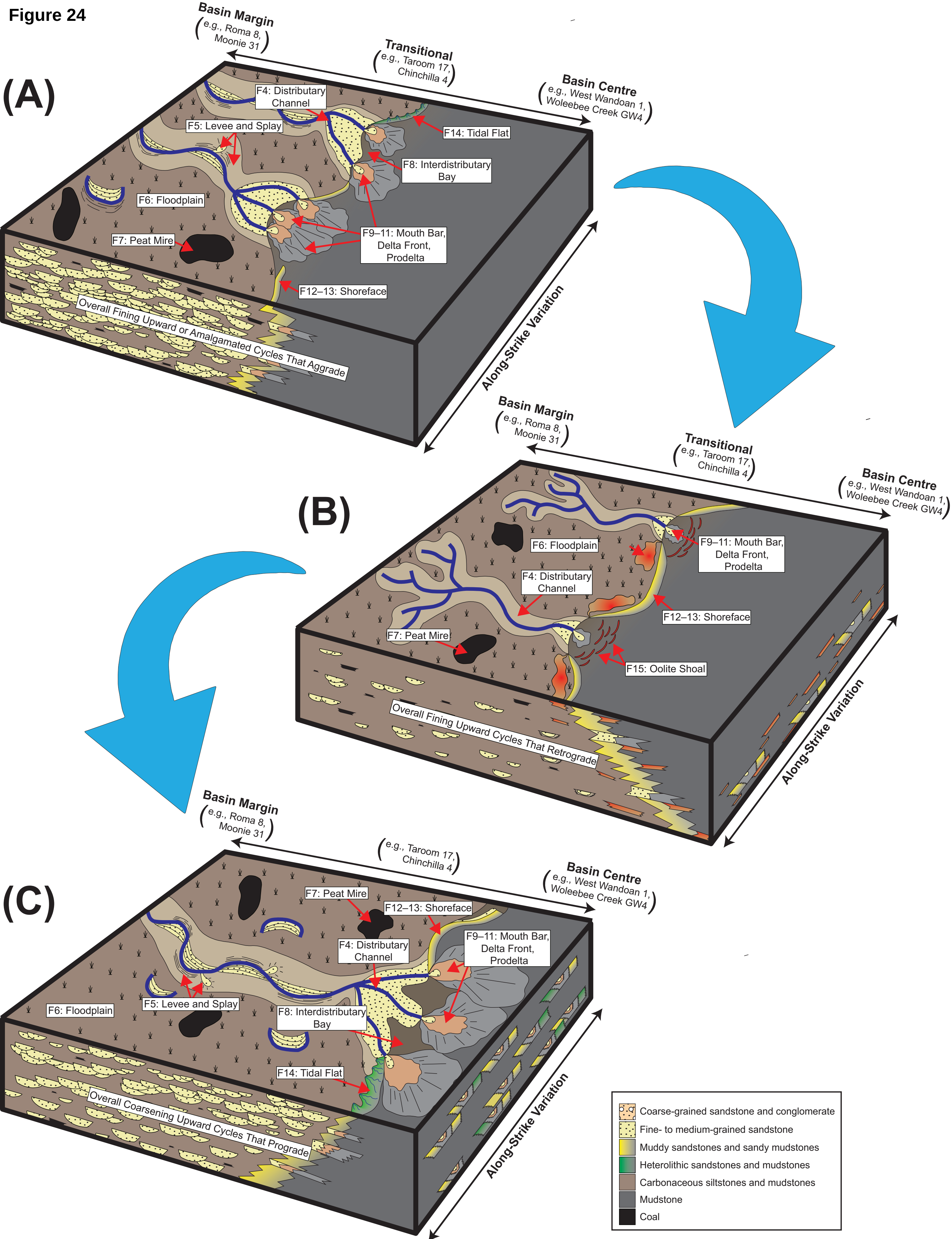
(A)
Basin Margin
(e.g., Roma 8, Moonie 31)
Transitional
(e.g., Taroom 17, Chinchilla 4)
Basin Centre
(e.g., West Wandoan 1, Woleebee Creek GW4)
F4: Distributary Channel
F5: Levee and Splay
F14: Tidal Flat
F8: Interdistributary Bay
F6: Floodplain
F7: Peat Mire
F9–11: Mouth Bar, Delta Front, Prodelta
F12–13: Shoreface
Overall Fining Upward or Amalgamated Cycles That Aggrade
Along-Strike Variation
(B)
Basin Margin
(e.g., Roma 8, Moonie 31)
Transitional
(e.g., Taroom 17, Chinchilla 4)
Basin Centre
(e.g., West Wandoan 1, Woleebee Creek GW4)
F6: Floodplain
F9–11: Mouth Bar, Delta Front, Prodelta
F4: Distributary Channel
F12–13: Shoreface
F7: Peat Mire
F15: Oolite Shoal
Overall Fining Upward Cycles That Retrograde
Along-Strike Variation
(C)
Basin Margin
(e.g., Roma 8, Moonie 31)
(e.g., Taroom 17, Chinchilla 4)
Basin Centre
(e.g., West Wandoan 1, Woleebee Creek GW4)
F7: Peat Mire
F12–13: Shoreface
F4: Distributary Channel
F9–11: Mouth Bar, Delta Front, Prodelta
F6: Floodplain
F5: Levee and Splay
F8: Interdistributary Bay
F14: Tidal Flat
Overall Coarsening Upward Cycles That Prograde
Along-Strike Variation
Coarse-grained sandstone and conglomerate
Fine- to medium-grained sandstone
Muddy sandstones and sandy mudstones
Heterolithic sandstones and mudstones
Carbonaceous siltstones and mudstones
Mudstone
Coal

Table 1

Well Name	Latitude	Longitude	Base (m, MD)	Top (m, MD)	Thickness (m)
Chinchilla 4	26°43'7.9721"S	150°12'5.0989"E	1227	979	248
Condabri MB3-H	26°48'32.9400"S	150°10'15.7900"E	1517	1300	217
Kenya East GW7	27°01'44.5100"S	150°34'27.8800"E	1228	972	256
Moonie 31	27°44'42.6577"S	150°15'13.9337"E	1731	1724	7
Moonie 34	27°45'50.6600"S	150°14'27.9384"E	1780	1758	22
Reedy Creek MB3-H	26°21'27.8000"S	149°25'35.8900"E	1351	1149	202
Roma 8	26°33'12.0538"S	148°36'14.4833"E	1060	950	110
Taroom 17	25°47'21.0026"S	148°44'57.7232"E	499	271	228
West Wandoan 1	26°10'53.8590"S	149°48'44.7444"E	1238	953	285
Woleebee Creek GW4	26°16'54.8917"S	149°42'50.9384"E	1575	1280	295
				Total	**1807**

Table 2

Facies Association	Facies	Grain Size	Physical Structures	Trace Fossils	Bioturbation Intensity and Distribution	Ichnofacies	Accessories	Sedimentary Environment
FA1: Braid plain	**F1:** Interbedded conglomerate and sandstone	Medium to very coarse-grained sand; granules to pebbles	Structureless to crudely laminated	None	BI 0	-	-	Lag deposit or channel base
	F2: Mud-clast breccia	Medium to very coarse-grained sand; granules to pebbles (angular)	Structureless to crudely laminated, mud rip-up clasts	None	BI 0	-	-	Channel base or channel bank collapse
	F3: Coarse-grained planar-tabular cross-bedded sandstone	Medium to very coarse-grained sand	Fining-upward, planar tabular cross-beds, rare current ripples, normal graded beds	None	BI 0	-	Rip-up clasts, pebbles, pebble lags	Fluvial channel
FA2: Lower delta plain	**F4:** Fine-grained planar-tabular grading into current ripple laminated sandstone	Very fine to fine grained sand	Fining-upward, planar tabular cross beds, current ripples	*Planolites, Taenidium*	BI 0-1, burrowed tops, sporadic distribution	*Scoyenia*	Carbonaceous detritus, rip-up clasts, pebbles and pebble lags	Distributary channel
	F5: Structureless to planar-parallel laminated sandstone	Fine to medium grained sand	Structureless to horizontal planar-parallel lamination	*Planolites*	BI 0-1, burrowed tops, sporadic distribution	*Scoyenia*	Rootlets, siderite horizons, coal fragments, spherulitic siderite	Channel levee or splay
	F6: Structureless, carbonaceous siltstone and mudstone	Very fine silt to coarse silt	Structureless, rare planar parallel or current ripple lamination	*Planolites, Taenidium, Naktodemasis*	BI 0-1	*Scoyenia*	Carbonaceous detritus, coal fragments, rare slickensides	Floodplain
	F7: Coal	Macerated plant material	N/A	None	BI 0	-	-	Peat Mire
	F8: Bioturbated muddy sandstone and sandy mudstone	Coarse silt to fine-grained sand	Rare horizontal planar parallel lamination, wavy or lenticular bedding, synaeresis cracks	*Planolites, Palaeophycus,* navichnia rare *Teichichnus*	BI 0-3, sporadic distribution	Impoverished *Cruziana*	-	Interdistributary Bay
FA3: Subaqueous delta	**F9**: Wave- to combined-flow ripple laminated sandstone	Very fine to fine grained sand	Coarsening-upward, wave or combined-flow ripples, soft sedimentary deformation, thin planar-parallel lamination and graded mudstone beds	*Planolites, Teichichnus, Lockeia,* fugichnia	BI 0-2, sporadic distribution	Skolithos	Rootlets, carbonaceous detritus, siderite horizons, rare coal fragments	Mouthbar
	F10: Sand-dominated to sub-equal sandy and muddy heterolithics (sandstone and mudstone); 90%>sand>30%	Medium to coarse silt and very fine to fine grained sand	Current to combined flow ripples, wave ripples, soft sedimentary deformation, micro-faults, synaeresis cracks, normal and inverse grading	*Planolties, Palaeophycus, Lockeia, Techichnus, Siphonichnus,* fugichnia	BI 0-3, sporadic distribution in mudstone, rare in sandstone	Impoverished Proximal *Cruziana*	Sideritized horizons	Delta front
	F11: Mud-dominated heterolithics (sandstone and mudstone); 30%>sand>10%	Medium to coarse silt and very fine to fine grained sand	Current to combined flow ripples, horizontal planar-parallel lamination, normal and inverse grading, wavy to lenticular bedding	*Planolites, Palaeophycus, Diplocraterion, Teichichnus, Thalassinoides, Siphonichnus.* navichnia, rare *Asterosoma*	BI 0-3, sporadic distribution in mudstone and sandstone	Impoverished Archetypal *Cruziana*	-	Prodelta
FA4: Delta-influenced shoreface	**F12**: Bioturbated muddy sandstone with wave-ripple lamination and HCS interbeds	Coarse silt to medium grained sand	Wave ripples, micro HCS, wavy undulatory lamination, normal-graded beds	*Asterosoma, Conichnus, Chondrites, Planolites, Scolicia, Teichichnus, Palaeophycus, Phycosiphon, Lockeia,* fugichnia	BI 0-5, laminated to scrambled	Proximal *Cruziana*	-	Lower shoreface
	F13: Bioturbated sandy mudstone with wave-ripple to HCS interbeds	Coarse silt with interstitial very fine to fine grained sand	Rare horizontal planar parallel lamination in muds; micro HCS in sandstone	*Asterosoma, Conichnus, Chondrites, Planolites, Teichichnus, Palaeophycus, Phycosiphon, Helminthopsis*	BI 0-6, laminated to scrambled	Archetypal *Cruziana*	-	Upper offshore
FA5: Tidally ~~e-~~ influenced shoreline	**F14**: Mixed sandy and muddy heterolithics with tide-generated structures (sandstone and mudstone) 90%>sand>10%	Medium to coarse silt and very fine to fine grained sand	Flaser, wavy, lenticular bedding, current to combined flow ripples, synaeresis cracks	*Planolites, Palaeophycus Cylindrichnus, Teichicnus, Diplocraterion, Siphonichnus,* navichnia	BI 2-5, sporadic distribution in mudstone and sandstone	Depauperate "Mixed *Skolithos-Cruziana"*	Carbonaceous detritus, rootlets, rare sideritized horizons	Tidal flats
FA 6: Restricted m~~M~~arine shoals	**F15A: Oolitic Ironstone**	Fine- to medium-grained sand	Horizontal planar-parallel lamination, structureless, rare wave ripples	None	BI 0	-	-	~~Shallow~~ Restricted marine shoals
	F15B: Cemented Ironstone	N/A	Cemented	None	BI 0	-	Stylolites	Diagenetic overprint related to faults

Table 3

Palynomorph	Type	Palynomorph	Type	Palynomorph	Type
Cymatiosphaera spp.	Achritarch	*Podocarpidites ellipticus*	Continental Pollen	*Klukisporites lacunus*	Continental Spore
Micrhystridium spp.	Achritarch	*Protohaploxypinus* spp.	Continental Pollen	*Klukisporites scaberis*	Continental Spore
Multiplicisphaeridium spp.	Achritarch	*Trisaccates undiff.*	Continental Pollen	*Klukisporites* spp.	Continental Spore
Veryhachium spp.	Achritarch	*Vitreisporites pallidus*	Continental Pollen	*Klukisporites variegatus*	Continental Spore
Algae spp.	Algae	*Vitreisporites signatus*	Continental Pollen	*Krauselisporites* spp.	Continental Spore
Bartenia communis	Algae	*Anapiculatisporites dawsonensis*	Continental Spore	*Laevigatosporites* spp.	Continental Spore
Botryococcus spp.	Algae	*Anapiculatisporites pristidentatus*	Continental Spore	*Leptolepidites* spp.	Continental Spore
cf. *Peltacystia* spp.	Algae	*Annulispora folliculosa*	Continental Spore	*Leptolepidites verrucatus*	Continental Spore
Cymatiosphaera spp.	Algae	*Annulispora microannulata*	Continental Spore	*Lundbladispora brevicula*	Continental Spore
Leiosphaeres spp.	Algae	*Antulsporites clavus*	Continental Spore	*Maratthesisporites crassibalteus*	Continental Spore
Micrhystridium spp.	Algae	*Antulsporites regius*	Continental Spore	*Matonisporites crassiangulatus*	Continental Spore
Multiplicisphaeridium spp.	Algae	*Antulsporites regius*	Continental Spore	*Neoraistrickia elongata*	Continental Spore
Veryhachium spp.	Algae	*Antulsporites saevus*	Continental Spore	*Neoraistrickia rugobacula*	Continental Spore
Araucariacites australis	Coastal Pollen	*Apiculatisporites* spp.	Continental Spore	*Neoraistrickia suratensis*	Continental Spore
Araucariacites fissus	Coastal Pollen	*Aratrisporites "miniparvispinosus"*	Continental Spore	*Neoraistrickia taylori*	Continental Spore
Callialasporites dampieri	Coastal Pollen	*Aratrisporites parvispinosus*	Continental Spore	*Neoraistrickia trichosa*	Continental Spore
Callialasporites segmentatus	Coastal Pollen	*Baculatisporites comaumensis*	Continental Spore	*Neoraistrickia truncata*	Continental Spore
Callialasporites trilobatus	Coastal Pollen	*Cadargasporites baculatus*	Continental Spore	*Nevesisporites vallatus*	Continental Spore
Callialasporites turbatus	Coastal Pollen	*Cadargasporites granulatus*	Continental Spore	*Obtusisporis modestus*	Continental Spore
Corollina spp.	Coastal Pollen	*Cadargasporites reticulatus*	Continental Spore	*Obtusisporites modestus*	Continental Spore
Densoisporites spp.	Coastal Spore	*Cadargasporites senectus*	Continental Spore	*Osmundacidites* spp.	Continental Spore
Densoisporites velatus	Coastal Spore	*Cadargasporites verrucosus*	Continental Spore	*Osmundacidites wellmanii*	Continental Spore
Retitriletes "net"	Coastal Spore	*Calamospora* spp.	Continental Spore	*Perotrilites whitfordensis*	Continental Spore
Retitriletes austroclavatidites	Coastal Spore	*Camarozonosporites ramosus*	Continental Spore	*Playfordiaspora velata*	Continental Spore
Retitriletes circolumenus	Coastal Spore	*Camarozonosporites rudis*	Continental Spore	*Polycingulatisporites clavus*	Continental Spore
Retitriletes clavatoides	Coastal Spore	*Cibotiumsporites juriensis*	Continental Spore	*Polycingulatisporites crenulatus*	Continental Spore
Retitriletes facetus	Coastal Spore	*Cingulatisporites* spp.	Continental Spore	*Polycingulatisporites mooniensis*	Continental Spore
Retitriletes huttonensis	Coastal Spore	*Clavatisporites* spp.	Continental Spore	*Rogalskaisporites cicatricosus*	Continental Spore
Retitriletes nodosus	Coastal Spore	*Concavissimisporites punctatus*	Continental Spore	*Rugulatisporites* spp.	Continental Spore
Retitriletes proxiradiatus	Coastal Spore	*Converrucosisporites pricei*	Continental Spore	*Sculptisporis moretonensis*	Continental Spore
Retitriletes semimuris	Coastal Spore	*Converrucosisporites verrucosus*	Continental Spore	*Staplinisporites caminus*	Continental Spore
Retitriletes watherooensis	Coastal Spore	*Coronatispora perforata*	Continental Spore	*Staplinisporites manifestus*	Continental Spore
Alisporites grandis	Continental Pollen	*Cyathidites australis*	Continental Spore	*Stereisporites antiquasporites*	Continental Spore
Alisporites lowoodensis	Continental Pollen	*Cyathidites minor*	Continental Spore	*Stereisporites pocockii*	Continental Spore
Alisporites similis	Continental Pollen	*Dictyophyllidites harrisii*	Continental Spore	*Stereisporites psilatus*	Continental Spore
Alisporites spp.	Continental Pollen	*Foraminisporis caelatus*	Continental Spore	*Striatella jurassica*	Continental Spore
Ashmoripollis reducta	Continental Pollen	*Foraminisporis* spp.	Continental Spore	*Striatella parva*	Continental Spore
Ashmoripollis reducta	Continental Pollen	*Foraminisporis tribulosus*	Continental Spore	*Striatella seebergensis*	Continental Spore
Cycadopites follicularis	Continental Pollen	*Foveosporites canalis*	Continental Spore	*Thymospora ipsviciensis*	Continental Spore
Cycadopites spp.	Continental Pollen	*Foveosporites moretonensis*	Continental Spore	*Todisporites major*	Continental Spore
Exesipollenites tumulus	Continental Pollen	*Foveosporites* spp.	Continental Spore	*Todisporites minor*	Continental Spore
Falcisporites australis	Continental Pollen	*Gleicheniidites senonicus*	Continental Spore	*Trilobosporites antiquus*	Continental Spore
Falcisporites grandis	Continental Pollen	*Granulatisporites* spp.	Continental Spore	*Verrucosisporites varians*	Continental Spore
Falcisporites similis	Continental Pollen	*Interulobites intraverrucatus*	Continental Spore	Copepod fragments	Copepoda
Perinopollenites elatoides	Continental Pollen	*Ischyosporites crateris*	Continental Spore	Dinocyst indet.	Dinocyst
Pinuspollenites parvisaccatus	Continental Pollen	*Ischyosporites spp.*	Continental Spore	*Mendicodinium* spp.	Dinocyst
Platysaccus queenslandi	Continental Pollen	*Kekryphalospora distincta*	Continental Spore	Fungal spores	Fungi

Table 4

Well	Total Count	Coastal Spores	Continental Spores	Coastal Pollen	Continental Pollen	Freshwater Algae	Fungal	Dino / Achritarch / Copepoda	Depth	Facies	Sequence Stratigraphy
Chinchilla 4	281	19	63	171	213	3	0	0	983.00	SM4	HST 3
Chinchilla 4	272	29	100	63	156	15	0	1	1017.40	M1	TST 3
Chinchilla 4	303	4	33	135	247	23	0	+	1045.45	SM3	TST 3
Chinchilla 4	276	24	104	137	166	6	0	0	1098.65	SM3	Sequence 2
Chinchilla 4	293	7	42	186	246	2	1	0	1126.70	SM3	HST 1
Chinchilla 4	277	23	92	136	179	4	0	0	1162.08	SM3	TST 1
Chinchilla 4	275	11	66	182	202	4	0	0	1199.64	SM3	LST1
Chinchilla 4	294	6	26	228	253	15	0	0	1217.60	SM3	LST 1
Condabri MB9-H	295	18	138	115	17	7	0	0	1326.06	M3	HST 3
Condabri MB9-H	300	25	137	116	18	4	0	0	1417.59	SM3	Sequence 2
Condabri MB9-H	300	41	157	74	23	5	0	0	1436.37	SM2	Sequence 2
Condabri MB9-H	300	29	104	142	20	5	0	0	1445.09	SM3	HST 1
Condabri MB9-H	300	19	103	144	25	9	0	0	1461.22	M1	TST 1
Condabri MB9-H	300	44	166	79	8	3	0	0	1501.41	SM1	LST 1
Condabri MB9-H	301	15	117	129	28	6	0	0	1508.70	SM2	LST 1
Kenya East GW7	310	44	107	66	77	13	0	3	981.35	SM3	HST 3
Kenya East GW7	300	17	32	129	95	27	0	0	1023.60	S6	TST 3
Kenya East GW7	300	7	38	93	120	37	0	5	1028.60	M2	TST 3
Kenya East GW7	300	12	54	196	33	5	0	0	1146.70	M1	TST 1
Kenya East GW7	300	13	62	166	54	5	0	0	1165.30	SM3	TST 1
Kenya East GW7	300	44	138	44	57	17	0	0	1181.50	SM3	TST 1
Kenya East GW7	300	11	116	112	52	9	0	0	1192.70	SM2	LST 1
Moonie 31	316	35	69	160	49	3	0	0	1724.25	M1	TST 1
Reedy Creek MB3-H	201	11	32	79	150	8	0	0	1208.35	M1	TST 3
Reedy Creek MB3-H	307	22	28	143	235	18	+	4	1215.17	M1	TST 3
Reedy Creek MB3-H	297	52	120	92	124	1	0	0	1243.30	M1	Sequence 2
Reedy Creek MB3-H	299	11	60	173	221	6	0	0	1270.42	SM2	HST 1
Reedy Creek MB3-H	294	33	128	69	124	6	0	0	1326.26	SM2	TST 1
Reedy Creek MB3-H	300	3	48	205	242	6	0	0	1337.68	SM2	LST 1
Roma 8	300	40	47	121	76	16	0	+	956.70	SM3	HST 3
Roma 8	300	21	87	100	89	2	0	1	967.87	SM3	HST 3
Roma 8	305	8	27	196	71	3	0	0	985.26	SM3	TST 3
Roma 8	300	47	108	120	7	18	0	0	995.85	SM2	Sequence 2
Roma 8	300	34	71	146	44	5	0	0	1011.40	M1	Sequence 2
Roma 8	300	19	68	174	38	1	0	0	1029.15	M1	HST 1
Roma 8	305	37	57	182	28	1	0	0	1041.00	M1	TST 1
Roma 8	301	16	65	185	26	9	0	0	1042.90	SM1	TST 1
Taroom 17	302	46	73	111	61	11	0	0	280.70	M3	TST 3
Taroom 17	301	4	71	182	35	6	0	0	297.65	SM2	TST 3
Taroom 17	300	51	75	88	66	18	0	0	331.37	S4	Sequence 2
Taroom 17	299	9	79	157	54	0	0	0	378.53	SM3	HST 1
Taroom 17	300	10	46	175	68	1	0	0	386.42	SM3	TST 1
Taroom 17	306	17	50	193	41	5	0	0	397.35	SM3	TST 1
Taroom 17	300	22	101	112	63	2	0	0	421.80	M1	TST 1
Taroom 17	300	0	19	252	28	1	0	0	483.25	SM2	LST 1
West Wandoan 1	405	11	108	198	81	7	0	0	980.45	SM2	TST 3
West Wandoan 1	304	41	98	117	43	5	0	0	990.84	SM3	TST 3
West Wandoan 1	327	40	73	142	65	7	0	0	993.51	M3	TST 3
West Wandoan 1	308	18	45	102	110	33	0	0	998.65	SM3	TST 3
West Wandoan 1	300	90	30	130	24	26	0	+	1010.56	SM3	TST 3
West Wandoan 1	307	15	40	114	82	37	0	19	1011.86	SM3	TST 3
West Wandoan 1	349	18	87	83	149	10	0	2	1013.40	M1	TST 3
West Wandoan 1	300	14	21	136	125	4	0	0	1027.61	SM2	TST 3
West Wandoan 1	300	0	22	255	15	8	0	0	1207.61	SM2	LST 1
Woleebee Creek GW4	300	49	77	102	57	15	0	0	1310.60	M2	TST 3
Woleebee Creek GW4	300	10	21	152	87	27	0	3	1336.70	M2	TST 3
Woleebee Creek GW4	299	93	110	76	7	13	0	0	1356.75	SM3	Sequence 2
Woleebee Creek GW4	300	25	110	135	28	2	0	0	1382.25	SM3	Sequence 2
Woleebee Creek GW4	300	14	83	155	45	3	0	0	1391.25	SM2	Sequence 2
Woleebee Creek GW4	300	14	64	182	40	0	0	0	1422.55	M1	TST 1
Woleebee Creek GW4	298	19	93	124	55	7	0	0	1489.55	SM4	LST 1